

NASA Technical Memorandum 80230

Simulation Study of Nonaxisymmetric
Nozzle for Air-Combat Maneuvering
for an F-15 Class Airplane (U)

Jack E. Pennington and Alfred J. Meintel, Jr.
Langley Research Center
Hampton, Virginia



National Aeronautics
and Space Administration

**Scientific and Technical
Information Office**

1980

[REDACTED]

1

2

3

4

5

6

7

8

9

10

11

12

13

14

15

16

17

18

19

20

21

22

23

24

25

26

27

28

29

30

31

32

33

34

35

36

[REDACTED]

UNCLASSIFIED

(U) SUMMARY (U)

(U) In 1978 an F-15 class airplane and a similar airplane having a nonaxisymmetric (two-dimensional) nozzle were simulated on the Langley Differential Maneuvering Simulator. A series of simulated engagements were flown by combat-qualified pilots to assess the benefits of the two-dimensional nozzle. This report presents the equations and data used to represent both airplanes, describes the tests used to validate the simulation, compares the performance characteristics of the two airplanes, and presents the results of the piloted simulation.

(U) INTRODUCTION (U)

(U) Jet airplanes that must operate at subsonic and supersonic speeds require exhaust nozzles with variable geometry in order to achieve high performance over a wide range of engine power settings and Mach numbers. Because of the high internal performance attainable with axisymmetric (circular) nozzles, this type nozzle has been used in past and current airplane designs. However, aft-end-closure drag problems can occur in multiengine configurations (ref. 1). Multiengine configurations usually have a large "gutter" interfaring between the nozzles that is subject to adverse interference effects, especially if the external flow separates from the aft body near the nozzle exits. Nonaxisymmetric (two-dimensional) nozzles properly integrated with the airframe can eliminate the boattail gutter and improve the thrust-minus-drag performance. Several different designs for nonaxisymmetric nozzles have been studied by government and industry (refs. 2 to 8). Figure 1 shows twin axisymmetric nozzles and one type of nonaxisymmetric nozzle installed on a fighter configuration.

(U) In addition to improved thrust-minus-drag performance, two-dimensional nozzles can provide other benefits such as thrust vectoring, in-flight thrust reversing, and reduced observables. Thrust vectoring supplies a vertical force which can augment the wing lift or which can be used as an independent control force. In-flight thrust reversing can provide deceleration at low speeds when a speed brake loses aerodynamic effectiveness.

(U) However, there are possible disadvantages. Thrust vectoring causes a pitching moment which must be countered by the flight control system, perhaps with another control surface such as a canard. Installation of both a two-dimensional nozzle and a canard would probably increase the airplane weight, perhaps negating some of the performance benefits obtained.

(U) Proper integration of the two-dimensional nozzle with the airframe would be critical. Studies have shown that with proper design integration, thrust vectoring can induce additional circulation and lift on the wing (refs. 2 and 3). Poor integration could cause interference with stability or control effectiveness.

UNCLASSIFIED

UNCLASSIFIED

(U) In 1977, NASA Langley Research Center and the McDonnell Aircraft Company participated in a study to design a two-dimensional nozzle suitable for installation on the F-15. References 9 and 10 present the results of the study. In 1978, an F-15 class airplane, with and without a two-dimensional nozzle, was simulated on the Langley Differential Maneuvering Simulator (DMS). The simulated two-dimensional nozzle provided thrust vectoring, in-flight thrust reversing, and induced lift. A large canard was simulated to counter the pitching moment due to thrust vectoring. This resulted in the modified airplane being about 4.3 percent heavier than the baseline airplane. This report presents the equations and data used to represent both airplanes, describes the tests used to validate the simulation, compares the performance characteristics of the two airplanes, and presents the results of a piloted simulation to assess the benefits of the two-dimensional nozzle in one-on-one air combat.

(U) Equations of motion, thrust, and aerodynamic data for F-15 simulation are given in appendix B by Fred L. Biessner, Jr., Kentron International, Inc.

(U) Use of trade names or names of manufacturers in this report does not constitute an official endorsement of such products or manufacturers, either expressed or implied, by the National Aeronautics and Space Administration.

(U) SYMBOLS AND ABBREVIATIONS (U)

(U) Values are given in both SI and U.S. Customary Units. The measurements and calculations were made in U.S. Customary Units.

AR	aspect ratio, dimensionless
A_g, E_g	gun azimuth and elevation angles, respectively
a_n	normal load factor, g units
$a_{n,vect}$	normal load factor increment due to thrust vectoring, g units
a_x	longitudinal acceleration, g units
a_y	lateral load factor, g units
b	wing span, m (ft)
C_D, C_L	drag and lift coefficients, respectively, dimensionless
$C_{D,aero}$	total aerodynamic drag coefficient, dimensionless
$C_{D,c}, C_{L,c}$	canard drag and lift coefficients, respectively, dimensionless
$C_{D,E}$	coefficient of engine drag, dimensionless
$C_{D,eff}, C_{L,eff}$	effective drag and lift coefficients, respectively, including both aerodynamic and thrust effects, dimensionless

UNCLASSIFIED

$C_{D,N}$	increment in afterbody drag of two-dimensional C-D nozzle at $\theta_j = 0$, referenced to a symmetric nozzle, dimensionless
$C_{D,R}$	ram drag coefficient, dimensionless
$C_{D,32}, C_{D,40}$	drag coefficient in afterburner at 9144 m (30 000 ft) altitude and $\alpha \leq 32^\circ$ and $\alpha \geq 40^\circ$, respectively
C_{ij}	direction cosines relating body to inertial axis system
$C_{L,aero}$	total aerodynamic lift coefficient, dimensionless
$C_{L,v}$	increment in aerodynamic lift coefficient due to thrust vectoring, dimensionless
C_L'	sum of coefficients of static and inertial lift effects, dimensionless
C_l, C_m, C_n	rolling-, pitching-, and yawing-moment coefficients, respectively, about body axes, dimensionless
C_T	thrust coefficient, dimensionless
$C_{X,b}, C_{Y,b}, C_{Z,b}$	nondimensional coefficients of aerodynamic and thrust force acting along X,Y,Z body axes, respectively
$C_{X,stab}, C_{Y,stab}, C_{Z,stab}$	nondimensional coefficients of aerodynamic and thrust force acting along X,Y,Z stability axes, respectively
C_y	side-force coefficient, dimensionless
c_g	center-of-mass position expressed as fraction of \bar{c}
\bar{c}	mean aerodynamic chord, m (ft)
$D_{max}, D_{mil}, D_{idle}$	single-engine ram drag at maximum, military (intermediate), and idle power settings, respectively, N (lb)
D_R	ram drag, N (lb)
dt	rate of change of time
E_H	expected number of bullet hits
$F_{max}, F_{mil}, F_{idle}$	single-engine fuel flow at maximum, military, and idle power settings, respectively, kg/sec (lb/hr)
F_1 to F_{14}	scheduled gains or functions in flight control system
g	acceleration due to gravity, $1g = 9.81 \text{ m/sec}^2$ (32.2 ft/sec^2)
H_L, H_D	thrust-induced amplification factors in lift and drag, respectively

UNCLASSIFIED

UNCLASSIFIED

h	altitude, m (ft)
I_{XX}, I_{YY}, I_{ZZ}	moments of inertia about roll, pitch, and yaw axes, respectively, referred to body axis system, $\text{kg}\cdot\text{m}^2$ ($\text{slug}\cdot\text{ft}^2$)
I_{XZ}	product of inertia, $\text{kg}\cdot\text{m}^2$ ($\text{slug}\cdot\text{ft}^2$)
$K_{\delta_r}, K_{\delta_{rl}}$	factors to adjust rudder effectiveness in side force and roll, respectively
K_1 to K_{10}	gain constants used in flight control system
$l_c l_t$	longitudinal distance to effective point of action of canard and thrust vectors, respectively, m (ft)
M	Mach number
m	mass, kg (slug)
P	Sciatti range
P_S	specific excess power, m/sec (ft/sec)
P_{HSS}	single shot probability of bullet hit
p, q, r	rolling, pitching, and yawing angular velocities, respectively, about X, Y, Z body axes, rad/sec
p_s	static pressure, N/m^2 (lb/ft^2)
p_T	total pressure, N/m^2 (lb/ft^2)
Q	gravity drop
\bar{q}	dynamic pressure, N/m^2 (lb/ft^2), $\bar{q} = p_T - p_s$
R	range between aircraft, m (ft)
R_{gcg}	displacement of gun from aircraft center of gravity
S	wing reference area, m^2 (ft^2)
S_x, S_y, S_z	components of windage jump in X_1, Y_1, Z_1 coordinate system, respectively
s	Laplace operator
T_{gross}	gross thrust, N (lb)
$T_{max}, T_{mil}, T_{idle}$	single-engine gross thrust at maximum, military, and idle power, respectively, N (lb)

UNCLASSIFIED

$t_{1/2}$	time to damp to one-half amplitude, sec
t_{90}	time to bank 90°
u, v, w	components of velocity along aircraft X, Y, Z body axes, respectively, m/sec (ft/sec)
u_M, v_M, w_M	components of bullet muzzle velocity along aircraft X, Y, Z body axes, respectively, m/sec (ft/sec)
v	total aircraft velocity, m/sec (ft/sec)
v_{bo}	initial bullet velocity, m/sec (ft/sec)
v_{cas}	calibrated airspeed, knots
v_M	muzzle velocity, m/sec (ft/sec)
v_p	total projectile velocity, m/sec (ft/sec)
w	weight, $W = mg$, N (lb)
w_f	rate of fuel flow
x_1, y_1, z_1 x_2, y_2, z_2	coordinate systems used in ballistic equations
x_I, y_I, z_I	components of inertial axis system
x_1, y_1, z_1	coordinates of projectile position in x_1, y_1, z_1 coordinate system, respectively
$\dot{x}_{Bbo}, \dot{y}_{Bbo}, \dot{z}_{Bbo}$	components of \bar{v}_{bo} in body axis system
$\dot{x}_{gcy}, \dot{y}_{gcy}, \dot{z}_{gcy}$	components of \bar{r}_{gcg} in body axis system
$\dot{x}_{Ibo}, \dot{y}_{Ibo}, \dot{z}_{Ibo}$	components of \bar{v}_{bo} in inertial axis system
x_{Ib}, y_{Ib}, z_{Ib}	components of projectile position in x_I, y_I, z_I system
α	angle of attack, deg or rad
β	angle of sideslip, deg
$\Delta C_D, alt$	increment in drag coefficient with altitude
$\Delta C_D, nozzle$	increment in nozzle drag coefficient at afterburning power setting
$\Delta C_D, sb, \Delta C_L, sb, \Delta C_l, sb,$ $\Delta C_m, sb, \Delta C_n, sb$	increments in drag coefficient, lift coefficient, rolling-moment coefficient, pitching-moment coefficient, and yawing-moment coefficient, respectively, at full speed-brake deflection

UNCLASSIFIED

UNCLASSIFIED

$\Delta C_{L,0}$	increment in lift coefficient at maximum speed brake deflection and $\alpha = 0^\circ$
$\Delta C_{L\alpha_1}$	increment in lift curve slope at maximum speed brake deflection and $\alpha \leq 10^\circ$
$\Delta C_{L\alpha_2}$	increment in lift curve slope at maximum speed brake deflection and $\alpha > 10^\circ$
$\Delta C_{l\delta_r}, \Delta C_{Y\delta_r}$	increments in rolling-moment and side-force coefficients, respectively, with rudder deflection
ΔN_o	transonic neutral point shift at $\delta_{sb} = 0$, expressed as fraction of \bar{c}
ΔN_{sb}	neutral point shift at full speed-brake deflection, expressed as fraction of \bar{c}
δ_o	projectile yaw angle, rad
δ_{AB}	fraction of afterburning power commanded
δ_a	aileron deflection, positive for right roll, deg
δ_d	differential horizontal-tail deflection, positive for right roll, deg
δ_h	symmetric horizontal-tail deflection, positive for aircraft nose down control, deg
$\delta_{h,L}, \delta_{h,R}$	deflection of left and right side of horizontal tail, respectively, deg
δ_{lat}	lateral stick position
δ_{long}	longitudinal stick position
δ_{mil}	fraction of nonafterburning power commanded
δ_r	rudder deflection, deg
δ_{rev}	fraction of available thrust reverser employed
δ_{sb}	speed-brake deflection, deg
δ_v	effective thrust-vector angle, deg
ζ	damping ratio
θ_j	geometric thrust-vector angle, deg

UNCLASSIFIED

$\theta_{j,c}$	commanded geometric thrust-vector angle, deg
$\theta_{j,max}$	maximum geometric thrust-vector angle, deg
θ_o, ψ_o	Euler angles used to transform from inertial axis system to x_2, y_2, z_2 axis system
λ	line-of-sight angle, deg
ρ	air density, kg/m ³ (slug/ft ³)
ϕ_o	projectile precession angle, deg
ω	total aircraft angular rate, rad/sec
ω_n	natural frequency, rad/sec

$$C_{D_h} = \frac{\partial C_D}{\partial h} \quad C_{L_{a_n}} = \frac{\partial C_L}{\partial a_n}$$

$$C_{\ell_p} = \frac{\partial C_\ell}{\partial \left(\frac{pb}{2v} \right)} \quad C_{\ell_r} = \frac{\partial C_\ell}{\partial \left(\frac{rb}{2v} \right)}$$

$$C_{\ell_{\delta_a}} = \frac{\partial C_\ell}{\partial \delta_a} \quad C_{\ell_{\delta_D}} = \frac{\partial C_\ell}{\partial \delta_D}$$

$$C_{m_{a_n}} = \frac{\partial C_m}{\partial a_n} \quad C_{m_q} = \frac{\partial C_m}{\partial \left(\frac{qc}{2v} \right)}$$

$$C_{m_{\alpha}} = \frac{\partial C_m}{\partial \left(\frac{\dot{\alpha} \bar{c}}{2v} \right)} \quad C_{n_{\delta_a}} = \frac{\partial C_n}{\partial \delta_a}$$

UNCLASSIFIED

UNCLASSIFIED

$$C_{n_p} = \frac{\partial C_n}{\partial \left(\frac{pb}{2v} \right)}$$

$$C_{n_r} = \frac{\partial C_n}{\partial \left(\frac{rb}{2v} \right)}$$

$$C_{n_{\delta_D}} = \frac{\partial C_n}{\partial \delta_D}$$

$$C_{n_{\delta_r}} = \frac{\partial C_n}{\partial \delta_r}$$

$$C_{Y_{\delta_a}} = \frac{\partial C_Y}{\partial \delta_a}$$

$$C_{Y_{\delta_D}} = \frac{\partial C_Y}{\partial \delta_D}$$

Subscripts:

A	attacker
basic	referenced to nominal aerodynamic configuration
max	maximum
min	minimum
o	opponent
p	pilot

Abbreviations:

ACM	air-combat maneuvering
ADV	adverse
AML	adaptive maneuvering logic
CAS	control augmentation system
C-D	convergent-divergent
DMS	Langley Differential Maneuvering Simulator
IFTR	in-flight thrust reversing
PLA	power-lever angle
PROV	proverse
SB	speed brake

UNCLASSIFIED

TED trailing edge down
TEU trailing edge up
TOA time on offense with advantage
TR thrust reverser
2D two dimensional

(U) A dot over a symbol denotes a time derivative of the variable. A bar over a symbol denotes a vector.

(U) SIMULATION FACILITY (U)

(U) The Langley Differential Maneuvering Simulator (DMS) (fig. 2) consists of two fixed-base cockpits, each located inside a 12-m (40-ft) projection sphere. The DMS is linked to a Control Data CYBER 175 real-time computer system operating at 32 iterations/sec. Each sphere also contains (1) a high-resolution, closed-circuit television projector with 10-to-1 range (zoom) capability to give the pilot a view of the opposing aircraft, (2) a point light source projector, which supplies a sky-Earth-horizon scene, and (3) a hydraulically driven cockpit buffet system. Each cockpit has (1) the principal flight instruments (airspeed, load factor, altitude, speed-brake/thrust-reverser position, angle of attack, etc.), (2) displacement-type rudder pedals and center stick with hydraulically driven force feel, (3) dual throttle quadrant with speed-brake/thrust-reverser command switch, and (4) computer-generated, wide-angle heads-up display showing range, closure rate, weapons status, target designator, airspeed, load factor, and lead computing sight.

(U) The target generator consists of a target model mounted in a four-axis gimbal system, which allows all-attitude positioning of the model, and a fixed television camera which views the model. The television is a standard black and white, 1029-line system with a standard 15-to-1 zoom lens that, with the 10-to-1 projector zoom lens, supplies a simulated range change of 150 to 1. With a 17.8-cm (7-in.) model of a fighter-type airplane, the simulated range can vary from 91 to 31 715 m (300 to 45 000 ft).

(U) Because of the lack of terrain growth or translational motion in the sky-Earth-horizon scene, a synthetic altitude cue is provided by a light in the cockpit which starts flashing at 1524-m (5000-ft) altitude and increases in frequency with decreasing altitude. A sound generator provides cues for engine noise, speed-brake or in-flight thrust-reverser (IFTR) deployment, gun firing, and infrared missile lock-on.

(U) The pilot's g-suit was inflated as a function of load factor to give an artificial load-factor cue. Pilot blackout was simulated by reducing the cockpit and target brightness as a function of time at high load factors. (See appendix A.) The simulation facility and its operation are described in more detail in reference 11.

UNCLASSIFIED

UNCLASSIFIED

(U) DESCRIPTION OF SIMULATED AIRPLANES (U)

(U) Two airplanes were simulated. The first was a single-place, twin-engine, fixed-wing fighter similar to the F-15A. The second (modified) airplane was similar, but with a nonaxisymmetric two-dimensional nozzle and a canard. Physical properties of the basic airplane are given in table 1. The modified airplane had the same physical characteristics but different mass and inertia values, as given in table 2. The combat weight in the tables is assumed to represent 50-percent internal fuel plus about 1350 kg (2976 lb) for weapons.

(U) Aerodynamics and flight-control-system data for the basic airplane were supplied by the F-15 Systems Program Office, Air Force Systems Command. Although representative of the F-15, the data used in the simulation (and

(U) TABLE 1.- PHYSICAL CHARACTERISTICS OF SIMULATED F-15 AIRPLANE (U)

Wing span, m (ft)	13.01 (42.7)
Wing reference area, m^2 (ft^2)	56.48 (604)
Mean aerodynamic chord, m (ft)	4.86 (15.94)
Center-of-gravity location, fraction of \bar{c}	0.2615
Aspect ratio	3.01
Maximum aileron deflection, deg	± 20
Maximum stabilator deflection, deg	+15 (TED)
Maximum rudder deflection, deg	-25 (TEU)
Maximum speed-brake deflection, deg	± 30
Weight (combat), kg (lb)	16 284 (35 906)
Moments of inertia:	
I_{XX} , $kg \cdot m^2$ ($slug \cdot ft^2$)	34 574 (25 500)
I_{YY} , $kg \cdot m^2$ ($slug \cdot ft^2$)	225 881 (166 600)
I_{ZZ} , $kg \cdot m^2$ ($slug \cdot ft^2$)	253 540 (187 000)
I_{XZ} , $kg \cdot m^2$ ($slug \cdot ft^2$)	-13 558 (-10 000)

(U) TABLE 2.- PHYSICAL CHARACTERISTICS OF SIMULATED F-15 WITH TWO-DIMENSIONAL C-D NOZZLES, INCLUDING CANARD AND BALLAST (U)

Canard reference area, m^2 (ft^2)	7.0 (75)
Weight, combat, kg (lb)	16 993 (37 463)
Center-of-gravity location, fraction of \bar{c}	0.2615
Moments of inertia:	
I_{XX} , $kg \cdot m^2$ ($slug \cdot ft^2$)	37 963 (28 000)
I_{YY} , $kg \cdot m^2$ ($slug \cdot ft^2$)	228 184 (168 300)
I_{ZZ} , $kg \cdot m^2$ ($slug \cdot ft^2$)	259 097 (191 100)
I_{XZ} , $kg \cdot m^2$ ($slug \cdot ft^2$)	-14 778 (-10 900)

UNCLASSIFIED

presented in this report) may not reflect the latest available data or the current airplane configuration. Thrust and fuel-flow data were supplied by the engine manufacturer. Data for the modified airplane are based on references 9 and 10 and on unpublished NASA data.

(U) The nonaxisymmetric nozzle used on the modified F-15 was assumed to be a convergent-divergent (C-D) type, which provided up to $\pm 15^\circ$ thrust vectoring. The nozzle also provided in-flight thrust reversing, but the simulated flight control system restricted thrust reversing to conditions when vectoring was not used and the engine was in dry power (nonafterburning). References 9 and 10 showed that the C-D nozzle exhibited the lowest weight and highest performance of the candidate nozzles evaluated. The modified F-15 was also assumed to have a canard to balance the pitching moment due to thrust vectoring.

(U) The simulated canard was larger than described in reference 9, thereby supplying more lift, pitching moment, and drag. When thrust vectoring was not used ($\theta_j = 0$), the canard provided no lift. When thrust vectoring was used, the canard was assumed to generate sufficient lift to exactly balance the pitching moment due to vectoring. At the simulated center-of-gravity position, the necessary canard lift was 1.447 times the lift generated by the two-dimensional nozzle. At low speeds, the maximum thrust-vector angle was limited to $\theta_{j,\max}$ to keep the pitching moment within the canard trim capability.

$$\theta_{j,\max} = \frac{K_{10}\bar{q}}{\text{Gross thrust}}$$

where $K_{10} = 250.2 \text{ deg-m}^2$. Canard sizing and effectiveness would be important considerations in designing a flight vehicle having thrust-vectoring capability.

(U) No data were available to indicate effects of wing/canard interaction or effect of the two-dimensional nozzle on aerodynamic stability and control, so these effects were not modeled in the simulation. Appendix B presents the equations of motion, aerodynamic data and equations, and thrust tables and equations used to simulate both aircraft.

(U) Two modes of thrust-vector control were simulated, an automatic mode and a manual mode. In the automatic mode, the thrust-vector angle was commanded by

$$\theta_{j,c} = 0 \quad (\alpha < 5^\circ)$$

$$\theta_{j,c} = (\alpha - 5) \quad (5^\circ \leq \alpha \leq 20^\circ)$$

$$\theta_{j,c} = 15^\circ \quad (\alpha > 20^\circ)$$

$$\theta_j = \min(\theta_{j,c}, \theta_{j,\max})$$

UNCLASSIFIED

In the manual mode, the pilot used a spring-loaded thumb wheel on the stick to command θ_j .

(U) Except for thrust vectoring, the same flight control system was used for the basic F-15 and the modified F-15; that is, symmetric deflection of the horizontal tail (stabilator) for longitudinal control, differential deflection of the horizontal tail plus ailerons for lateral control, and deflection of twin rudders for directional control. The pilot applied controls with conventional center-mounted stick and rudder pedals. A retract/hold/extend switch on the throttle lever commanded speed brakes for the basic airplane and thrust reversing for the modified airplane. The flight-control-system simulation is described in appendix C.

(U) SIMULATION VALIDATION (U)

(U) Before the simulated basic F-15 airplane was flown for data, a series of tests was conducted to evaluate its flying qualities and performance and validate the simulation program. The tests included longitudinal and lateral stability and control checks and performance checks. Results were compared with available flight test data. A description of the checks and the results obtained are presented in appendix D.

(U) Two U.S. Air Force F-15 pilots participated in the validation. They agreed that the simulation was generally satisfactory. The major disagreement noted by the pilots was a tendency for a delay or reversal in roll response at high speeds and with back stick in the simulator, which did not occur in flight. Since data based on flight-test results were not available, the data in appendix B reflect this characteristic. However, it was not considered a factor in simulated engagements, which generally occurred at subsonic speeds.

COMPARISON OF SIMULATED AIRPLANE (U)

(C) Figure 3 shows the maximum sustained turn rate and the maximum instantaneous turn rate for the basic F-15 and the modified F-15 with automatic thrust-vector-angle control. At high speeds both airplanes were limited by the assumed 7.33-g structural limit. At lower speeds, the modified airplane had better sustained and instantaneous turn rates, despite being 706 kg heavier.

(U) Figure 4 shows the thrust-vector angle θ_j corresponding to the modified F-15 turn rates presented in figure 3. Below $M = 0.50$ at $h = 3048$ m and below $M = 0.53$ at $h = 9144$ m, the maximum vector angle $\theta_{j,max}$ was less than 15° because of the limited canard trim capability at low q .

(C) The canard and the vectored thrust worked together to produce the high instantaneous turn rates shown in figure 3. Figure 5 shows the effective lift coefficient $C_{L,eff}$ plotted as a function of angle of attack, where $C_{L,eff}$ includes both wing and canard lift and vectored thrust effect.

$$C_{L,eff} = C_L + C_T \sin(\alpha + \delta_v)$$

(C) The sustained turn rate for the modified F-15 shown in figure 3 was better than the basic F-15 because the automatic thrust-vectoring schedule improved the lift versus drag characteristics. This is illustrated by the drag polar in figure 6, where the effective drag coefficient $C_{D,\text{eff}}$ included longitudinal thrust effects as well as drag.

$$C_{D,\text{eff}} = C_D - C_T \cos(\alpha + \delta_v)$$

(C) An alternative form of figure 6 is the specific excess power P_S plotted in figure 7, where

$$P_S = (\text{Thrust} - \text{drag}) \left(\frac{V}{W} \right) = (-\bar{q} S C_{D,\text{eff}}) \left(\frac{V}{W} \right)$$

The sustained load factor (a_n at $P_S = 0$) determines the sustained turn rate (fig. 3) at that flight condition.

(C) Figure 8 compares the deceleration capability of the simulated speed brake of the basic airplane and the thrust reverser of the modified airplane. The thrust reverser was considerably more effective than the speed brake at all speeds.

(U) ANALYSIS AND SCORING (U)

(U) Several different criteria were used to evaluate the outcome of simulated engagements. These are described in references 12 and 13 and include (1) time on offense with advantage, (2) adaptive-maneuvering-logic (AML) value, (3) missile-launch opportunities, launches, and successes, and (4) gun analysis. Each of these is discussed in the following sections.

(U) Time on Offense With Advantage (U)

(U) Time on offense with advantage (TOA) for an aircraft is defined as the time that the aircraft is behind the opponent (the opponent's line-of-sight angle λ_o exceeds 90°) and the opponent is in front of the aircraft (the attacker's line-of-sight angle λ_A is less than 90°). The line-of-sight angle λ is defined as the angle between the X body axis and the line-of-sight vector to the other aircraft. Time on offense with advantage provides a quantitative measure of aircraft capability and, in previous studies (refs. 14 to 16), has correlated well with pilot opinion and other quantitative measures.

(U) Adaptive-Maneuvering-Logic Value (U)

(U) The AML value is based on a quantitative criteria used by the Langley Adaptive-Maneuvering-Logic (AML) computer program. This program (ref. 13) is

~~UNCLASSIFIED~~

a digital model of a one-on-one air-combat engagement. The program can be run in an off-line (batch) mode, or the decision and maneuvering logic can be used to supply a computer-driven opponent for a pilot in the DMS. The decision logic in the program tries to adaptively improve the AML value, which is calculated based on the questions in table 3. If an airplane (assumed to be the attacker) can answer a question positively, a one is assigned; if not, a zero is assigned. The AML value is just the sum of the 11 values.

(U) TABLE 3.- QUESTIONS USED TO ASSIGN AML VALUE (U)

Question	Criteria (a)
1. Is opponent ahead of attacker?	$\lambda_A < 90^\circ$
2. Is attacker behind opponent?	$\lambda_O > 90^\circ$
3. Can attacker see opponent?	$-30^\circ < \lambda_{A,e} < 150^\circ$
4. Is opponent unable to see attacker?	$\lambda_{O,e} > 150^\circ$ or $\lambda_{O,e} < -30^\circ$
5. Is attacker in volume behind opponent?	$(\lambda_O > 150^\circ \text{ and } R < 914 \text{ m}) \text{ or } (\lambda_O > 135^\circ \text{ and } 914 \text{ m} < R < 1524 \text{ m})$
6. Is opponent outside of volume behind attacker?	$(R > 1524 \text{ m}) \text{ or } (\lambda_A < 150^\circ \text{ if } R < 914 \text{ m}) \text{ or } (\lambda_A < 135^\circ \text{ if } 914 \text{ m} < R < 1524 \text{ m})$
7. Can attacker fire at opponent?	$\lambda_A < 30^\circ \text{ and } R < 914 \text{ m}$
8. Is opponent unable to fire at attacker?	$\lambda_O > 30^\circ \text{ or } R > 914 \text{ m}$
9. Are aircraft closing slowly?	$-91 \text{ m/sec} < \dot{R} < 0$
10. Is attacker deviation angle below 60°?	$\xi_A < 60^\circ$
11. Is attacker line-of-sight angle decreasing?	$\dot{\lambda}_A < 0^\circ/\text{sec}$

$914 \text{ m} = 3000 \text{ ft}$; $1524 \text{ m} = 5000 \text{ ft}$; and $-91 \text{ m/sec} = -300 \text{ ft/sec}$.

(U) For each simulated engagement the AML value was computed for each airplane every 0.5 sec and then averaged over the time of the engagement (3 min). Previous studies have shown that a difference of 1.0 in AML values indicates a definite aircraft superiority.

(U) The elevation component of the attacker's line-of-sight angle $\lambda_{A,e}$ is measured from the X-Y plane of his body axes to the opponent's center of gravity (positive upward). The deviation angle ξ is defined as the angle between an airplane's velocity vector and the line-of-sight vector to the opponent.

~~UNCLASSIFIED~~

[REDACTED] Missile Analysis (U)

(U) The pilot's ability to achieve a missile-launch opportunity and then to successfully launch the missile was analyzed by two methods.

[REDACTED] The first method employs a postflight computer program to determine missile-launch opportunities. The program compares the recorded trajectory information from the simulator with precalculated envelopes (launch acceptability regions) for the AIM-9G missile involving range, target deviation angle ξ_T , off-boresight angle, maximum tracking rate, altitude, Mach number, plus delays for sensor acquisition and lock-on. For example, the program requires that the attacker's line-of-sight angle λ_A be less than 30° for 3.5 sec for acquisition, and less than 20° for an additional 1.5 sec for lock-on before launch. If all the constraints are satisfied, the program assumes that the missile can be launched and will impact. Up to four launch opportunities are allowed per engagement for each airplane.

(U) The second method involves a subprogram in the real-time simulation program which "launches" and "flies" the AIM-9G missile when the pilot has a missile selected and pulls the trigger. In addition, the following cues are supplied in the DMS: (1) the pilot is given an aural tone whenever $\lambda_A < 20^\circ$, (2) the pilot in the target airplane sees a flashing light under the wing of the attacking airplane when the missile is in flight, and (3) the pilot in the attacking airplane sees a bright light superimposed on the target airplane on missile impact. Some of the current limitations of the on-line missile program are (1) only one missile can be in flight at a time; in a situation where both airplanes might employ missiles, the first pilot to pull the trigger would, in effect, lock out the opponent's ability to fire until after the missile completed its flight and (2) a missile is assumed to be successful (impact) if it closes to within 10 m (32.8 ft) of the target inasmuch as no calculations of weapons effects or vulnerability are made.

(U) Neither of the missile programs is completely realistic. Each has particular advantages and disadvantages. The postflight program includes time delays for sensor acquisition and lock-on but does not consider postlaunch maneuvers. The on-line program has simple time delays, but realistically flies the missile against the maneuvering target. Thus, the successful launches indicated by the two programs would not necessarily be the same, and a completely realistic program which included delays and postlaunch maneuvering plus sensor characteristics might show even fewer launches.

(U) Gun Analysis (U)

(U) Like the missile analysis, the pilot's ability to achieve a gun-firing opportunity was analyzed by two methods, that is, off-line in a postflight computer program, and on-line with bullet trajectories calculated in real time.

(U) The postflight program compared the recorded trajectories of the two airplanes to determine when an airplane was within a "gun zone," which is defined as (1) range less than 914 m (3000 ft), (2) line-of-sight angle λ_A less than 10° , and (3) opponent's line of sight angle λ_O greater than 120° . Time in

~~UNCLASSIFIED~~

gun zone was the total time the airplane satisfied ~~these~~ criteria. An airplane was assumed to have achieved a gun conversion when it was the first to reach this envelope. Probability of conversion was computed as the number of engagements in which a conversion occurred divided by total number of engagements (24). Time in gun zone was averaged over the number of engagements in which a gun conversion occurred.

(U) The on-line gun scoring was added to the real-time simulation to provide an alternate, and perhaps more realistic, scoring criteria. The DMS engagements often involved hard maneuvering at close range and high aspect angles (angle between velocity vectors). In such situations, the pilot would observe the predicted bullet trajectory on his heads-up display and then fire the gun so the target "flew through" the bullet stream rather than trying to maneuver to a tracking position. Most of the firings during the simulation occurred in high aspect angle and head-on situations. These "snap-shot" gun opportunities were not addressed by the off-line gun-zone criteria, which assumed an attack from a tail chase position.

(U) For DMS simulation, it is assumed that the airplane carries one gun, similar to the M61, with 500 rounds of ammunition. The only limitation on gun employment was that, if a pilot had fired a missile, his gun was locked out until the missile flight ended. Otherwise, both aircraft could fire guns at any time. It is assumed that when the pilot pulls the trigger, one "tracer" bullet is fired every 1/8 sec, with 9 bullets between each tracer, given 80 rounds/sec or 4800 rounds/min firing rate. Firing rate buildup is not modeled. The choice of 8 tracers/sec was based on the computer frame rate (32 iterations/sec) and the available compute time. The position of up to 16 tracers is computed (so maximum flight time is 2 sec) and displayed on the pilots' heads-up display. As a tracer bullet reaches the target range, its single-shot probability of hit is computed based on its position with respect to the center of the targets's projected area, and then multiplied by 10 to obtain the expected number of hits in that 1/8-sec burst. Appendix E presents the equations used in the gun model simulation.

(U) On-line gun scoring included (1) number of runs in which the gun was fired, (2) total rounds fired, (3) number of runs in which a hit occurred, and (4) total number of hits in all engagements.

(U) SIMULATION PROCEDURE (U)

(U) Four sets of simulated engagements were flown, in the following order:

- (1) Basic F-15 versus basic F-15 (equal airplanes)
- (2) Basic F-15 versus F-15 with two-dimensional nozzle, using automatic thrust-vectoring control
- (3) Basic F-15 versus F-15 with two-dimensional nozzle, using manual thrust-vectoring control

~~UNCLASSIFIED~~

(4) Basic F-15 versus F-15 with two-dimensional nozzle, using thrust reversing but without thrust vectoring

(U) For the study it was assumed that both airplanes carried two AIM-9 missiles and a gun. Engagements started with the airplanes head-on with a separation of 2 n. mi. at an altitude of 4572 m (15 000 ft) and a Mach number of 0.9. The ground rules for the engagements were as follows:

(1) Both airplanes were to attempt to employ their weapons by using the best maneuvers for their airplane system.

(2) No weapons would be employed on the first pass.

(3) All engagements lasted 3 min. Any run which ended earlier because of impacting the ground was recorded but was not used for data.

(U) Four combat-qualified pilots participated in the study. In each set of engagements, each pilot flew two engagements against each of the other three pilots in each airplane, giving a total of 24 engagements per set. Before a set was flown, the pilots were briefed on the capabilities of the two simulated airplanes, using information like that in appendix B. Before taking data, the pilots were given as much time as they desired to develop maneuvers and to become familiar with the airplane. Generally, this required 1 to 4 hr per data set.

~~RESULTS~~ (U)

(U) In analyzing the results from the four sets of data, more emphasis is placed on TOA, probability of conversion, and AML values than on missile and gun results for three reasons. First, previous studies (refs. 14 and 15) have shown good correlation between TOA, probability of conversion, AML values, and pilot opinion. Second, the number of successful missile launches (either post-analysis or on-line impacts) have in some cases been inconsistent. A pilot might be able to achieve an offensive position at close range but be unable to successfully employ a missile. Third, gun results can also be inconsistent. The number of gun firings and bullet hits vary considerably from run to run, so a large number of runs might be required for gun data to be statistically stable.

(U) Despite the use of qualified pilots, large variations are sometimes seen in the results, particularly for more evenly matched airplanes. Past experience has indicated that a 50-percent or more difference in TOA is necessary to indicate a superior airplane configuration. A 2-to-1 or greater difference would indicate a definite superiority. A difference of 0.5 in AML value would indicate some advantage, with a difference of 1.0 or more showing definite superiority. However, the reader is cautioned that the use of the results as an absolute indication of airplane exchange ratios is not recommended.

ORIGINAL PAGE IS
OF POOR QUALITY

~~UNCLASSIFIED~~

[REDACTED]
[REDACTED]
Equal Airplanes (U)

[REDACTED] The first study conducted was a set of simulated engagements between two basic F-15 airplanes. Table 4 summarizes the results with each DMS cockpit treated as a separate airplane (denoted A and B).

[REDACTED]
TABLE 4.- RESULTS FOR EQUAL AIRPLANES (U)

Scoring criteria	A	B
Average TOA at 180 sec	35.9	40.4
Average AML value	5.2	5.3
Launch opportunities (off-line)	1	2
Missile launches (on-line)	4	10
Impacts (on-line)	1	2
Probability of conversion	5/24	8/24
Average time in gun zone, sec	9.0	11.6
Total rounds fired	5060	4170
Runs in which gunfire occurred	21	17
Total number of hits	66	27
Runs in which hits occurred	4	5

(C) The data in table 4 show that the airplane [REDACTED] were evenly matched. Only the number of bullet hits were substantially different, and that occurred because sphere A got 39 hits in one run.

[REDACTED]
Dissimilar Airplanes (U)

[REDACTED] Scoring criteria.- Tables 5 and 6 present the results of engagements between the simulated basic F-15 and the F-15 with nonaxisymmetric (two-dimensional) nozzle. The data in table 5 are for automatic thrust-vector control. Data in table 6 are for manual thrust-vector control. Both tables show an overwhelming superiority for the airplanes with the two-dimensional nozzle, despite its 4.3-percent-heavier weight. Some superiority had been anticipated based on results in reference 16 for a simulated airplane with 15° vectoring and a 2.9-percent weight increase and 30° vectoring with a 5.9-percent weight increase, but the extent of the superiority was somewhat surprising.

(U) Participating pilots were divided on their preference for manual or automatic thrust-vector control. The reasons cited for preferring manual control were that it gave the decision of using thrust vectoring to the pilot and the pilot could avoid thrust-reverser lockout by the flight control system. Reasons cited for preferring automatic control were that it provided improved aerodynamic performance and eliminated the work load of making manual control inputs. All the pilots agreed that it would take additional practice to become proficient with manual thrust-vector control.

TABLE 5.- RESULTS FOR BASIC F-15 VERSUS F-15 WITH
AUTOMATIC THRUST-VECTOR CONTROL (U)

Scoring criteria	Basic F-15	F-15 with 2D nozzle
Average TOA at 180 sec	9.7	112.0
Average AML value	3.9	6.9
Launch opportunities (off-line)	0	0
Missile launches (on-line)	0	22
Impacts (on-line)		8
Probability of conversion	0	24/24
Time in gun zone, sec	0.5	36.8
Total rounds fired	1150	6240
Runs in which gunfire occurred	13	24
Total number of hits	18	297
Runs in which hits occurred	3	12

TABLE 6.- RESULTS FOR BASIC F-15 VERSUS F-15 WITH MANUAL
THRUST-VECTOR CONTROL (U)

Scoring criteria	Basic F-15	F-15 with 2D nozzle
Average TOA at 180 sec	6.9	115.5
Average AML value	3.9	6.8
Launch opportunities (off-line)	0	10
Missile launches (on-line)	1	19
Impacts (on-line)	1	7
Probability of conversion	1/24	18/24
Time in gun zone, sec	0.5	35.2
Total rounds fired	3770	6460
Runs in which gunfire occurred	20	21
Total number of hits	44	506
Runs in which hits occurred	5	14

(C) Tables 5 and 6 indicate that the results were nearly the same with the two control modes. Table 5 shows a higher probability of conversion with automatic vectoring control, but the TOA and time in gun zone are essentially equal. The only significant difference in tables 5 and 6 is the number of AIM-9G missile-launch opportunities predicted by the off-line computer program. Ten launch opportunities (occurring in six runs) were predicted with manual vectoring, and

no launch opportunities were predicted with automatic vectoring. This suggests a difference in flight conditions in the two cases, so the flight conditions were examined in more detail.

Flight conditions. - The altitude, Mach number, turning radius, and range were averaged over 18-sec intervals (10 percent of run) during the simulated engagements, and the results are shown in figure 9. Average values during the intervals are plotted at the end of the interval in the figures. Turn radius corresponds to the theoretical horizontal turn radius at the airplane load factor a_n .

$$\text{Turn radius} = \frac{v^2}{g \sqrt{a_n^2 - 1}}$$

Both cases (manual thrust-vector control and automatic control) show the same altitude trends (fig. 9(a)), a gradual decrease in altitude as the pilot trades altitude for airspeed during the engagement. This is typical of the results from other DMS simulations.

The other three variables are considerably different between the two cases. Figure 9(b) shows two important results: (1) the modified airplane (with two-dimensional nozzle) was always slower than the basic airplane; (2) in the case of automatic thrust vectoring, the average Mach number was about 40 percent slower than in the case of manual thrust vectoring.

The tendency for the superior airplane to be slower has been seen in all of the ACM simulations in the DMS. This occurs because, in one-on-one combat, the best offensive position is also the least vulnerable position (i.e., behind the opponent). The superior airplane will be able to maneuver to a tail attack position, and then a slightly slower speed will enable it to stay there. A slightly lower speed also prevents an overshoot and possible loss of advantage, and it tends to shorten the turning radius. If the defender tries to exploit the attacker's slower speed by unloading and accelerating, he becomes vulnerable to a missile attack. To the extent possible, the "inferior" airplane (in this case, the basic F-15) will try to operate in a speed regime which minimizes the opponent's advantage.

Pilots were not told the strategy or tactics to use in the DMS. These evolved from initial briefings on the capabilities and differences of the two airplanes, using data such as figures 3 to 8, and from familiarization and practice engagements flown prior to collecting data.

The slow speeds in engagements involving automatic thrust vectoring (fig. 9(b)) were probably not as much a "strategy" as a result of the modified airplane's clear superiority. It could turn quicker (because of higher maximum lift) and more efficiently (because of its better drag polar) and soon reached a position behind the defender. As the defender pulled near maximum g to turn rapidly in trying to evade, the speed decreased rapidly. The very low speeds helped the defender in two ways. First, at slow speeds the maximum

vector angle was automatically limited to keep the pitching moment within the canard trim capability. This reduced the attacker's lift and turn-rate advantage, as shown in figure 3, thereby slowing the attacker's rate of improvement. Second, as the speed decreased, the turn radius (fig. 9(c)) and range (fig. 9(d)) decreased also. At the very short range, it was more difficult to hold a sensor lock-on and track long enough to satisfy the pilot delay time plus launch delay time that is built into the off-line missile program. This may account for the lack of missile-launch opportunities in table 5. Only the arming delay had to be satisfied in the on-line missile program, and some on-line launches were successful.

Engagements with manual thrust-vector control were flown after obtaining data for automatic control, and the defender employed a considerably different strategy, as indicated by the differences in speed and range in figures 9(b) and 9(d). The strategy employed by the basic F-15 flying against the manual thrust-vectoring airplane was to keep the speed up, make head-on passes (employing guns where feasible), unload (release g) and accelerate after passing, then turn back for another head-on pass. This accounted for the higher speed engagements with manual control (fig. 9(b)). Several considerations may have been involved in adopting this strategy: it was tactically sound, it gave the defender a little more offensive potential, and it was more fun to fly.

In the automatic thrust-vector mode, only positive vector angles (causing positive a_n) were commanded; but in the manual mode, the pilot could command either positive or negative vector angles (fig. C10). However, in familiarization flights, the pilots found no benefits from negative vectoring, so they used $\theta_j \geq 0$. Manual thrust-vector control was used in an on/off manner - on at high α to make a quicker turn, and off at low α to minimize drag. Without vectoring, the modified airplane had essentially the same drag polar as the basic airplane but poorer acceleration because of its increased weight. The strategy adopted by the defender was that employed against an opponent having superior turning capability but inferior acceleration. And it worked reasonably well. It took longer for the attacker to reach the gun conversion position (not achieved in six runs). However, the number of off-line missile-launch opportunities were substantial for the modified airplane because of the longer ranges (fig. 9(d)).

With more time spent in head-on and high aspect angle passes, there were more opportunities for the defender to use his gun. All of the basic F-15 bullet hits (44) occurred during high aspect angle passes. This accounts for the tripling of the number of rounds fired by the basic F-15 in table 6 as compared with table 5. However, table 6 shows that the modified airplane achieved more hits in more runs with fewer rounds fired than in the previous data set (table 5).

Speed-brake/thrust-reverser usage. - Thrust-reverser and speed-brake use in engagements involving automatic or manual thrust-vector control is summarized in tables 7 and 8 for conditions in which the airplane was offensive (in a position to accumulate TOA), defensive (opponent accumulating TOA), or neutral. Flying the airplane with manual thrust-vector control (table 8), pilots decelerated 2 to 3 times more often than when flying the other simulated airplane. Actually, manual thrust-vector control was the only situation which

~~UNCLASSIFIED~~

(U) TABLE 7.- SPEED-BRAKE AND THRUST-REVERSER USE IN ENGAGEMENTS
INVOLVING AUTOMATIC THRUST-VECTOR CONTROL (U)

Airplane position	Basic F-15 (speed brake)			Automatic thrust vector with IFTR		
	Offensive	Neutral	Defensive	Offensive	Neutral	Defensive
Uses	5	11	11	5	8	0
Time of employment - Average, sec	67.4	11.7	115.7	143.6	12.6	
Standard deviation, sec	19.2	21.4	36.7	25.0	24.4	
Duration - Average, sec	2.9	5.4	3.0	7.0	9.3	
Standard deviation, sec	1.0	3.4	1.4	5.5	5.6	

(U) TABLE 8.- SPEED-BRAKE AND THRUST-REVERSER USE IN ENGAGEMENTS
INVOLVING MANUAL THRUST-VECTOR CONTROL (U)

Airplane position	Basic F-15 (speed brake)			Manual vector with IFTR		
	Offensive	Neutral	Defensive	Offensive	Neutral	Defensive
Uses	0	10	10	36	31	4
Time of employment - Average, sec		22.7	93.7	105.8	30.8	85.3
Standard deviation, sec		34.7	48.1	45.5	35.9	60.3
Duration - Average, sec		4.7	3.6	5.1	5.5	7.5
Standard deviation, sec		2.3	1.6	3.6	2.7	1.8

enabled the pilot to use thrust reversing as much as desired. When pilots [REDACTED] the basic F-15 and the F-15 with automatic thrust-vector control, they complained that they would command the speed brake or IFTR, but nothing would happen. This occurred because the simulated flight control system restricted the use of the deceleration devices. The flight control system retracted the speed brake whenever α exceeded 15° , as indicated in figure C9. The flight control system also gave priority to thrust vectoring over thrust reversing. In the automatic vectoring mode, the vector angle was commanded as

$$\theta_j = \alpha - 5^\circ \quad (\alpha > 5^\circ)$$

Thus, the pilot could only employ IFTR when $\alpha \leq 5^\circ$. With manual thrust-vector control, the pilot could command $\theta_j = 0^\circ$ and then deploy IFTR at any time. After discussions, the pilots agreed that the vectoring-over-reversing priority was reasonable, particularly since the airplane tends to decelerate when the thrust is deflected. However, they questioned the desirability of limiting speed-brake deployment to $\alpha < 15^\circ$. The $\alpha = 15^\circ$ deployment limit was based on information available at the time the simulation was conducted. In 1979, U.S. Air Force F-15's could deploy the speed brake up to $\alpha = 25^\circ$.

(U) In order to investigate the effect of having only thrust reversing, another set of engagements was flown with the modified airplane having $\theta_j \equiv 0$. Results of these engagements are presented in a later section. The flight conditions at the time of speed-brake/thrust-reverser deployment were examined to see if the pilot's reason for slowing down could be determined.

(U) From a defensive position, a likely reason for wanting to slow down rapidly is to cause the attacker to overshoot and lose his advantage. However, few overshoots occurred during SB/IFTR deployment, and no trends were apparent in the data.

(C) Deceleration from neutral conditions occurred early in the engagement. Pilots frequently decelerated from the initial airspeed ($M = 0.9$) to obtain a higher instantaneous turn rate near the corner velocity (fig. 3). Generally, neutral conditions only occurred early in the engagements because the modified airplane was soon able to convert to an offensive position, as indicated by the large TOA in tables 5 and 6.

(C) A trend was seen in the data for decelerations in offensive situations. Figure 10 shows R/R and the attacker's Mach number at the start and the end of IFTR/SB employment plotted against the range R at the start of the employment. The figure contains data for both the basic and the modified airplanes in offensive situations. Figure 10 shows that most of the TR/SB employments occurred at ranges less than 500 m (1640 ft). At these short ranges the speeds were already slow (generally less than $M = 0.6$), so the deceleration was not used just to slow down. Apparently, it was used to control closure rate and prevent overshooting the target. At ranges less than 300 m, the value of R was generally positive at the end of the TR/SB employment, indicating separation between the vehicles. This suggests that the pilot may have decelerated until he began to see the target recede.

Thus, even at relatively slow speeds there were still situations in which deceleration was desirable. At slow speeds, thrust reversing would be more effective than a speed brake, as shown in figure 8. Since DMS engagements tend to reach these conditions, thrust reversing alone, without thrust vectoring, might provide an advantage. This was investigated in a set of engagements described in the following section.

Thrust reversing without vectoring. - The modified airplane flown in the fourth set of engagements was the same as flown in previous engagements, except that thrust vectoring was disabled. That is, the modified airplane was 607 kg heavier than the basic F-15 and had IFTR instead of a speed brake.

Table 9 summarizes the results of the simulated engagements. The missile and gun criteria indicate that the airplanes were evenly matched. The TOA and AML values indicate a slight superiority of the airplane with IFTR. The advantage afforded by IFTR apparently offsets the disadvantage of the increased weight.

TABLE 9.- RESULTS FOR BASIC F-15 VERSUS F-15 WITH THRUST REVERSER (U)

Scoring criteria	Basic F-15	F-15 with IFTR
Average TOA at 180 sec	37.0	53.7
Average AML value at 180 sec	5.1	5.5
Launch opportunities (off-line)	0	0
Missile launches (on-line)	6	7
Impacts (on-line)	1	1
Probability of conversion	8/24	6/24
Time in gun zone, sec	8.3	23.5
Total rounds fired	3760	3720
Runs in which gunfire occurred	19	20
Total number of hits	62	43
Runs in which hits occurred	5	5

Table 10 summarizes the IFTR and speed-brake usage for the two airplanes. Like the results for manual thrust-vector control (table 8), there were about three times as many IFTR deployments as speed-brake deployments. As noted earlier, the simulated flight-control-system limit prevented speed-brake use above $\alpha = 15^\circ$. This was a disadvantage for the basic F-15, but its effect is uncertain. Table 10 shows a different distribution than table 8 of IFTR/SB deployments in offensive, neutral, and defensive positions. This appears consistent with the trends of the engagements - considerable time on offense with thrust vectoring (table 8), and considerable time in a neutral position with IFTR alone (table 10).

TABLE 10.- SPEED-BRAKE AND THRUST-REVERSER USE IN
ENGAGEMENTS WITHOUT THRUST VECTORING (U)

Airplane position	Basic F-15 with speed brake			Modified F-15 with IFTR		
	Offensive	Neutral	Defensive	Offensive	Neutral	Defensive
Uses	13	16	4	14	52	31
Time of use - Average, sec	96.7	46.1	71.1	111.9	58.5	114.3
Standard deviation, sec	25.1	39.8	34.4	31.2	48.0	33.3
Duration - Average, sec	4.2	4.6	2.0	5.6	5.9	7.1
Standard deviation, sec	2.3	2.4	1.5	2.6	2.7	5.0

(U) Participating pilots commented that they liked the capability provided by in-flight thrust reversing (i.e., the ability to decelerate quickly to prevent an overshoot if on offense, or to cause an overshoot if on defense). However, they were reluctant to accept a weight increase to obtain this capability. The general feeling was that IFTR (without vectoring) would be nice to have if it did not cost too much.

CONCLUDING REMARKS (U)

(U) Simulated one-on-one air-combat engagements between a basic F-15 and an F-15 with a nonaxisymmetric (two-dimensional) nozzle have been conducted on the Langley Differential Maneuvering Simulator. The simulated nonaxisymmetric nozzle was assumed to provide up to $\pm 15^\circ$ vectored thrust to augment the lift generated by the wing and to provide in-flight thrust reversing for deceleration. Three sets of engagements were flown - manual thrust-vector control, automatic thrust-vector control through an angle-of-attack schedule, and thrust reversing only (no thrust vectoring capability).

(U) Results showed that the modified airplane with thrust-vectoring capability was clearly superior to the basic airplane, despite being considerably heavier. No significant difference was seen in the results for manual or automatic thrust-vector control. Pilots were divided on their preference for manual or automatic thrust-vector control. However, all pilots agreed that it would take additional practice to become proficient with manual control.

(U) The simulated flight control system assumed a vectoring-over-reversing priority, which prevented in-flight thrust reversing when thrust vectoring was used. This restricted thrust-reverser deployment in the automatic vectoring mode because vectoring was commanded above an angle of attack of 5°. This was partially compensated for by a flight-control-system limit in the basic airplane that prevented speed-brake deployment above an angle of attack of 15°. Pilots agreed that the vectoring/reversing logic was probably reasonable, but they objected to the speed-brake limit in the simulator. (This limit is not applicable to current inventory F-15's.)

Results of engagements in which the modified airplane had thrust-reversing but not thrust-vectoring capability showed that the basic and modified airplanes were evenly matched. The advantage afforded by the in-flight thrust reverser apparently offset the disadvantage of its heavier weight. Thrust reversing provided rapid deceleration, particularly at low speeds where the speed brake lost effectiveness. The general feeling of the pilots was that thrust reversing (without vectoring) would be nice to have if it did not cost too much.

From neutral starting conditions (a Mach number of 0.9 and a range of 4572 m (15 000 ft)), engagements tended to decrease in energy to low altitude and low speed. Despite this trend, the thrust reverser and speed brake were used in many engagements, often by the attacker at short ranges to reduce closer rate and prevent overshooting the target.

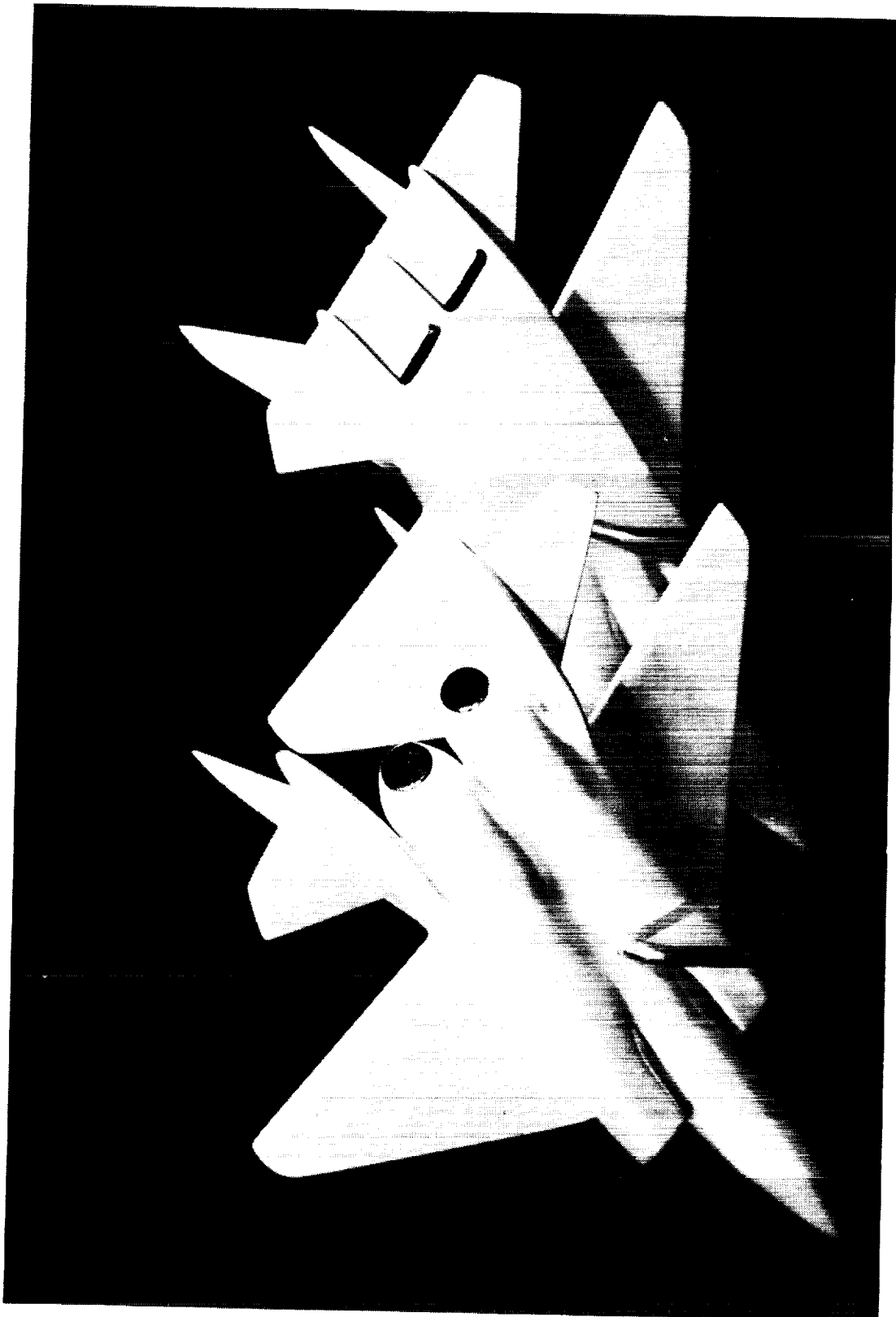
(U) The simulation assumed that the modified airplane had a canard which automatically countered the pitching moment generated by thrust vectoring. To provide an adequate restoring moment, a relatively large canard was required, which was about 12 percent of the wing area. Canard sizing and effectiveness would be important considerations in designing a flight vehicle having thrust-vectoring capability.

(U) Another important assumption in the study was that thrust vectoring and reversing did not affect the stability characteristics of the F-15. Limited wind-tunnel tests on other configurations have shown that thrust vectoring/reversing can reduce the effectiveness of the rudder/horizontal tail unless carefully integrated. Such effects should be determined and studied prior to any flight tests.

Langley Research Center
National Aeronautics and Space Administration
Hampton, VA 23665
March 31, 1980

ORIGINAL PAGE IS
OF POOR QUALITY

UNCLASSIFIED

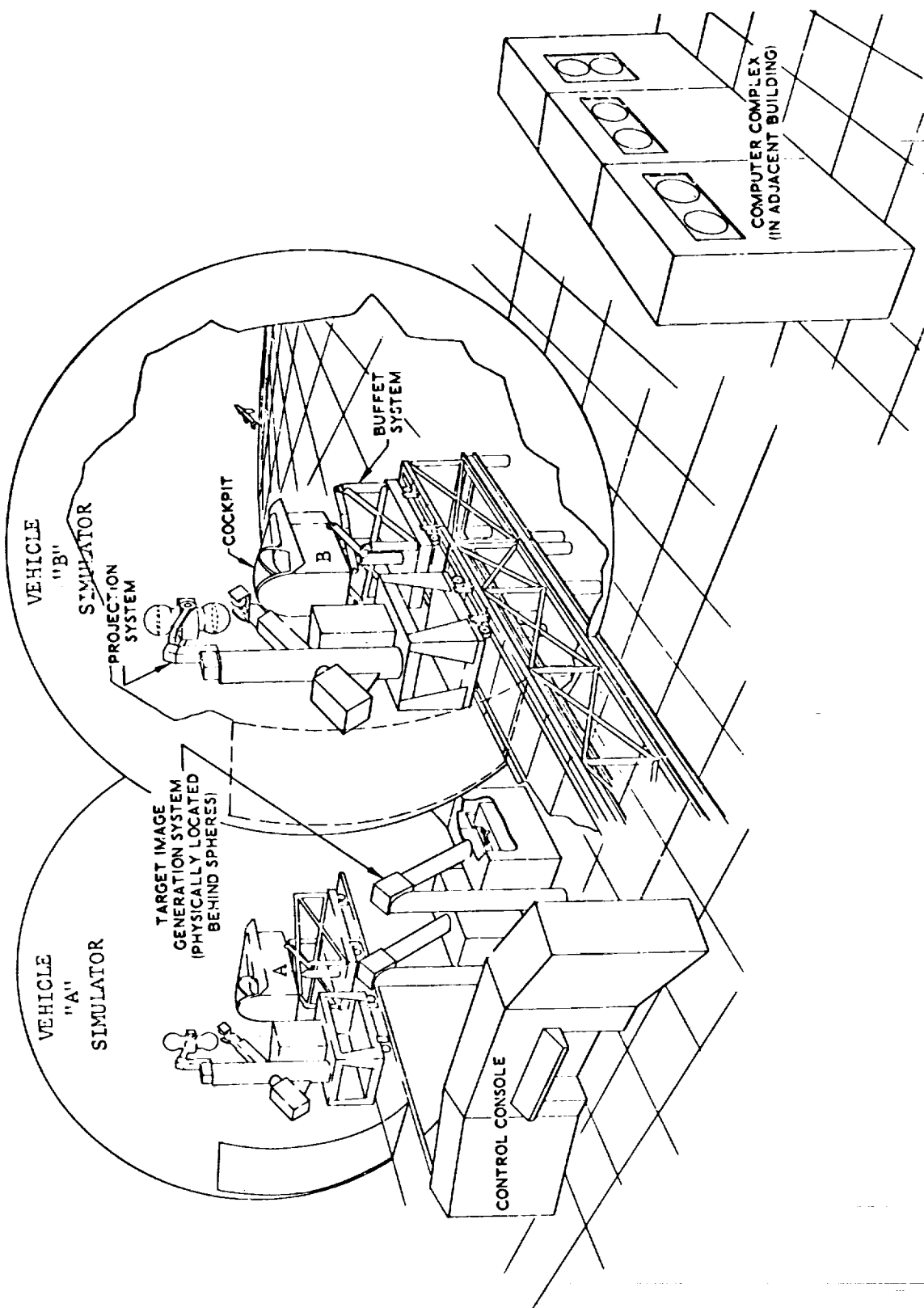


(U) Figure 1.- Twin axisymmetric and two-dimensional nozzle concepts. (U) L-74-3694

UNCLASSIFIED

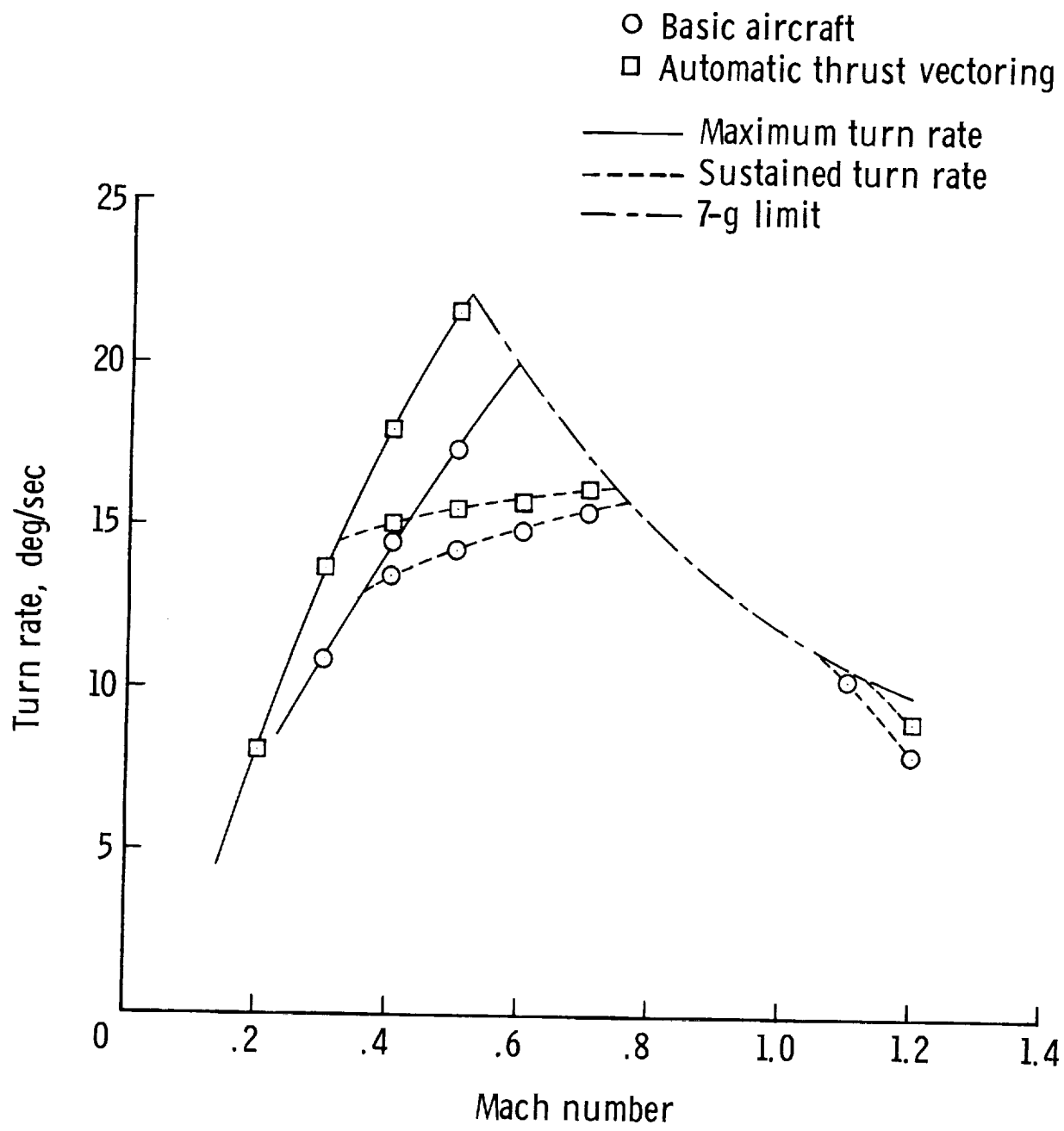
ORIGINAL PAGE IS
OF POOR QUALITY

UNCLASSIFIED



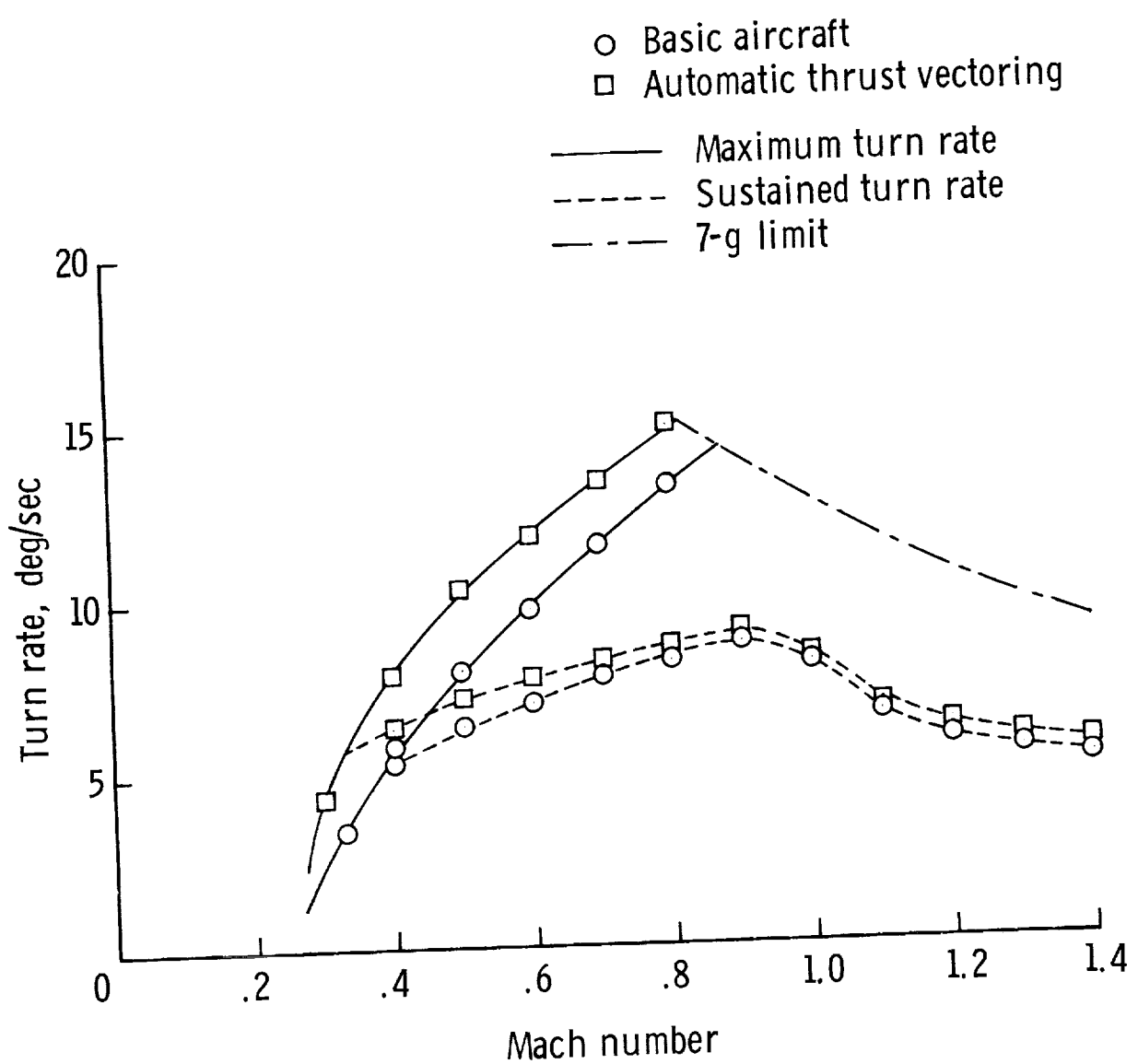
(U) Figure 2.- Differential maneuvering simulator. (U)

UNCLASSIFIED



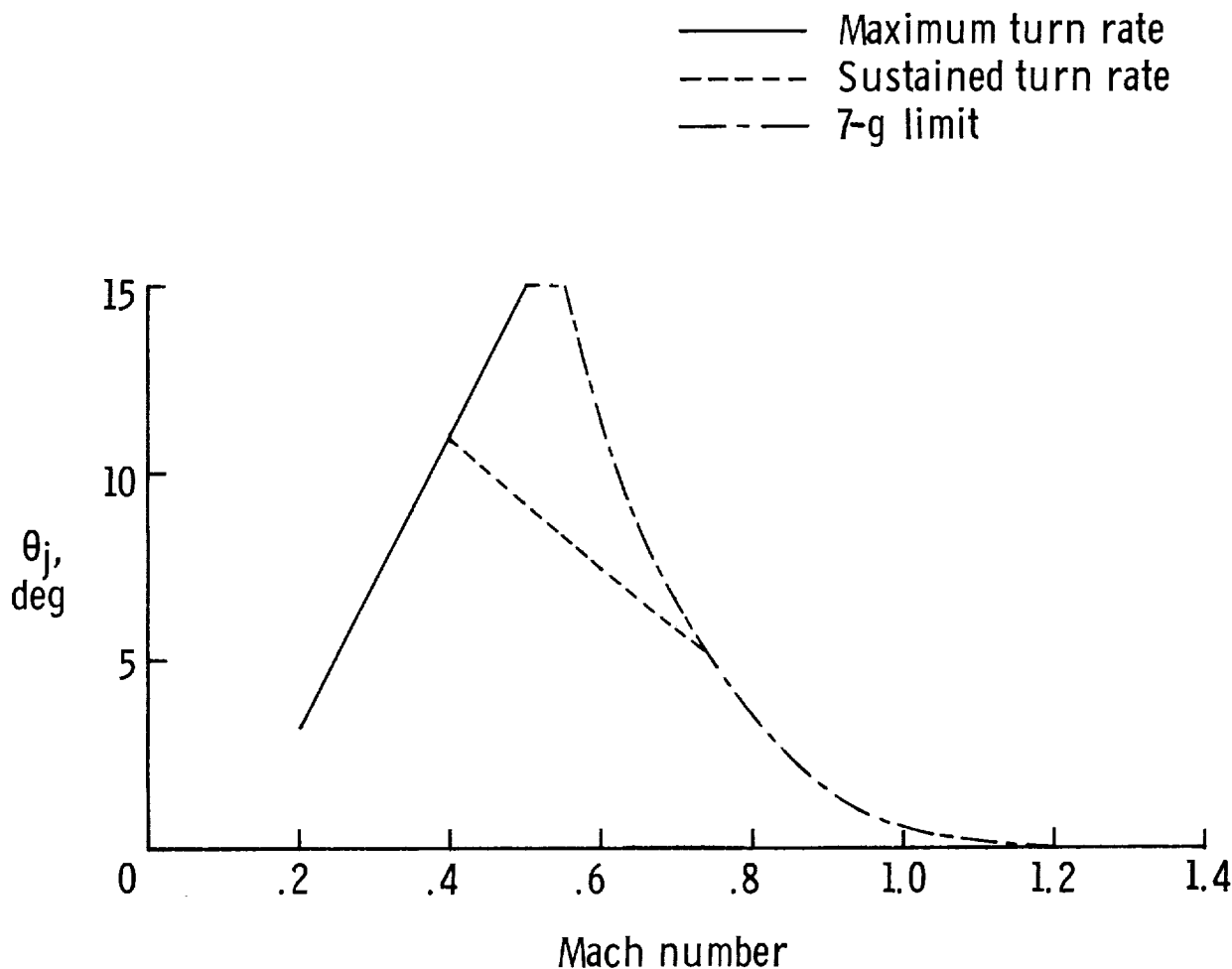
(a) $h = 3048 \text{ m (10 000 ft)}$.

Figure 3.- Turn-rate comparison. (U)



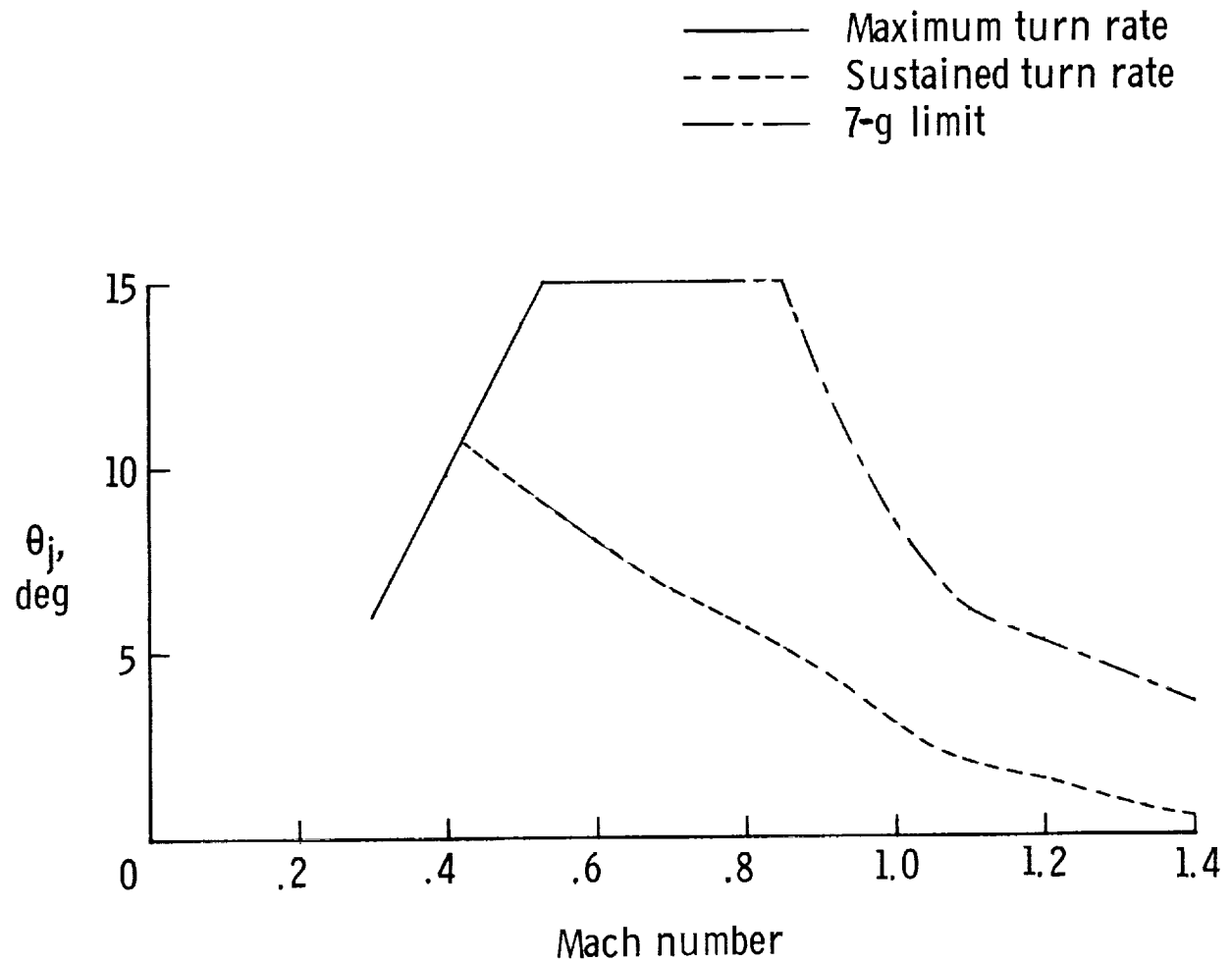
(b) $h = 9144 \text{ m} (30000 \text{ ft})$.

(C) Figure 3.- Concluded. (U)



(a) $h = 3048 \text{ m (10 000 ft)}$.

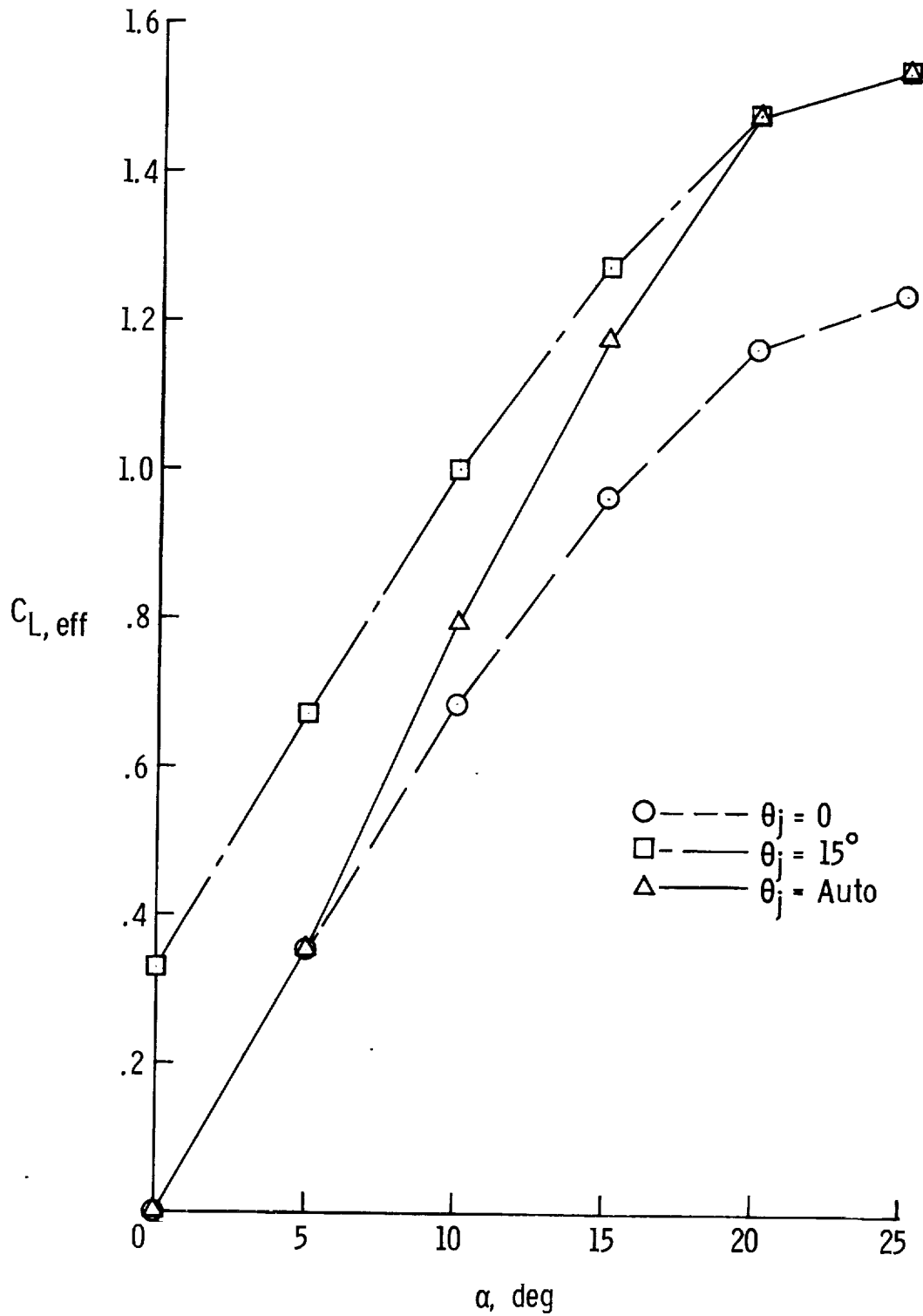
Figure 4.- Thrust-vector angle corresponding to maximum and sustained turn rates. (U)



(b) $h = 9144 \text{ m} (30,000 \text{ ft})$.

(C) Figure 4.- Concluded. (U)

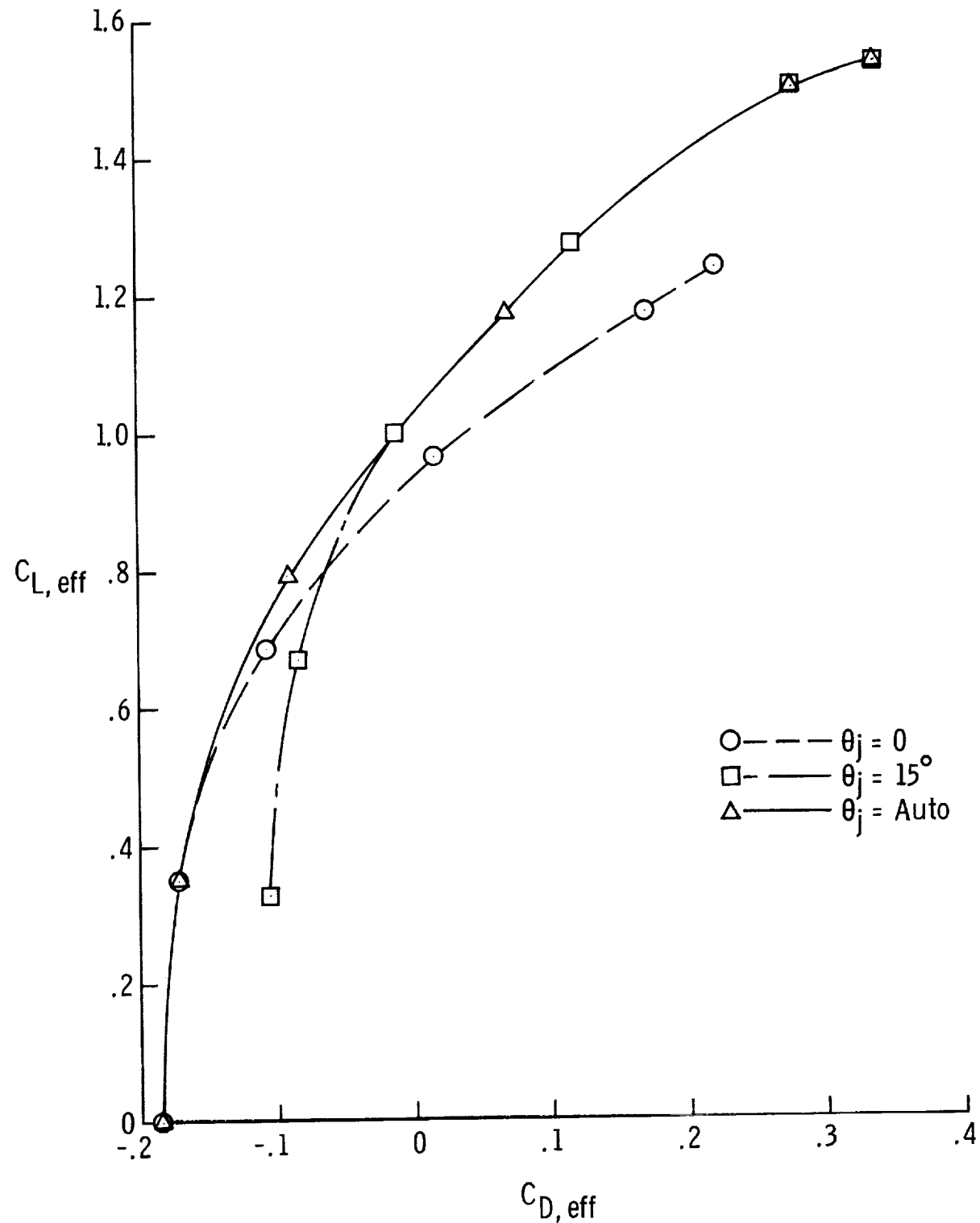
UNCLASSIFIED



(U) Figure 5.- Modified F-15 lift capability at $M = 0.6$ and altitude of 9144 m (30 000 ft). (U)

UNCLASSIFIED

UNCLASSIFIED



(U) Figure 6.- Modified F-15 drag polar at $M = 0.6$ and altitude of 9144 m (30 000 ft). (U)

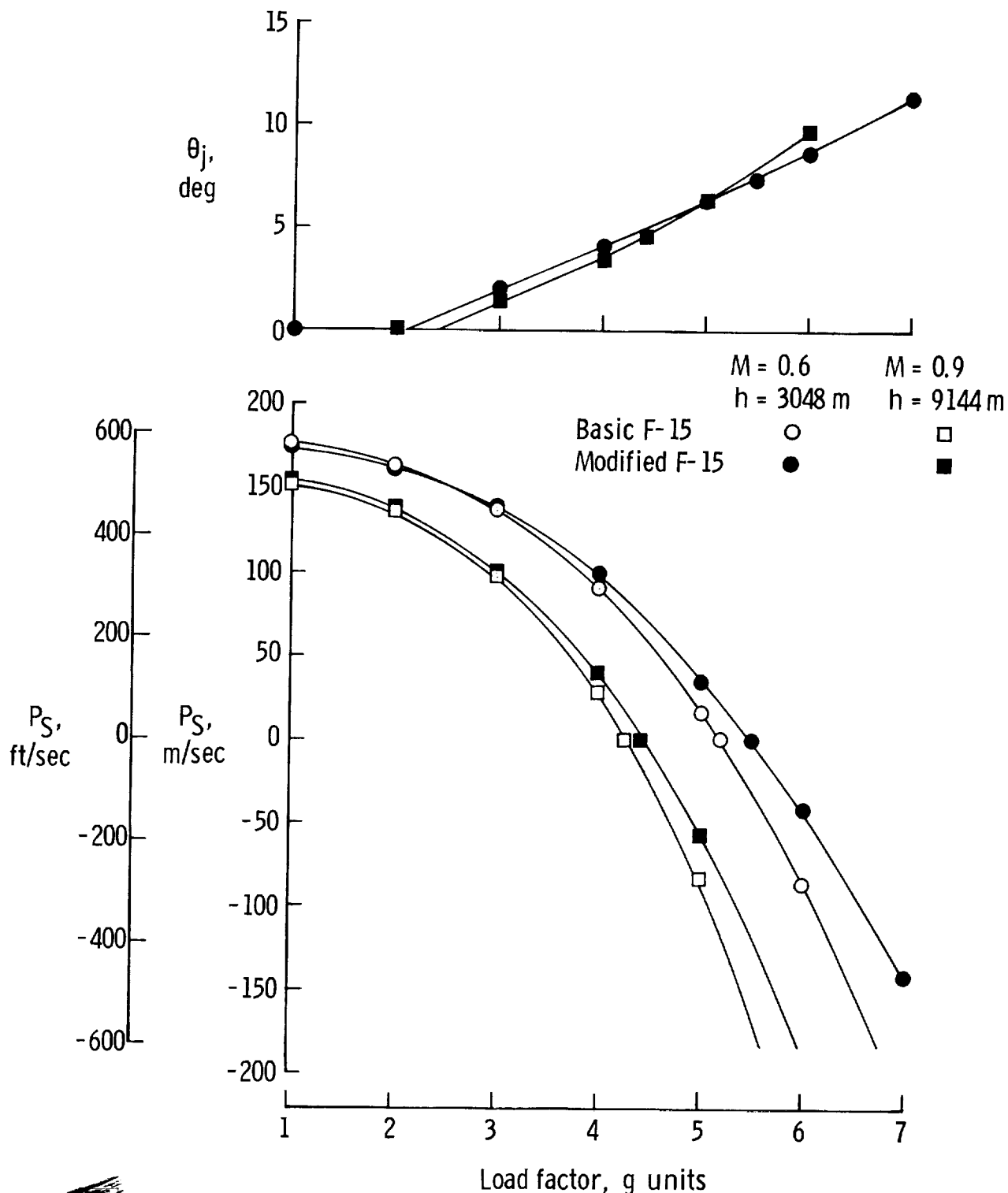
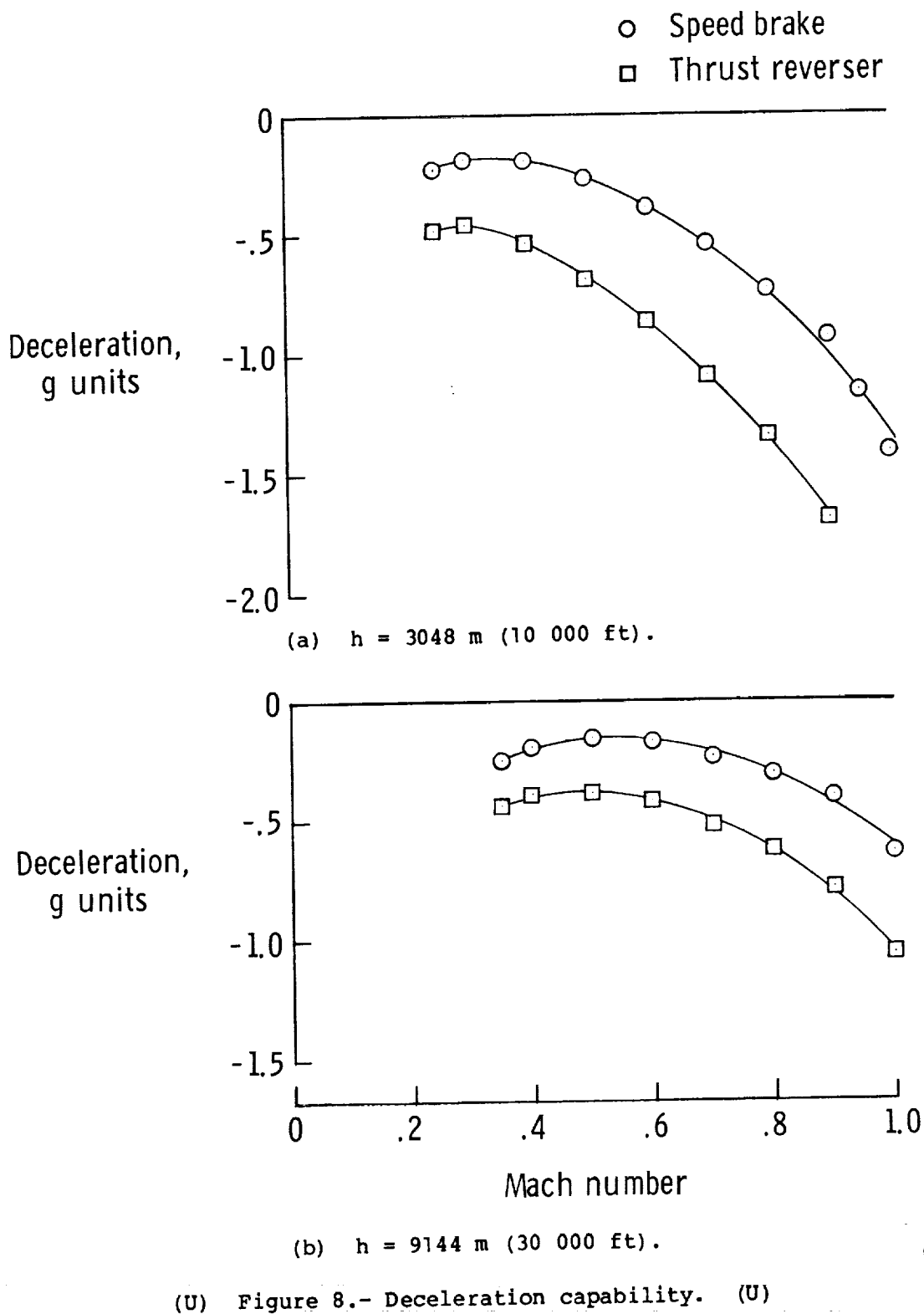
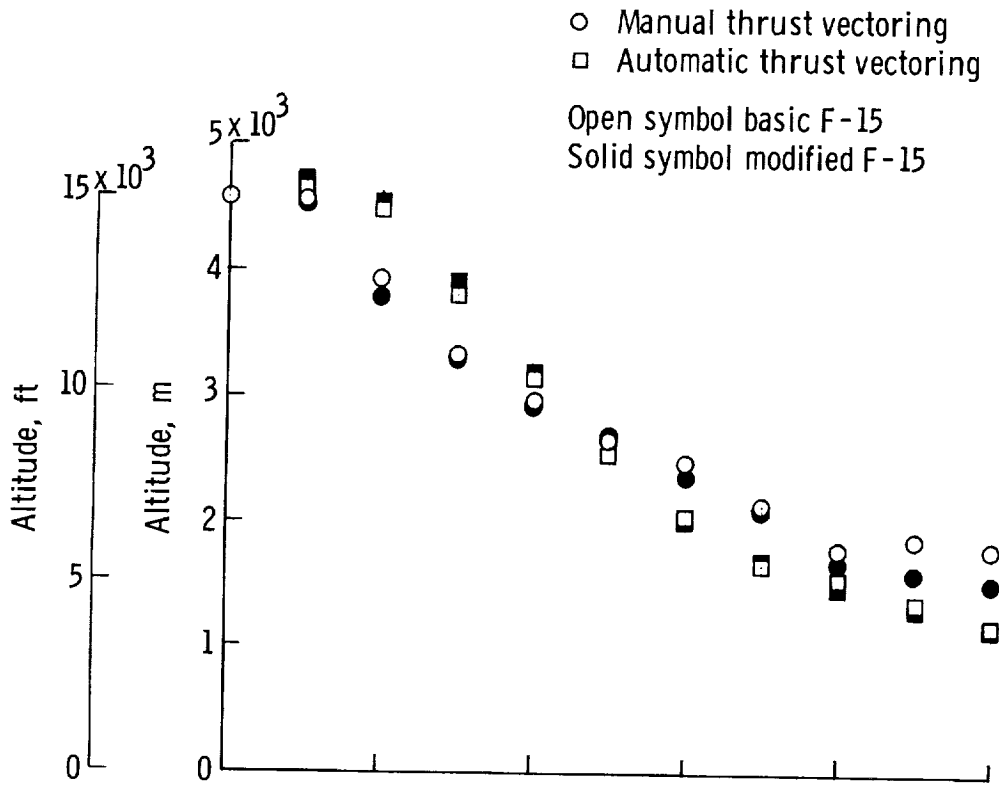


Figure 7.- Specific excess power and thrust-vector angle for basic F-15 and F-15 with automatic thrust vectoring. (U)

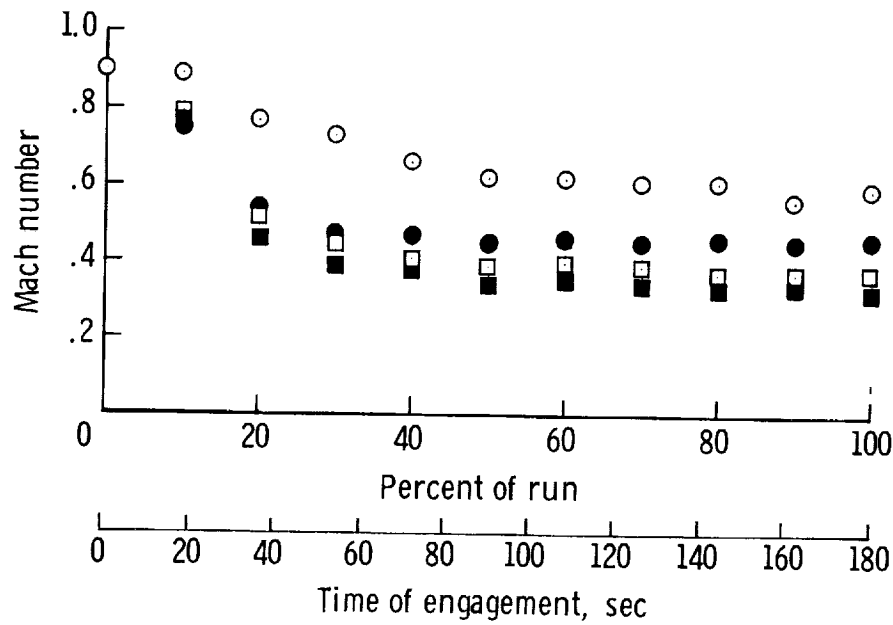
~~UNCLASSIFIED~~



~~UNCLASSIFIED~~



(a) Altitude.



(b) Average Mach number.

Figure 9.- Average flight conditions in engagements between basic and modified F-15. (U)

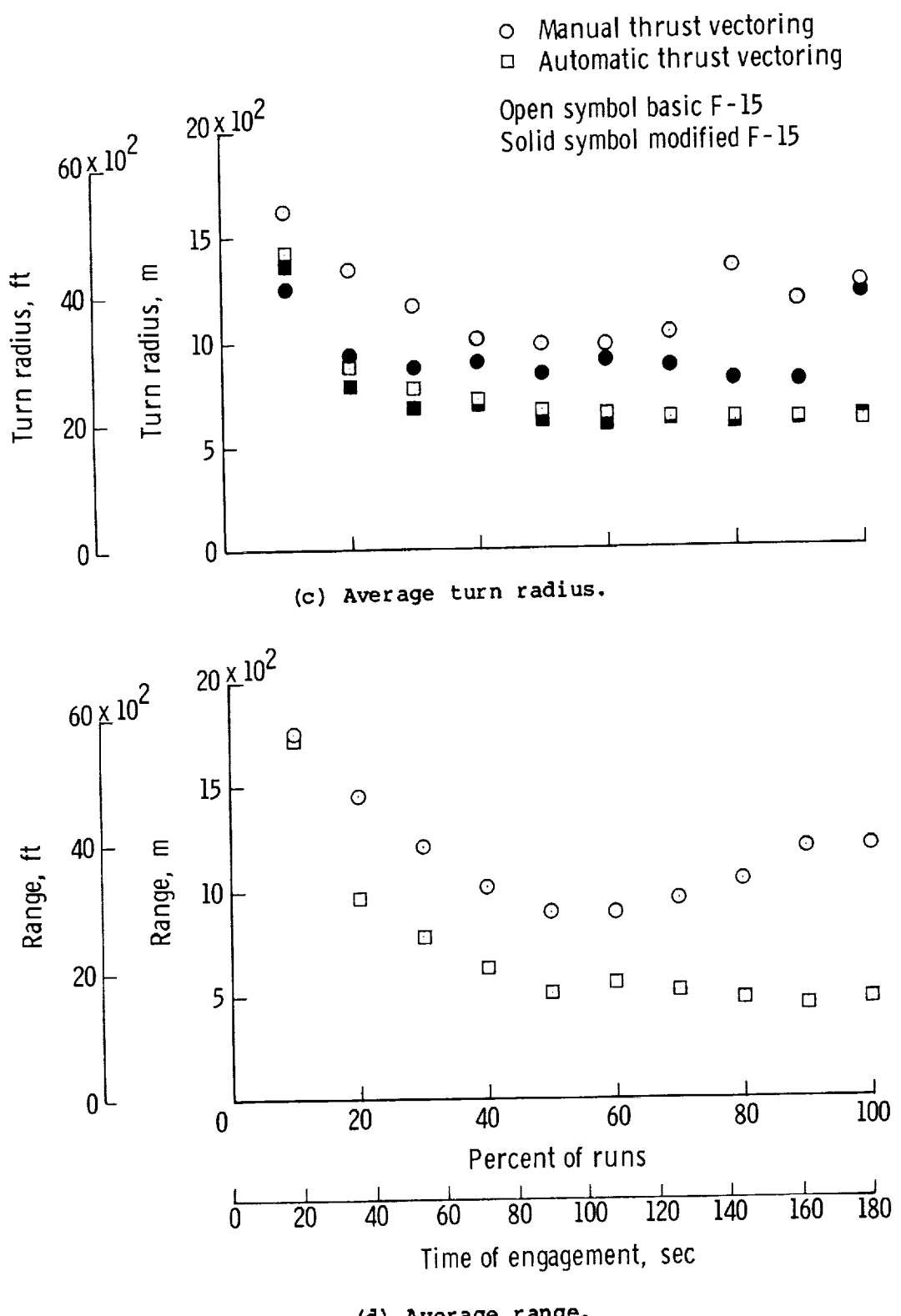
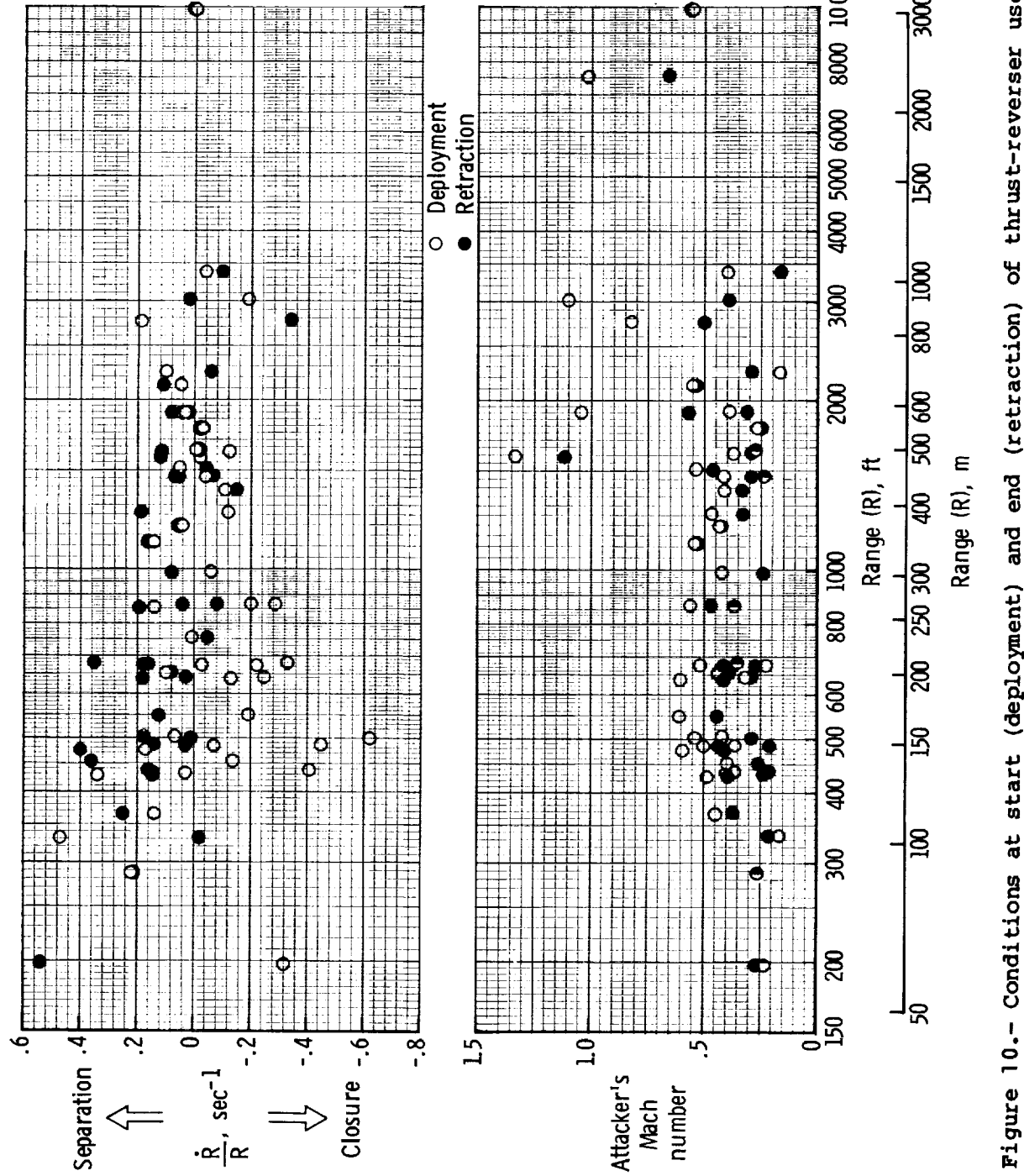


Figure 9.- Concluded. (U)



(C) Figure 10.— Conditions at start (deployment) and end (retraction) of thrust-reverser use. (U)

~~UNCLASSIFIED~~

APPENDIX A

(U) SIMULATION OF BLACKOUT (U)

(U) Pilot blackout or "grayout" under sustained high values of normal acceleration was simulated in the Langley Differential Maneuvering Simulator by decreasing the brightness of the projected scene and the cockpit instruments as a function of the cumulative time spent at high load factors. At the same time, dimming of the target image was delayed relative to the projected scene in order to partially simulate tunnel vision for steady tracking maneuvers. This simulation of blackout provided a cue, in addition to the inflatable g-suit, of the extent of operation at high normal accelerations, and it penalized the pilot who flew at unrealistically high load factors. The blackout representation assumed that a pilot will experience grayout if exposed to a value of normal acceleration greater than 7g and will tend to recover when returning to below this level. The 7g threshold was chosen as representing high-g cockpit capability; earlier simulations involving F-4 airplanes used a 5g threshold.

(U) The visual-scale brightness varied linearly with the variable K_{BO} , with full brightness at $K_{BO} = 0$ and complete blackout at $K_{BO} \geq 1$. The variable K_{BO} was computed as

$$K_{BO} = \int \dot{K}_{BO} dt \quad \text{and} \quad K_{BO} \geq 0$$

$$\dot{K}_{BO} = \left(\frac{1}{300} \right) \left(\frac{a_n}{7} \right)^{7.525} \quad (a_n \geq 7)$$

$$\dot{K}_{BO} = \frac{-2}{(a_n - 2)} \quad (3 < a_n < 7)$$

$$\dot{K}_{BO} = -2 \quad (a_n \leq 3)$$

This resulted in 300 sec to blackout at 7g and 10 sec to blackout at 11g, with very rapid recovery at low load factors.

UNCLASSIFIED

APPENDIX B

EQUATIONS OF MOTION, THRUST, AND AERODYNAMIC DATA**FOR F-15 SIMULATION (U)**

Fred L. Biessner, Jr.
Kentron International, Inc.

(U) This appendix presents the equations of motion, aerodynamic data, and engine data used to simulate the basic F-15 on the Langley Differential Maneuvering Simulator (DMS). Also included are the assumptions, equations, and data required to modify the basic F-15 simulation to represent the installation of two-dimensional convergent-divergent (C-D) nozzles in place of the standard axisymmetric (round) nozzles. Other changes required to support this modification include the installation of a canard and ballast. These modifications as applied in this simulation are discussed in a later section.

(U) Simulation of Basic F-15 (U)

(U) The F-15A airplane simulated is a single-place, twin-engine, high-performance fighter airplane. Physical data for the F-15 are given in table 1. The following sections describe the simulation of the basic F-15.

(U) Equations of Motion (U)

(U) The aircraft is programmed for the DMS using nonlinear six-degree-of-freedom rigid body equations of motion (refs. 17 and 18) referenced to the body axis system.

$$\dot{I_{XX}P} = (r + pq) I_{XZ} + qr(I_{YY} - I_{ZZ}) + \bar{q}SbC_\ell$$

$$\dot{I_{YY}q} = (r^2 - p^2) I_{XZ} + pr(I_{ZZ} - I_{XX}) + \bar{q}Sc\bar{C}_m$$

$$\dot{I_{ZZ}r} = (p - qr) I_{XZ} + pq(I_{XX} - I_{YY}) + \bar{q}SbC_n$$

$$\dot{u} = rv - qw + C_{13}g + \frac{\bar{q}}{m} \bar{S} C_{X,b}$$

$$\dot{v} = pw - ru + C_{23}g + \frac{\bar{q}}{m} \bar{S} C_{Y,b}$$

$$\dot{w} = qu - pv + C_{33}g + \frac{\bar{q}}{m} \bar{S} C_{Z,b}$$

UNCLASSIFIED

UNCLASSIFIED

APPENDIX B

The direction cosines C_{ij} were computed using quaternions, as described in reference 19.

(U) The aerodynamic force coefficients were transformed from the stability axis system to the body axis system by

$$\begin{Bmatrix} C_{X,b} \\ C_{Y,b} \\ C_{Z,b} \end{Bmatrix} = \begin{vmatrix} \cos \alpha & 0 & -\sin \alpha \\ 0 & 1 & 0 \\ \sin \alpha & 0 & \cos \alpha \end{vmatrix} \begin{Bmatrix} C_{X,stab} \\ C_{Y,stab} \\ C_{Z,stab} \end{Bmatrix}$$

The auxiliary equations included

$$\alpha = \tan^{-1} (w/u)$$

$$\beta = \sin^{-1} (v/V)$$

$$V = \sqrt{u^2 + v^2 + w^2}$$

$$a_n = \frac{\bar{q}SC_{Z,b}}{mg}$$

$$a_y = \frac{\bar{q}SC_{Y,b}}{mg}$$

(U) Data Format (U)

(U) The aerodynamic and propulsion data used to simulate the F-15 airplane were defined in tabular form as functions of up to three of the following independent variables: Mach number, angle of attack, horizontal-tail deflection, lift coefficient, angle of sideslip, rudder deflection, altitude, and power-lever angle. Data at any specific flight condition were obtained by one-, two-, or three-dimensional linear interpolation. If the simulated airplane operated beyond the data range, the computer program would not extrapolate but would use the closest stored data point.

(U) Data were programmed for $M \leq 1.6$, despite the greater speed capability of the F-15. Past experience has shown that in the DMS simulation of one-on-one visual air combat, pilots maneuver aggressively and frequently exceed the maximum sustained turn rate, resulting in subsonic and only low supersonic speeds.

APPENDIX B

(U) Table B1 summarizes the functional dependence of the aerodynamic and engine variables used in the simulation.

Modifications For Two-Dimensional C-D Nozzle Simulation (U)

(U) The modifications to the F-15A that are incorporated for simulation of the two-dimensional C-D nozzle on the DMS are the result of a joint NASA/U.S. Air Force/industry study reported in references 9 and 10. Several nonaxisymmetric candidate nozzles were considered and the two-dimensional C-D nozzle was selected for simulation on the DMS. Some alterations and additional assumptions were identified as necessary as modeling progressed. The complete modification is discussed in the following sections.

(U) In addition to the desired forces obtained by deflecting the thrust with the two-dimensional nozzles, there is a substantial pitching moment to be addressed. The method chosen to control the pitching moment was with a canard.

(U) For purposes of this simulation, the canard was used only to trim out (by opposing) the pitching moment due to the deflected thrust (including induced effects). To better utilize the thrust-vectoring feature in ACM, it was found necessary to increase the size of the canard substantially over the size featured in reference 9. Wing-canard interactions were not addressed, nor were possible secondary effects due to deflecting thrust (such as changes in control effectiveness).

(C) The nozzle changes plus the addition of the canard contribute to substantial changes in the mass properties. When ballasting is included to maintain the center of gravity in the same longitudinal position as the basic airplane (to try to assure the same handling qualities throughout the flight envelope), a net weight increase of 706 kg (1557 lb) results. The final mass characteristics for the modified aircraft are listed in table 2.

Engine Simulation (U)

(U) Thrust and fuel flow varied linearly with power-lever angle (PLA) between idle thrust ($PLA = 18^\circ$) and intermediate (military) thrust ($PLA = 83^\circ$), and between intermediate thrust and maximum thrust ($PLA = 129^\circ$). The pilot's throttle setting corresponded to a commanded power-lever angle. The actual PLA response to the throttle command was simulated by using a nonlinear dynamic model supplied by the engine manufacturer.

(U) Installed gross thrust per engine was defined as a function of altitude and Mach number at maximum, intermediate (military thrust), and idle power settings. Table B2 presents the data for the basic airplane. Table B3 presents the data for the airplane with two-dimensional nozzle. The coefficient of gross thrust C_T was computed as

~~CONFIDENTIAL~~

APPENDIX B

$$C_T = \frac{2(T_{gross})}{\bar{q}s} \left(1 - K_T |\theta_j| \right)$$

where K_T is the loss in nozzle efficiency per degree of vectoring ($K_T = 0.00096/\text{deg}$). For the basic F-15, without thrust-vectoring capability, $\theta_j \equiv 0$. Gross thrust T_{gross} for the basic F-15 was computed as

$$T_{gross} = (T_{max} - T_{mil}) \delta_{AB} + (T_{mil} - T_{idle}) \delta_{mil} + T_{idle}$$

where

$$\delta_{AB} = \frac{PLA - 83^\circ}{46^\circ} \quad (0 \leq \delta_{AB} \leq 1)$$

$$\delta_{mil} = \frac{PLA - 18^\circ}{65^\circ} \quad (0 \leq \delta_{mil} \leq 1)$$

(C) Gross thrust for the modified F-15 was computed as discussed previously when thrust reversing was not employed. Thrust reversing could only be employed when $PLA \leq 83^\circ$ (nonafterburning) and $\theta_j = 0$ (vectoring had priority over reversing). When thrust reversing was employed, gross thrust was calculated as a function of the fraction of maximum reverser deployment used, δ_{rev} .

$$T_{gross} = \delta_{rev} [0.22T_{mil} + (K_{rev}\bar{q})(0.0326 - 0.0186M)]$$

$$(0 \leq \delta_{rev} \leq 1)$$

where $K_{rev} = 56.5 \text{ m}^2 (608 \text{ ft}^2)$. The second term of the equation, involving dynamic pressure and Mach number, accounts for the base drag of the reverser panels and was obtained from wind-tunnel test data. Operation of simulated speed brake and thrust reverser is described in appendix C.

(U) Fuel flow was assumed to be the same with either the axisymmetric (basic) or nonaxisymmetric (two-dimensional) nozzle. Values of fuel flow are defined as functions of altitude and Mach number at maximum, intermediate, and idle power settings (table B4). Theoretical fuel use was computed in simulated flights, but because of the short duration (3 min), engagements were flown at constant weight.

ORIGINAL PAGE IS
OF POOR QUALITY

UNCLASSIFIED

APPENDIX B

$$\text{Fuel used} = 2 \int (\text{Fuel flow}) dt$$

$$\text{Fuel flow} = (F_{\max} - F_{\text{mil}})\delta_{AB} + (F_{\text{mil}} - F_{\text{idle}})\delta_{\text{mil}} + F_{\text{idle}}$$

(U) Ram drag D_R was assumed to be the same with either nozzle. Ram drag is defined as a function of altitude and Mach number at maximum, intermediate, and idle power setting (table B5).

$$D_R = (D_{\max} - D_{\text{mil}})\delta_{AB} + (D_{\text{mil}} - D_{\text{idle}})\delta_{\text{mil}} + D_{\text{idle}}$$

$$C_{D,R} = \frac{2D_R}{qS}$$

(U) The coefficient of engine drag $C_{D,E}$ includes the ram drag coefficient $C_{D,R}$ plus a term $\Delta C_{D,\text{nozzle}}$, which accounts for the change in afterbody/nozzle drag in going from afterburning to nonafterburning power setting.

$$C_{D,E} = C_{D,R} + \Delta C_{D,\text{nozzle}}$$

For $\text{PLA} > 83^\circ$ ($\delta_{AB} > 0$), $\Delta C_{D,\text{nozzle}} = 0$. For $\text{PLA} \leq 83^\circ$, $\Delta C_{D,\text{nozzle}}$ is defined in table B6 for the basic airplane and in table B7 for the airplane with the two-dimensional nozzle.

(U) The use of gross thrust and ram drag rather than net thrust was done to provide more realistic thrust effects at high angles of attack for the basic airplane and is more appropriate in the modified configuration for vectoring and reversing simulation. Gross thrust (coefficient C_T) acts along the X body axis while engine drag (coefficient $C_{D,E}$) acts along the X stability axis.

(U) Aerodynamic Forces and Moments (U)

(U) The aerodynamic forces and moments are computed using nondimensional aerodynamic coefficients including stability and control derivatives. The representations of the data were selected from aerodynamic data furnished by the F-15 Systems Program Office (SPO), propulsion data from the engine manufacturer, and thrust-vectoring and reversing data from NASA and industry studies.

UNCLASSIFIED

UNCLASSIFIED

APPENDIX B

(C) Vertical Force Coefficient (U)

(U) The equation for the vertical (lift) force coefficient is

$$C_{Z,stab} = -C_{L,eff}$$

The effective lift coefficient includes both the aerodynamic effects $C_{L,aero}$ and thrust effects.

$$C_{L,eff} = C_{L,aero} + C_T \sin (\alpha + \delta_v)$$

(U) The effective thrust-vector angle δ_v was related to the geometric thrust-vector angle θ_j by

$$\delta_v = 1.16\theta_j$$

The relationship between effective and geometric thrust-vector angle was determined from static test data on a two-dimensional C-D nozzle at afterburning power setting. The geometric thrust-vector angle of the modified airplane could be controlled by the pilot or by an automatic schedule, as described in appendix C. For the basic airplane, $\delta_v = \theta_j \equiv 0$.

$$C_{L,aero} = C_L' + \left(\frac{\delta_{sb}}{45} \right) \Delta C_{L,sb} + C_{L,v}$$

The term C_L' is the sum of the static lift characteristics and inertial effects and is used in calculating the drag coefficient.

$$C_L' = C_{L,basic} + C_{L,a_n} a_n$$

Table B8 presents the data for $C_{L,basic}$.

(U) The increment in the lift coefficient at full speed-brake deflection $\Delta C_{L,sb}$ is given by

$$\Delta C_{L,sb} = \Delta C_{L,o} + \Delta C_{L,\alpha_1} \alpha_1 + \Delta C_{L,\alpha_2} \alpha_2$$

UNCLASSIFIED

APPENDIX B

where

$$\alpha_1 = \alpha \text{ and } \alpha_2 = 0 \quad (\alpha \leq 10^\circ)$$

$$\alpha_1 = 10^\circ \text{ and } \alpha_2 = (\alpha - 10^\circ) \quad (\alpha > 10^\circ)$$

Table B9 presents the data for $C_{L\alpha_n}$, $\Delta C_{L,\alpha}$, $\Delta C_{L\alpha_1}$, and $\Delta C_{L\alpha_2}$. For the basic airplane, the maximum speed-brake deflection was limited as a function of aerodynamic loading, as described subsequently. For the modified airplane, which was assumed to have a thrust reverser but no speed brake, $\delta_{sb} \equiv 0$.

(U) The last term in the aerodynamic lift equation $C_{L,v}$ is the increment in aerodynamic lift coefficient produced by thrust vectoring. It is composed of an induced lift $C_{L,\Gamma}$ caused by induced circulation and canard lift $C_{L,c}$ required to balance the pitching moment due to vectored thrust

$$C_{L,v} = C_{L,\Gamma} + C_{L,c}$$

The induced lift due to thrust vectoring $C_{L,\Gamma}$ is given by

$$C_{L,\Gamma} = [(H_L - 1)C_T] [\sin(\alpha + \delta_v) - \sin \alpha]$$

where H_L is the thrust-induced lift amplification factor as defined in reference 9 and

$$H_L = 1.9$$

(U) The canard lift was assumed just sufficient to balance the pitching moment due to vectoring such that

$$C_{m,thrust} = \frac{-l_t}{c} (C_{L,\Gamma} \cos \alpha + C_T \sin \delta_v)$$

and

$$C_{m,canard} = \frac{l_c}{c} (\cos \alpha) C_{L,c}$$

[REDACTED]

APPENDIX B

where l_t and l_c are longitudinal distance to the effective point of action of the thrust vector and canard respectively, and

$$C_{L,c} = \frac{l_t}{l_c} \left(C_{L,\Gamma} + C_T \frac{\sin \delta_v}{\cos \alpha} \right)$$

$$\frac{l_t}{l_c} = 1.447$$

Combining terms, the lift-coefficient increment for simulation with thrust vectoring becomes

$$C_{L,v} = \left(1 + \frac{l_t}{l_c} \right) \left[C_T (H_L - 1) \right] \left[\sin (\alpha + \delta_v) - \sin \alpha \right] \\ + \frac{l_t}{l_c} C_T \frac{\sin \delta_v}{\cos \alpha}$$

(U) For the basic airplane (without thrust vectoring), $\theta_j = \delta_v \equiv 0$ and $C_{L,v} = 0$.

(C) The canard used in this simulation had $7.0-m^2$ (75-ft 2) exposed area with an exposed aspect ratio (AR_{exp}) of 2.0 ($AR_{eff} = 2.6$), and a maximum lift coefficient of 2.0. Based on the airplane reference area, the maximum lift coefficient is 0.25.

(U) In order to maintain realistic canard sizing (and lift), the maximum geometric thrust-vector angle $|\theta_j|$ was limited to the smaller of either 15° or

$$\frac{K_{10}\bar{q}}{T_{gross}}$$

where $K_{10} = 250.2 \text{ deg-m}^2$ (2693 deg-ft 2). This prevented the pitching moment due to vectoring from overpowering the canard moment and causing the airplane to pitch nose down at low speeds. Figure 3 shows that even with the limit, the modified airplane still had a considerable margin in instantaneous turn capability over the basic F-15.

UNCLASSIFIED

APPENDIX B

(U) Longitudinal Force Coefficient (U)

(U) The equation for net longitudinal force coefficient is

$$C_{X,stab} = -C_{D,eff}$$

The effective drag coefficient $C_{D,eff}$ includes longitudinal thrust effects as well as drag.

$$C_{D,eff} = C_D - C_T \cos (\alpha + \delta_v)$$

The drag coefficient C_D includes aerodynamic drag $C_{D,aero}$ and engine drag $C_{D,E}$

$$C_D = C_{D,aero} + C_{D,E}$$

$$C_{D,aero} = C_{D,basic} + \Delta C_{D,alt} + \frac{\delta_{sb}}{45} (\Delta C_{D,sb})$$

$$+ C_{D,C} + C_{D,\Gamma} + C_{D,N}$$

(U) $C_{D,basic}$ is the drag coefficient in afterburner at 9144-m (30 000-ft) altitude.

$$C_{D,basic} = C_{D,32} \quad (\alpha \leq 32^\circ)$$

$$C_{D,basic} = C_{D,32} + \left(\frac{\alpha - 32}{8} \right) (C_{D,40} - C_{D,32}) \quad (32^\circ < \alpha < 40^\circ)$$

$$C_{D,basic} = C_{D,40} \quad (\alpha \geq 40^\circ)$$

$$C_{D,40} = C_L' \tan \alpha$$

(U) $C_{D,32}$, the value of $C_{D,basic}$ at $\alpha \leq 32^\circ$, is defined in table B10 as a function of C_L' and Mach number.

UNCLASSIFIED

APPENDIX B

(U) The effect of altitude on drag coefficient is given by $\Delta C_{D,alt}$, where

$$\Delta C_{D,alt} = \frac{C_{D_h}}{0.3048} (h - 9144)$$

$$C_{D_h} = 5 \times 10^{-8} \text{ m}^{-1}$$

(U) Drag coefficient at maximum speed-brake deflection $\Delta C_{D,sb}$ is defined in table B11. For the basic airplane, the speed-brake deflection δ_{sb} was limited to the smaller of 45° or the deflection that would result in 55 600-N (12 500-lb) force.

$$\delta_{sb} \leq 45^\circ$$

and

$$\delta_{sb} \leq \frac{45K_8}{\bar{q}s \Delta C_{D,sb}}$$

where $K_8 = 55 600 \text{ N}$ (12 500 lb). For the modified airplane, which was assumed to have a thrust reverser but no speed brake, $\delta_{sb} \equiv 0$.

(U) The canard drag coefficient $C_{D,c}$ is defined as $C_{D,c} = 0$ for the basic airplane (no canards) and $C_{D,c} = 0.00075 + 1.537C_{L,C}^2$ for the modified airplane (with canard).

(U) The component of aerodynamic drag induced by thrust vectoring is

$$C_{D,\Gamma} = [C_T(H_D - 1)] [\cos \alpha - \cos (\alpha + \delta_v)]$$

where H_D is the thrust-induced amplification factor in drag as defined in reference 9.

$$H_D = 1.6$$

Drag associated with vectoring is included in the amplification factor H_D . For the basic aircraft $\theta_j = \delta_v = 0$ and $C_{D,\Gamma} = 0$.

UNCLASSIFIED

APPENDIX B

(U) The last term in the aerodynamic drag equation $C_{D,N}$ is the increment in afterbody drag of the two-dimensional C-D nozzle at $\theta_j = \delta_v = 0$ referenced to the axisymmetric nozzle. Therefore, $C_{D,N} = 0$ for the basic airplane. For the modified airplane

$$C_{D,N} = -0.0006 - 0.0028 K_{nozzle}$$

where $K_{nozzle} = (M - 0.6)/0.3$ and $0 \leq K_{nozzle} \leq 1$.

(U) Pitching-Moment Coefficient (U)

(U) The equation for the net pitching-moment coefficient is

$$\begin{aligned} C_m &= C_{m,basic} + C_{m,a_n} a_n + \frac{\bar{c}}{2V} \left(C_{m_q} q + C_{m_\alpha} \dot{\alpha} \right) \\ &+ C_{L,aero} \left[c_g - 0.2565 + \Delta N_o + \Delta N_{sb} \left(\frac{\delta_{sb}}{45} \right) \right] \\ &+ \frac{\delta_{sb}}{45^\circ} \Delta C_{m,sb} \end{aligned}$$

(U) The pitching-moment equation was the same for the basic and modified airplanes. The pitching moment resulting from thrust vectoring was assumed to be balanced by the canard, so these effects do not appear in the equation. The terms ΔN_o and ΔN_{sb} account for the transonic shift of the neutral point. Tables B12 to B15 present the data for $C_{m,basic}$, C_{m_q} , C_{m_α} , C_{m,a_n} , $\Delta C_{m,sb}$, ΔN_{sb} , and ΔN_o .

(U) Side-Force Coefficient (U)

(U) The equation for the net side-force coefficient is

$$C_y,stab = C_{y,basic} + C_{y\delta_D} \delta_D + \Delta C_{y\delta_r} K_{\delta_r} \text{ sign } (\delta_r) + C_{y\delta_a} \delta_a$$

UNCLASSIFIED

UNCLASSIFIED

APPENDIX B

where

$$C_{Y,\text{basic}} = C_{Y,2}$$

when $\alpha \geq 25^\circ$, $\beta \leq 10^\circ$, $M \leq 0.6$; otherwise

$$C_{Y,\text{basic}} = C_{Y,1} \text{ sign } (\beta)$$

The special static side-force coefficient $C_{Y,2}$ is necessary to reflect asymmetries in the airplane characteristics. The other contributions are due to differential horizontal tail, rudder, and ailerons, respectively.

(U) In table B16, $C_{Y,1}$ is defined as a function of the absolute value of β in 4° increments, from $|\beta| = 4^\circ$ to $|\beta| = 28^\circ$. At $\beta = 0^\circ$, $C_{Y,1}$ was zero. Tables B17 to B21 present the data for $C_{Y,2}$, $C_{Y\delta_a}$, $C_{Y\delta_D}$, $\Delta C_{Y\delta_r}$, and K_{δ_r} , respectively. In table B20, $\Delta C_{Y\delta_r}$ is defined at $|\delta_r| = 10^\circ$, 20° , and 30° . At $\delta_r = 0^\circ$, $\Delta C_{Y\delta_r}$ is zero.

(U) Rolling-Moment Coefficient (U)

(U) The equation for the net rolling-moment coefficient is

$$C_l = C_{l,\text{basic}} + C_{l\delta_a} \delta_a + C_{l\delta_D} \delta_D + \Delta C_{l\delta_r} K_{\delta_r} \text{ sign } (\delta_r)$$

$$+ \left(\frac{b}{2V} \right) \left(C_{l_p} p + C_{l_r} r \right) + \Delta C_{l,sb} \frac{\delta_{sb}}{45}$$

where

$$C_{l,\text{basic}} = C_{l,2}$$

when $\alpha \geq 25^\circ$, $\beta \leq 10^\circ$, $M \leq 0.6$, and $PLA \leq 35^\circ$; otherwise,

UNCLASSIFIED

APPENDIX B

$$C_{\ell,\text{basic}} = C_{\ell,1} \text{ sign } (\beta)$$

In table B22, $C_{\ell,1}$ is defined from $|\beta| = 4^\circ$ to $|\beta| = 28^\circ$. At $\beta = 0^\circ$ $C_{\ell,1}$ is zero. Tables B23 to B29 present the data for $C_{\ell,2}$, $C_{\ell,p}$, $C_{\ell,r}$, $C_{\ell\delta_a}$, $C_{\ell\delta_D}$, $\Delta C_{\ell\delta_r}$, and $K_{\delta_r\ell}$, respectively. In table B28, $\Delta C_{\ell\delta_r}$ is defined at $|\delta_r| = 10^\circ$, 20° , and 30° . At $\delta_r = 0^\circ$, $\Delta C_{\ell\delta_r} = 0$. In table B30, $\Delta C_{\ell,sb}$ is defined from $|\beta| = 4^\circ$ to $|\beta| = 16^\circ$. At $\beta = 0^\circ$, $\Delta C_{\ell,sb} = 0$.

(U) Yawing-Moment Coefficient (U)

(U) The equation for the net yawing-moment coefficient is

$$C_n = C_{n,\text{basic}} + C_{n\delta_a} \delta_a + C_{n\delta_D} \delta_D + C_{n\delta_r} \delta_r K_{\delta_r} + \frac{b}{2V} (C_{np} p + C_{nr} r) \\ + \Delta C_{n,sb} \frac{\delta_{sb}}{45} + C_{Y,\text{basic}} (cg - 0.2565) \frac{-c}{b}$$

where

$$C_{n,\text{basic}} = C_{n,2}$$

when $\alpha \geq 25^\circ$, $\beta \leq 10^\circ$, and $M \leq 0.6$; otherwise

$$C_{n,\text{basic}} = C_{n,1} \text{ sign } (\beta)$$

In table B31, $C_{n,1}$ is defined from $|\beta| = 4^\circ$ to $|\beta| = 28^\circ$. At $\beta = 0^\circ$, $C_{n,1}$ is zero. Tables B32 to B38 present the data for $C_{n,2}$, C_{np} , C_{nr} , $C_{n\delta_a}$, $C_{n\delta_D}$, $C_{n\delta_r}$, and $\Delta C_{n,sb}$, respectively. In table B38, $\Delta C_{n,sb}$ is defined from $|\beta| = 4^\circ$ to $|\beta| = 16^\circ$. At $\beta = 0$, $\Delta C_{n,sb} = 0^\circ$.

UNCLASSIFIED

UNCLASSIFIED

APPENDIX B

(U) TABLE B1.- ENGINE CHARACTERISTICS AND AERODYNAMIC

COEFFICIENTS USED IN SIMULATION (U)

Variable	Functional dependence	Table
Gross thrust for basic airplane	M h	B2
Gross thrust for basic airplane	M h	B3
Fuel flow	M h	B4
Ram drag	M h	B5
ΔC_D , nozzle (basic)	M	B6
ΔC_D , nozzle (2-D)	M	B7
C_L , basic	$M \alpha \delta_h$	B8
$C_{L_{a_n}}$	M	B9
ΔC_{L_o}	M	B9
$\Delta C_{L_{\alpha_1}}$	M	B9
$\Delta C_{L_{\alpha_2}}$	M	B9
C_D , 32	$M C_L'$	B10
ΔC_D , sb	M	B11
C_m , basic	$M \alpha \delta_h$	B12
C_{m_q}	$M \alpha$	B13
$C_{m_{\dot{\alpha}}}$	$M \alpha$	B14
$C_{m_{a_n}}$	M	B15
ΔC_m , sb	M	B15
ΔN_{sb}	M	B15
ΔN_o	M	B15
C_y , 1	$M \alpha \beta$	B16

APPENDIX B

(U) TABLE B1.- Concluded

Variable	Functional dependence	Table
$C_Y, 2$	$M \alpha \beta$	B17
$C_{Y\delta_a}$	$M \alpha$	B18
$C_{Y\delta_D}$	$M \alpha$	B19
$\Delta C_{Y, \delta_r}$	$M \alpha \delta_r$	B20
K_{δ_r}	M	B21
$C_\ell, 1$	$M \alpha \beta$	B22
$C_\ell, 2$	$M \alpha \beta$	B23
$C_{\ell p}$	$M \alpha$	B24
$C_{\ell r}$	$M \alpha$	B25
$C_{\ell\delta_a}$	$M \alpha$	B26
$C_{\ell\delta_D}$	$M \alpha$	B27
$\Delta C_{\ell\delta_r}$	$M \alpha \delta_r$	B28
$K_{\delta_r\ell}$	M	B29
$\Delta C_{\ell, sb}$	$M \alpha \beta$	B30
$C_n, 1$	$M \alpha \beta$	B31
$C_n, 2$	$M \alpha \beta$	B32
C_{np}	$M \alpha$	B33
C_{nr}	$M \alpha$	B34
$C_{n\delta_a}$	$M \alpha$	B35
$C_{n\delta_D}$	$M \alpha$	B36
$C_{n\delta_r}$	$M \alpha \beta$	B37
$\Delta C_{n, sb}$	$M \alpha \beta$	B38

UNCLASSIFIED

ORIGINAL PAGE IS
OF POOR QUALITY

APPENDIX B

TABLE B2.- GROSS THRUST VALUES USED IN SIMULATION
OF BASIC AIRPLANE (U)

(a) SI Units

Mach number	Thrust, N, at altitude, m, of -						
	0	3 048	6 096	9 144	12 192	15 240	18 288
T_{\max}							
0.2	96 668	73 324	52 907	34 091	22 241	13 344	8 896
.4	109 817	85 957	61 447	41 724	24 852	14 341	8 896
.6	129 269	99 364	73 791	50 398	30 430	17 859	9 185
.8	148 548	118 349	88 884	63 320	38 308	22 783	11 752
1.0	178 907	139 055	105 876	77 559	51 038	28 103	14 843
1.2	211 223	166 737	125 751	92 780	61 901	36 221	19 447
1.4	222 410	204 417	154 588	113 469	76 189	44 286	23 869
1.6	222 410	217 962	190 535	141 680	94 426	56 007	32 325
T_{mil}							
0.2	60 131	45 211	31 689	20 702	13 344	8 896	4 448
.4	67 755	52 182	36 720	24 087	15 012	9 065	4 448
.6	78 439	60 055	44 201	29 304	18 308	11 107	6 472
.8	90 521	70 659	52 515	36 777	23 050	14 060	7 926
1.0	107 855	83 235	62 412	44 860	29 362	17 383	9 763
1.2	128 927	101 148	75 512	54 957	36 101	21 293	11 876
1.4	133 446	123 589	93 061	67 141	44 482	26 053	14 572
1.6	133 446	128 998	114 701	84 863	55 900	33 615	19 941
T_{idle}							
0.2	4 804	4 248	5 075	6 458	8 006	8 006	8 006
.4	6 387	4 821	5 475	6 774	8 478	9 065	8 006
.6	9 230	6 294	6 174	7 232	8 767	10 021	6 472
.8	13 758	9 390	7 157	7 891	9 216	10 466	7 926
1.0	35 799	30 452	21 840	14 020	9 995	10 898	9 763
1.2	79 022	64 850	50 909	37 338	25 377	15 288	11 698
1.4	133 446	123 589	93 061	67 141	44 482	26 053	14 576
1.6	133 446	128 998	114 701	84 863	55 900	33 615	19 941

APPENDIX B

TABLE B2.- Concluded (U)

(b) U.S. Customary Units

Mach number	Thrust, lb, at altitude, ft, of -						
	0	10 000	20 000	30 000	40 000	50 000	60 000
T_{max}							
0.2	21 732	16 484	11 894	7 664	5 000	3 000	2 000
.4	24 688	19 324	13 814	9 380	5 587	3 224	2 000
.6	29 061	22 338	16 589	11 330	6 841	4 015	2 065
.8	33 395	26 606	19 982	14 235	8 612	5 122	2 642
1.0	40 220	31 261	23 802	17 436	11 474	6 318	3 337
1.2	47 485	37 484	28 270	20 858	13 916	8 143	4 372
1.4	50 000	45 955	34 753	25 509	17 128	9 956	5 366
1.6	50 000	49 000	42 834	31 851	21 228	12 591	7 267
T_{mil}							
0.2	13 518	10 164	7 124	4 654	3 000	2 000	1 000
.4	15 232	11 731	8 255	5 415	3 375	2 038	1 000
.6	17 634	13 501	9 937	6 588	4 116	2 497	1 455
.8	20 350	15 885	11 806	8 268	5 182	3 161	1 782
1.0	24 247	18 712	14 031	10 085	6 601	3 908	2 195
1.2	28 984	22 739	16 976	12 355	8 116	4 787	2 670
1.4	30 000	27 784	20 921	15 094	10 000	5 857	3 276
1.6	30 000	29 000	25 786	19 078	12 567	7 557	4 483
T_{idle}							
0.2	1 080	955	1 141	1 452	1 800	1 800	1 800
.4	1 436	1 084	1 231	1 523	1 906	2 038	1 800
.6	2 075	1 415	1 388	1 626	1 971	2 253	1 455
.8	3 093	2 111	1 609	1 774	2 072	2 353	1 782
1.0	8 048	6 846	4 910	3 152	2 247	2 450	2 195
1.2	17 765	14 579	11 445	8 394	5 705	3 437	2 630
1.4	30 000	27 784	20 921	15 094	10 000	5 857	3 277
1.6	30 000	29 000	25 786	19 078	12 567	7 557	4 483

APPENDIX B

TABLE B3.- GROSS THRUST WITH TWO-DIMENSIONAL NOZZLE (U)

(a) SI Units

Mach number	Thrust, N, at altitude, m, of -						
	0	3 048	6 096	9 144	12 192	15 240	18 288
T _{max} for two-dimensional nozzle							
0.2	99 568	75 744	54 757	35 354	22 241	13 344	8 896
.4	112 562	88 279	63 231	43 018	25 670	14 857	8 896
.6	131 854	101 548	75 561	51 710	31 284	18 393	9 479
.8	151 964	120 600	90 485	64 588	39 148	23 330	12 068
1.0	184 988	142 810	108 207	79 031	51 959	28 637	15 155
1.2	220 938	172 737	129 145	94 729	63 013	36 800	19 758
1.4	231 307	213 412	159 691	116 191	77 559	44 904	24 131
1.6	231 307	222 410	197 776	145 363	96 126	56 679	32 552
T _{mil} for two-dimensional nozzle							
0.2	60 851	45 843	32 227	21 115	13 344	8 896	4 448
.4	68 297	52 702	37 196	24 447	15 284	9 247	4 448
.6	78 755	60 415	44 597	29 625	18 566	11 285	6 587
.8	91 063	71 296	53 147	37 293	23 419	14 314	8 091
1.0	108 825	84 235	63 284	45 620	29 918	17 748	9 999
1.2	130 475	102 562	76 798	56 003	36 857	21 805	12 161
1.4	133 446	125 688	94 827	68 618	45 505	26 756	14 937
1.6	133 446	128 998	116 881	86 731	57 244	34 522	20 421

APPENDIX B

TABLE B3.- Concluded (U)

(b) U.S. Customary Units

Mach number	Thrust, lb, at altitude, ft, of -						
	0	10 000	20 000	30 000	40 000	50 000	60 000
T_{max} for two-dimensional nozzle							
0.2	22 384	17 028	12 310	7 948	5 000	3 000	2 000
.4	25 305	19 846	14 215	9 671	5 771	3 340	2 000
.6	29 642	22 829	16 987	11 625	7 033	4 135	2 131
.8	34 163	27 112	20 342	14 520	8 801	5 245	2 713
1.0	41 587	32 105	24 326	17 767	11 681	6 438	3 407
1.2	49 669	38 833	29 033	21 296	14 166	8 273	4 442
1.4	52 000	47 977	35 900	26 121	17 436	10 095	5 425
1.6	52 000	50 000	44 462	32 679	21 610	12 742	7 318
T_{mil} for two-dimensional nozzle							
0.2	13 680	10 306	7 245	4 747	3 000	2 000	1 000
.4	15 354	11 848	8 362	5 496	3 436	2 079	1 000
.6	17 705	13 582	10 026	6 660	4 174	2 537	1 481
.8	20 472	16 028	11 948	8 384	5 265	3 218	1 819
1.0	24 465	18 937	14 227	10 256	6 726	3 990	2 248
1.2	29 332	23 057	17 265	12 590	8 286	4 902	2 734
1.4	30 000	28 256	21 318	15 426	10 230	6 015	3 358
1.6	30 000	29 000	26 276	19 498	12 869	7 761	4 591

APPENDIX B

TABLE B4.- FUEL-FLOW VALUES USED IN SIMULATION (U)

(a) SI Units

Mach number	Fuel flow, kg/sec, at altitude, m, of -						
	0	3048	6096	9144	12 192	15 240	18 288
$\dot{w}_f,_{max}$							
0.2	353.9	265.6	188.4	104.8	68.0	37.8	15.1
.4	385.9	293.0	207.9	131.5	73.0	43.7	22.7
.6	435.5	319.1	235.6	159.1	84.7	50.9	28.8
.8	489.0	362.3	267.2	190.0	101.2	61.2	33.8
1.0	572.4	415.2	299.1	220.7	146.1	72.6	39.7
1.2	659.0	499.1	351.6	247.3	167.4	98.6	54.3
1.4	680.4	583.7	427.8	295.3	193.4	112.4	61.5
1.6	680.4	604.8	508.2	367.4	241.0	142.4	82.7
$\dot{w}_f,_{mil}$							
0.2	74.7	56.4	38.8	24.7	16.6	7.6	7.6
.4	79.9	62.0	43.2	27.7	17.1	10.8	7.6
.6	87.0	67.4	50.1	32.6	20.2	12.7	7.7
.8	92.2	74.0	56.5	39.9	24.8	15.6	8.9
1.0	100.3	79.5	62.1	46.5	30.8	18.5	10.5
1.2	108.4	87.6	68.0	51.7	35.0	20.8	11.8
1.4	113.4	95.3	75.3	57.5	39.7	23.4	13.1
1.6	113.4	98.3	82.5	64.8	44.4	26.7	15.9
$\dot{w}_f,_{idle}$							
0.2	9.7	7.2	6.3	7.2	7.6	7.6	7.6
.4	10.0	7.1	6.1	6.9	8.7	10.8	7.6
.6	10.5	7.1	5.9	6.4	8.2	11.0	7.7
.8	11.9	8.0	5.9	6.0	7.6	10.2	8.9
1.0	24.1	20.8	14.8	9.3	6.9	9.5	10.5
1.2	55.6	48.0	38.8	29.5	20.6	12.8	11.5
1.4	105.8	95.3	75.3	57.5	39.7	23.4	13.1
1.6	105.8	98.3	82.5	66.3	44.4	26.7	15.9

APPENDIX B

TABLE B4.- Concluded (U)

(b) U.S. Customary units

Mach number	Fuel flow, lb/hr, at altitude, ft, of -						
	0	10 000	20 000	30 000	40 000	50 000	60 000
\dot{w}_f, max							
0.2	46 814	35 130	24 919	13 860	9 000	5 000	2 000
.4	51 041	38 754	27 501	17 400	9 659	5 787	3 000
.6	57 613	42 210	31 170	21 047	11 205	6 731	3 816
.8	64 684	47 925	35 344	25 129	13 390	8 099	4 467
1.0	75 720	54 926	39 559	29 190	19 328	9 609	5 256
1.2	87 172	66 024	46 504	32 715	22 141	13 049	7 189
1.4	90 000	77 217	56 588	39 061	25 582	14 872	8 135
1.6	90 000	80 000	67 230	48 594	31 885	18 832	10 940
\dot{w}_f, mil							
0.2	9 878	7 461	5 126	3 263	2 200	1 000	1 000
.4	10 573	8 197	5 720	3 664	2 266	1 425	1 000
.6	11 513	8 911	6 628	4 315	2 675	1 679	1 021
.8	12 199	9 784	7 476	5 273	3 285	2 063	1 183
1.0	13 267	10 522	8 208	6 149	4 080	2 451	1 388
1.2	14 342	11 593	8 996	6 836	4 625	2 755	1 557
1.4	15 000	12 612	9 957	7 612	5 255	3 091	1 727
1.6	15 000	13 000	10 911	8 574	5 876	3 535	2 104
\dot{w}_f, idle							
0.2	1 283	958	830	959	1 000	1 000	1 000
.4	1 324	940	803	912	1 154	1 425	1 000
.6	1 389	944	781	851	1 090	1 450	1 021
.8	1 568	1 059	786	800	1 008	1 350	1 183
1.0	3 191	2 745	1 956	1 236	913	1 251	1 388
1.2	7 351	6 354	5 132	3 896	2 728	1 690	1 523
1.4	14 000	12 612	9 957	7 612	5 255	3 091	1 728
1.6	14 000	13 000	10 911	8 774	5 876	3 535	2 104

APPENDIX B

TABLE B5.- RAM DRAG VALUES USED IN SIMULATION (U)

(a) SI Units

Mach number	Drag, N, at altitude, m, of -							
	0	3 048	6 096	9 144	12 192	15 240	18 288	
D_R, max								
0.2	6 663	4 759	3 180	2 050	1 334	444	444	
.4	14 514	10 355	7 041	4 670	2 815	1 730	889	
.6	23 926	17 210	12 027	7 757	4 812	2 958	1 783	
.8	37 058	26 066	18 046	12 116	7 517	4 621	2 682	
1.0	53 418	38 161	26 306	17 583	11 222	6 583	3 749	
1.2	72 977	54 019	37 485	25 145	15 840	9 465	5 440	
1.4	80 067	72 777	52 075	35 385	22 290	13 273	7 726	
1.6	80 067	75 619	69 694	49 095	32 085	19 331	11 738	
D_R, mil								
0.2	6 672	4 799	3 184	2 050	1 334	444	444	
.4	14 532	10 377	7 041	4 537	2 815	1 730	889	
.6	23 971	17 241	12 036	7 757	4 817	2 958	1 792	
.8	37 093	26 093	18 077	12 116	7 521	4 621	2 708	
1.0	54 521	38 223	26 351	17 628	11 236	6 690	3 896	
1.2	76 415	55 411	37 529	25 190	15 866	9 488	5 449	
1.4	80 067	76 673	53 783	35 434	22 334	13 313	7 739	
1.6	80 067	75 619	73 973	51 029	32 218	19 727	11 979	
D_R, idle								
0.2	2 201	1 787	1 539	1 338	889	444	444	
.4	5 159	3 705	3 238	2 793	2 290	1 730	889	
.6	9 390	6 441	5 235	4 417	3 580	2 873	1 792	
.8	15 421	10 577	7 517	6 240	5 022	4 127	2 708	
1.0	30 430	22 979	15 862	10 213	6 739	5 457	3 896	
1.2	54 802	41 025	29 816	20 599	13 446	8 162	5 413	
1.4	80 067	76 673	53 783	35 434	22 334	13 317	7 744	
1.6	80 067	80 067	73 973	51 029	32 218	19 727	11 979	

APPENDIX B

TABLE B5.- Concluded (U)

(b) U.S. Customary Units

Mach number	Drag, lb, at altitude, ft, of -						
	0	10 000	20 000	30 000	40 000	50 000	60 000
$D_{R,\max}$							
0.2	1 498	1 070	715	461	300	100	100
.4	3 263	2 328	1 583	1 050	633	389	200
.6	5 379	3 869	2 704	1 744	1 082	665	401
.8	8 331	5 860	4 057	2 724	1 690	1 039	603
1.0	12 009	8 579	5 914	3 953	2 523	1 480	843
1.2	16 406	12 144	8 427	5 653	3 561	2 128	1 223
1.4	18 000	16 361	11 707	7 955	5 011	2 984	1 737
1.6	18 000	17 000	15 668	11 037	7 213	4 346	3 639
$D_{R,\text{mil}}$							
0.2	1 500	1 079	716	461	300	100	100
.4	3 267	2 333	1 583	1 020	633	389	200
.6	5 389	3 876	2 706	1 744	1 083	665	403
.8	8 339	5 866	4 064	2 724	1 691	1 039	609
1.0	12 257	8 593	5 924	3 963	2 526	1 504	876
1.2	17 179	12 457	8 437	5 663	3 567	2 133	1 225
1.4	18 000	17 237	12 091	7 966	5 021	2 993	1 740
1.6	18 000	17 000	16 630	11 472	7 243	4 435	2 693
$D_{R,\text{idle}}$							
0.2	495	386	346	301	200	100	100
.4	1 160	833	728	628	515	389	200
.6	2 111	1 448	1 177	993	805	646	403
.8	3 467	2 378	1 690	1 403	1 129	928	609
1.0	6 841	5 166	3 566	2 296	1 515	1 227	876
1.2	12 320	9 223	6 703	4 631	3 023	1 835	1 217
1.4	18 000	17 237	12 091	7 966	5 021	2 994	1 741
1.6	18 000	18 000	16 630	11 472	7 243	4 435	2 693

APPENDIX B

(U) TABLE B6.- AFTERBODY DRAG

COEFFICIENT FOR AXISYMMETRIC

NOZZLE AT NONAFTERBURNING

POWER SETTING (U)

Mach number	ΔC_D , nozzle
0.2	-0.0021
.4	-.0021
.6	-.0023
.8	-.0031
.9	-.0023
1.0	.0032
1.1	.0052
1.2	.0049
1.4	.0050
1.6	.0050

TABLE B7.- AFTERBODY DRAG

COEFFICIENT OF 2-D C-D NOZZLE

AT NONAFTERBURNING POWER

SETTING (U)

Mach number	ΔC_D , nozzle
0.2	0.0015
.6	.0015
.9	.0052
1.6	.0052

(U) TABLE B8.- $C_{L,\text{basic}}$ (U)(a) $\delta_h = -25^\circ$

ALPHA	MACH NUMBER						1.4	1.5
	0.2	0.4	0.6	0.8	0.9	1.0		
-12.	-1.00	-1.01	-1.03	-1.10	-1.13	-1.25	-1.20	-1.10
-8.	-0.74	-0.74	-0.74	-0.78	-0.81	-0.89	-0.80	-0.69
-4.	-0.48	-0.48	-0.47	-0.47	-0.48	-0.52	-0.46	-0.39
0.	-0.22	-0.21	-0.20	-0.19	-0.18	-0.18	-0.16	-0.13
4.	0.04	0.05	0.07	0.11	0.14	0.20	0.19	0.15
8.	0.32	0.33	0.34	0.41	0.45	0.49	0.48	0.43
12.	0.56	0.57	0.59	0.62	0.64	0.70	0.75	0.69
16.	0.78	0.78	0.79	0.82	0.84	0.90	0.97	0.91
20.	0.98	0.98	0.98	1.00	1.01	1.10	1.22	1.14
24.	1.13	1.12	1.10	1.12	1.13	1.24	1.22	1.14
28.	1.24	1.22	1.19	1.20	1.20	1.32	1.22	1.14
32.	1.32	1.30	1.25	1.26	1.27	1.38	1.22	1.14
36.	1.35	1.33	1.29	1.30	1.30	1.39	1.22	1.14
40.	1.32	1.32	1.31	1.30	1.30	1.39	1.22	1.14
44.	1.25	1.25	1.24	1.30	1.30	1.39	1.22	1.14
48.	1.16	1.16	1.17	1.30	1.30	1.39	1.22	1.14
52.	1.10	1.10	1.10	1.30	1.30	1.39	1.22	1.14
56.	1.04	1.04	1.04	1.30	1.30	1.39	1.22	1.14
60.	.97	.97	.97	1.30	1.30	1.39	1.22	1.14

UNCLASSIFIED

APPENDIX B

(U) TABLE B8.- Continued (U)

(b) $\delta_h = -15^\circ$

ALPHA	MACH NUMBER					
	0.2	0.4	0.6	0.8	0.9	1.0
-12.	-0.93	-0.97	-1.05	-1.10	-1.14	-1.20
-8.	-0.66	-0.69	-0.75	-0.78	-0.81	-0.87
-4.	-0.39	-0.41	-0.45	-0.46	-0.47	-0.50
0.	-0.12	-0.13	-0.15	-0.15	-0.14	-0.15
4.	.13	.14	.15	.16	.18	.22
8.	.42	.42	.43	.46	.51	.55
12.	.65	.66	.68	.70	.73	.79
16.	.86	.87	.88	.90	.93	1.00
20.	1.07	1.07	1.08	1.11	1.15	1.19
24.	1.24	1.23	1.20	1.21	1.23	1.32
28.	1.34	1.32	1.28	1.28	1.29	1.40
32.	1.41	1.38	1.34	1.34	1.35	1.45
36.	1.42	1.40	1.38	1.38	1.38	1.46
40.	1.38	1.38	1.38	1.38	1.38	1.46
44.	1.30	1.30	1.30	1.38	1.39	1.46
48.	1.20	1.20	1.21	1.38	1.38	1.46
52.	1.12	1.12	1.12	1.38	1.38	1.46
56.	1.04	1.04	1.04	1.38	1.38	1.46
60.	.97	.97	.97	1.38	1.39	1.46

UNCLASSIFIED

UNCLASSIFIED

APPENDIX B

ORIGINAL PAGE IS
OF POOR QUALITY

(U) TABLE B8.- Continued (U)

(C) $\delta_h = -5^\circ$

ALPHA	MACH NUMBER					1.4	1.6
	0.4	0.6	0.8	0.9	1.0		
-12.	-.79	-.84	-.89	-.98	-1.07	-1.10	-1.00
-8.	-.53	-.57	-.61	-.65	-.73	-.80	-.73
-4.	-.27	-.30	-.33	-.36	-.38	-.43	-.39
0.	-.01	-.03	-.05	-.05	-.05	-.07	-.07
4.	.25	.24	.23	.25	.27	.29	.28
8.	.49	.50	.52	.56	.61	.63	.59
12.	.75	.76	.78	.80	.82	.88	.89
16.	.98	.99	1.00	1.02	1.03	1.10	1.16
20.	1.18	1.18	1.19	1.20	1.20	1.27	1.37
24.	1.33	1.32	1.30	1.32	1.33	1.42	1.37
28.	1.44	1.40	1.36	1.38	1.40	1.51	1.37
32.	1.50	1.46	1.41	1.43	1.44	1.53	1.37
36.	1.50	1.47	1.43	1.45	1.46	1.53	1.37
40.	1.45	1.45	1.45	1.45	1.45	1.53	1.37
44.	1.35	1.35	1.36	1.45	1.45	1.53	1.37
48.	1.25	1.25	1.26	1.45	1.45	1.53	1.37
52.	1.15	1.15	1.15	1.45	1.45	1.53	1.37
56.	1.05	1.05	1.05	1.45	1.45	1.53	1.37
60.	.96	.96	.95	1.45	1.45	1.53	1.37

UNCLASSIFIED

(U) TABLE B8.- Continued (U)

(d) $\delta_h = 5^\circ$

ALPHA	MACH NUMBER						1.4	1.6
	0.2	0.4	0.6	0.8	0.9	1.0		
-12.	-75	-78	-82	-87	-92	-100	-80	-70
-8.	-48	-50	-52	-56	-60	-69	-57	-49
-4.	-21	-22	-24	-26	-28	-35	-31	-22
0.	.06	.06	.05	.05	.05	.03	.02	.02
4.	.33	.33	.34	.36	.37	.39	.36	.32
8.	.58	.60	.62	.67	.71	.74	.67	.61
12.	.84	.86	.89	.91	.92	1.00	.96	.89
16.	1.07	1.10	1.13	1.13	1.13	1.18	1.21	1.15
20.	1.29	1.30	1.31	1.30	1.30	1.40	1.47	1.41
24.	1.44	1.43	1.41	1.42	1.42	1.52	1.47	1.41
28.	1.54	1.52	1.49	1.50	1.50	1.62	1.47	1.41
32.	1.59	1.57	1.54	1.54	1.54	1.63	1.47	1.41
36.	1.58	1.57	1.55	1.54	1.54	1.63	1.47	1.41
40.	1.53	1.53	1.52	1.52	1.52	1.63	1.47	1.41
44.	1.42	1.43	1.44	1.52	1.52	1.63	1.47	1.41
48.	1.29	1.29	1.30	1.52	1.52	1.63	1.47	1.41
52.	1.17	1.17	1.17	1.52	1.52	1.63	1.47	1.41
56.	1.05	1.05	1.06	1.52	1.52	1.63	1.47	1.41
60.	.93	.93	.94	1.52	1.52	1.63	1.47	1.41

UNCLASSIFIED

UNCLASSIFIED

APPENDIX B

(U) TABLE B8.- Concluded (U)

(e) $\delta_h = 150$

ALPHA	MACH NUMBER						1.4	1.5
	0.2	0.4	0.6	0.8	1.0	1.1		
-12.	-.62	-.66	-.70	-.77	-.85	-.90	-.80	-.70
-8.	-.36	-.36	-.37	-.44	-.52	-.68	-.70	-.57
-4.	-.10	-.10	-.10	-.15	-.19	-.35	-.37	-.23
0.	.16	.16	.17	.14	.12	.05	.05	.07
4.	.42	.44	.46	.45	.45	.48	.43	.37
8.	.66	.69	.73	.76	.78	.79	.72	.66
12.	.92	.96	1.00	.99	.98	.99	1.02	.95
16.	1.17	1.18	1.20	1.20	1.20	1.22	1.28	1.21
20.	1.40	1.40	1.39	1.38	1.38	1.43	1.51	1.47
24.	1.55	1.53	1.51	1.53	1.55	1.50	1.51	1.47
28.	1.65	1.61	1.57	1.60	1.62	1.60	1.51	1.47
32.	1.68	1.64	1.60	1.63	1.65	1.61	1.51	1.47
36.	1.66	1.64	1.61	1.63	1.65	1.61	1.51	1.47
40.	1.60	1.60	1.60	1.60	1.60	1.61	1.51	1.47
44.	1.50	1.50	1.50	1.60	1.60	1.61	1.51	1.47
48.	1.36	1.36	1.36	1.60	1.60	1.61	1.51	1.47
52.	1.22	1.22	1.21	1.60	1.60	1.61	1.51	1.47
56.	1.08	1.08	1.07	1.60	1.60	1.61	1.51	1.47
60.	.93	.93	.93	1.60	1.60	1.61	1.51	1.47

UNCLASSIFIED

ORIGINAL PAGE IS
POOR QUALITY

UNCLASSIFIED

APPENDIX B

(U) TABLE B9.- LIFT FORCE COEFFICIENTS (U)

Mach number	$C_{L_{\alpha_n}}$	$\Delta C_{L,0}$	$\Delta C_{L\alpha_1}'$ per deg	$\Delta C_{L\alpha_2}'$ per deg
0.2	0	-0.0060	-0.0024	0.020
.4	0	-.0060	-.0024	.020
.6	.00180	-.0060	-.0023	.020
.8	.00187	-.0065	-.0019	.030
.9	.00190	-.0055	-.0012	.035
1.0	.00166	-.0025	-.0006	.035
1.1	.00142	-.0006	0	-.035
1.2	.00123	0	0	-.055
1.4	.00099	0	0	-.050
1.6	.00082	0	0	-.035

(U) TABLE B10.- DRAG COEFFICIENT AT $\alpha \leq 32^\circ$ FOR $C_D, 32$ (U)

C_L	MACH NUMBER					
	0.2	0.4	0.6	0.8	0.9	1.0
-1.0	.2582	.2582	.2691	.2862	.2993	.3166
-.8	.1517	.1517	.1545	.1583	.1809	.2136
-.6	.0778	.0778	.0768	.0745	.0753	.1037
-.4	.0376	.0376	.0376	.0370	.0380	.0554
-.2	.0218	.0218	.0218	.0218	.0227	.0321
-.0	.0196	.0196	.0196	.0201	.0204	.0261
.2	.0218	.0218	.0218	.0218	.0227	.0321
.4	.0376	.0376	.0376	.0370	.0380	.0554
.6	.0778	.0778	.0768	.0745	.0753	.1037
.8	.1517	.1517	.1545	.1583	.1809	.2136
1.0	.2582	.2582	.2691	.2862	.2993	.3166
1.2	.4438	.4438	.4663	.5092	.5275	.5370
1.4	.8559	.8559	.8774	.9000	.9050	.8787
1.6	1.2873	1.2873	1.3118	1.3220	1.3230	1.5000

UNCLASSIFIED

ORIGINAL PAGE IS
OF POOR QUALITY

UNCLASSIFIED

APPENDIX B

(U) TABLE B11.- INCREMENT IN DRAG

COEFFICIENT AT FULL SPEED-BRAKE

DEFLECTION (U)

Mach number	$\Delta C_D, sb$
0.2	0.0430
.4	.0430
.6	.0430
.8	.0470
.9	.0510
1.0	.0570
1.1	.0620
1.2	.0620
1.4	.0550
1.6	.0490

(U) TABLE B12.- C_m , basic (U)(a) $\delta_h = -25^\circ$

ALPHA	MACH NUMBER							1.6
	0.2	0.4	0.6	0.8	0.9	1.0	1.1	
-12.	.285	.300	.290	.280	.270	.320	.440	.440
-8.	.267	.287	.281	.265	.257	.309	.363	.368
-4.	.249	.269	.261	.239	.226	.245	.276	.270
0.	.234	.252	.244	.215	.202	.210	.217	.203
4.	.225	.238	.230	.203	.187	.178	.151	.133
8.	.205	.219	.211	.191	.181	.145	.096	.080
12.	.190	.195	.191	.180	.156	.106	.054	.032
16.	.171	.165	.165	.143	.106	.055	.026	-.015
20.	.128	.116	.109	.082	.053	.012	-.044	-.084
24.	.063	.056	.050	.035	.015	-.048	-.044	-.084
28.	0.000	.004	0.000	-.008	-.025	-.120	-.044	-.084
32.	-.045	-.040	-.044	-.050	-.070	-.170	-.044	-.084
36.	-.090	-.090	-.090	-.100	-.120	-.220	-.044	-.084
40.	-.143	-.140	-.140	-.150	-.170	-.270	-.044	-.084
44.	-.213	-.210	-.210	-.150	-.170	-.270	-.044	-.084
48.	-.283	-.280	-.280	-.150	-.170	-.270	-.044	-.084
52.	-.342	-.340	-.340	-.150	-.170	-.270	-.044	-.084
56.	-.391	-.390	-.390	-.150	-.170	-.270	-.044	-.084
60.	-.439	-.440	-.440	-.150	-.170	-.270	-.044	-.084

UNCLASSIFIED

(U) TABLE B12.- Continued (U)

(b) $\delta_h = -15^\circ$

ALPHA	MACH NUMBER						1.4	1.6
	0.2	0.4	0.6	0.8	0.9	1.0		
-12.	.203	.200	.200	.200	.210	.280	.340	.400
-8.	.194	.190	.189	.194	.207	.262	.320	.342
-4.	.185	.179	.171	.172	.175	.205	.236	.241
0.	.166	.166	.161	.158	.157	.166	.170	.165
4.	.150	.149	.145	.140	.140	.116	.092	.075
8.	.122	.124	.123	.121	.117	.060	.016	-.005
12.	.097	.095	.096	.091	.070	.008	-.045	-.070
16.	.070	.071	.072	.042	-.014	-.044	-.096	-.129
20.	.027	.036	.036	-.016	-.045	-.102	-.165	-.191
24.	-.026	-.029	-.029	-.058	-.099	-.175	-.165	-.191
28.	-.077	-.093	-.080	-.110	-.149	-.240	-.165	-.191
32.	-.146	-.160	-.160	-.160	-.200	-.300	-.165	-.191
36.	-.220	-.240	-.240	-.220	-.240	-.340	-.165	-.191
40.	-.300	-.320	-.320	-.320	-.360	-.460	-.165	-.191
44.	-.370	-.390	-.390	-.320	-.360	-.460	-.165	-.191
48.	-.425	-.440	-.440	-.320	-.360	-.460	-.165	-.191
52.	-.470	-.490	-.490	-.320	-.360	-.460	-.165	-.191
56.	-.507	-.520	-.520	-.320	-.360	-.460	-.165	-.191
60.	-.535	-.550	-.550	-.320	-.360	-.460	-.165	-.191

UNCLASSIFIED

UNCLASSIFIED

APPENDIX B

(U) TABLE B12.- Continued (U)

	(C) $\delta_h = -50$									
	MACH NUMBER									
ALPHA	0.2	0.4	0.6	0.8	0.9	1.0	1.1	1.2	1.4	1.6
-12.	-.111	.105	.105	.105	.120	.200	.260	.300	.290	.260
-8.	-.093	.089	.088	.090	.111	.180	.243	.252	.236	.196
-4.	.075	.071	.069	.070	.082	.120	.146	.149	.137	.112
0.	.060	.059	.059	.059	.063	.071	.075	.077	.072	.057
4.	.040	.040	.040	.041	.042	.012	-.020	-.010	.006	.008
8.	.017	.014	.016	.020	.012	-.052	-.100	-.095	-.075	-.048
12.	-.006	-.009	-.004	0.000	-.016	-.092	-.150	-.155	-.132	-.113
16.	-.034	-.029	-.021	-.035	-.062	-.148	-.210	-.216	-.206	-.189
20.	-.068	-.077	-.072	-.095	-.126	-.198	-.263	-.280	-.280	-.258
24.	-.108	-.130	-.129	-.147	-.176	-.252	-.263	-.280	-.280	-.258
28.	-.159	-.188	-.179	-.192	-.222	-.308	-.263	-.280	-.280	-.258
32.	-.217	-.240	-.240	-.240	-.280	-.380	-.263	-.280	-.280	-.258
36.	-.284	-.300	-.300	-.300	-.340	-.440	-.263	-.280	-.280	-.258
40.	-.338	-.350	-.350	-.350	-.390	-.490	-.263	-.280	-.280	-.258
44.	-.380	-.400	-.400	-.350	-.390	-.490	-.263	-.280	-.280	-.258
48.	-.415	-.430	-.430	-.350	-.390	-.490	-.263	-.280	-.280	-.258
52.	-.460	-.480	-.480	-.350	-.390	-.490	-.263	-.280	-.280	-.258
56.	-.490	-.510	-.510	-.350	-.390	-.490	-.263	-.280	-.280	-.258
60.	-.525	-.540	-.540	-.350	-.390	-.490	-.263	-.280	-.280	-.258

UNCLASSIFIED

(U) TABLE B12.- Continued (U)

(d) $\delta_h = 5^\circ$

ALPHA	MACH NUMBER						1.6
	1.0	1.1	1.2	1.4	1.6		
0.2	0.4	0.6	0.8	0.9	1.0	.200	.180
-12.	-0.40	-0.40	-0.40	-0.10	.140	.163	.138
-8.	-0.40	-0.41	-0.39	-0.05	.100	.045	.060
-4.	-0.47	-0.49	-0.43	-0.04	-0.023	.045	.049
0.	-0.61	-0.64	-0.62	-0.06	-0.064	-0.035	.040
4.	-0.81	-0.89	-0.80	-0.07	-0.085	-0.114	-0.106
8.	-1.02	-1.14	-1.04	-0.08	-0.106	-0.150	-0.140
12.	-1.25	-1.35	-1.27	-0.117	-0.146	-0.210	-0.185
16.	-1.50	-1.60	-1.51	-0.159	-0.199	-0.266	-0.211
20.	-1.75	-1.96	-1.89	-0.208	-0.240	-0.310	-0.267
24.	-2.02	-2.30	-2.20	-0.240	-0.286	-0.390	-0.358
28.	-2.38	-2.53	-2.48	-0.270	-0.320	-0.420	-0.36
32.	-2.88	-3.00	-3.00	-0.300	-0.340	-0.420	-0.336
36.	-3.45	-3.60	-3.60	-0.360	-0.400	-0.500	-0.420
40.	-3.80	-4.00	-4.00	-0.400	-0.440	-0.540	-0.420
44.	-4.00	-4.20	-4.20	-0.400	-0.440	-0.600	-0.420
48.	-4.25	-4.40	-4.40	-0.400	-0.440	-0.640	-0.420
52.	-4.60	-4.80	-4.80	-0.400	-0.440	-0.640	-0.420
56.	-4.90	-5.10	-5.10	-0.400	-0.440	-0.640	-0.420
60.	-5.25	-5.40	-5.40	-0.400	-0.440	-0.640	-0.420

UNCLASSIFIED

(U) TABLE B12.- Concluded (U)

ALPHA	MACH NUMBER						1.4	1.6
	0.2	0.4	0.6	0.8	0.9	1.0		
-12.	-.155	-.150	-.140	-.120	-.080	-.040	.120	.110
-8.	-.161	-.152	-.144	-.120	-.086	-.010	.065	.062
-4.	-.175	-.156	-.146	-.131	-.128	-.102	-.064	-.040
0.	-.205	-.188	-.173	-.149	-.159	-.172	-.140	-.116
4.	-.240	-.214	-.199	-.166	-.180	-.217	-.237	-.200
8.	-.270	-.240	-.219	-.182	-.204	-.260	-.300	-.282
12.	-.297	-.264	-.244	-.211	-.239	-.288	-.354	-.344
16.	-.314	-.270	-.253	-.236	-.269	-.340	-.396	-.400
20.	-.315	-.278	-.263	-.284	-.325	-.402	-.448	-.456
24.	-.310	-.280	-.280	-.310	-.340	-.440	-.448	-.456
28.	-.320	-.290	-.290	-.350	-.390	-.490	-.448	-.456
32.	-.365	-.330	-.330	-.380	-.420	-.520	-.448	-.456
36.	-.405	-.370	-.370	-.450	-.490	-.590	-.448	-.456
40.	-.420	-.390	-.390	-.500	-.540	-.640	-.448	-.456
44.	-.450	-.420	-.420	-.500	-.540	-.640	-.448	-.456
48.	-.470	-.440	-.440	-.500	-.540	-.640	-.448	-.456
52.	-.490	-.460	-.460	-.500	-.540	-.640	-.448	-.456
56.	-.510	-.480	-.480	-.500	-.540	-.640	-.448	-.456
60.	-.535	-.500	-.500	-.500	-.540	-.640	-.448	-.456

UNCLASSIFIED

APPENDIX B

UNCLASSIFIED

(U) TABLE B13.- DATA FOR C_{mq} (PER RADIAN) (U)

	MACH NUMBER					
	0.2	0.4	0.6	0.8	0.9	1.0
ALPHA						
-12.	-10.0	-10.0	-10.0	-7.6	-6.0	-6.5
-8.	-10.0	-10.0	-10.0	-7.6	-6.0	-6.5
-4.	-10.0	-10.0	-10.0	-7.6	-6.0	-6.5
0.	-10.0	-10.0	-10.0	-7.6	-6.0	-6.5
4.	-10.0	-10.0	-10.0	-7.6	-6.4	-6.5
8.	-10.0	-10.0	-10.0	-7.6	-6.6	-6.5
12.	-10.0	-10.0	-10.0	-7.6	-6.6	-6.5
16.	-10.0	-10.0	-10.0	-7.7	-6.8	-6.5
20.	-10.0	-10.0	-10.0	-8.0	-7.3	-6.5
24.	-10.0	-10.0	-10.1	-8.5	-7.8	-6.5
28.	-10.0	-10.0	-10.4	-9.0	-8.6	-6.5
32.	-10.0	-10.0	-10.9	-9.8	-9.6	-6.5
36.	-10.0	-10.0	-11.5	-11.5	-11.5	-6.5
40.	-10.0	-10.0	-12.2	-12.2	-12.2	-6.5
44.	-10.0	-10.0	-12.9	-12.9	-12.9	-6.5
48.	-10.0	-10.0	-11.2	-11.2	-11.2	-6.5
52.	-10.0	-10.0	-6.9	-6.9	-6.9	-6.5
56.	-10.0	-10.0	-6.0	-6.0	-6.0	-6.5
60.	-10.0	-10.0	-6.5	-6.5	-6.5	-6.5

UNCLASSIFIED

APPENDIX B

(U) TABLE 14.- $C_{m\dot{\alpha}}$ (PER RADIAN) (U)

ALPHA	MACH NUMBER						
	0.2	0.4	0.6	0.8	0.9	1.0	1.1
-12.	-1.25	-1.25	-1.25	-1.30	-1.60	1.90	2.00
-8.	-1.25	-1.25	-1.25	-1.30	-1.60	1.90	2.00
-4.	-1.25	-1.25	-1.25	-1.30	-1.60	1.90	2.00
0.	-1.25	-1.25	-1.25	-1.30	-1.60	1.90	2.00
4.	-1.25	-1.25	-1.25	-1.30	-1.60	1.90	2.00
8.	-1.10	-1.10	-1.10	-1.20	-1.35	1.90	2.00
12.	-0.75	-0.75	-0.75	-0.85	-0.95	1.90	2.00
16.	-0.35	-0.35	-0.35	-0.40	-0.50	1.90	2.00
20.	.05	.05	.05	.05	.05	1.90	2.00
24.	.20	.20	.20	.20	.20	1.90	2.00
28.	.15	.15	.15	.15	.15	1.90	2.00
32.	.05	.05	.05	.05	.05	1.90	2.00
36.	0.00	0.00	0.00	0.00	0.00	1.90	2.00
40.	0.00	0.00	0.00	0.00	0.00	1.90	2.00
44.	0.00	0.00	0.00	0.00	0.00	1.90	2.00
48.	0.00	0.00	0.00	0.00	0.00	1.90	2.00
52.	0.00	0.00	0.00	0.00	0.00	1.90	2.00
56.	0.00	0.00	0.00	0.00	0.00	1.90	2.00
60.	0.00	0.00	0.00	0.00	0.00	1.90	2.00

UNCLASSIFIED

UNCLASSIFIED

APPENDIX B

(U) TABLE B15.- PITCHING-MOMENT COEFFICIENT (U)

Mach number	$C_{m_{an}}$	$\Delta C_{m, sb}$	ΔN_{sb}	ΔN_o
0.2	0	-0.0075	0.020	-0.0130
.4	0	-.0075	.020	-.0130
.6	-.00109	-.0100	.020	-.0090
.8	-.00119	-.0200	.023	-.0035
.9	-.00123	-.0290	.030	-.0060
1.0	-.00119	-.0310	.032	-.0130
1.1	-.00109	-.0290	.026	-.0120
1.2	-.00099	-.0270	.016	-.0110
1.4	-.00080	-.0240	.002	-.0070
1.6	-.00065	-.0220	-.007	-.0020

(U) TABLE B16.- DATA FOR $C_{Y,1}$ (U)(a) $|\beta| = 4^\circ$

ALPHA	MACH NUMBER						
	0.2	0.4	0.6	0.8	0.9	1.0	1.1
-12.	-.062	-.061	-.060	-.062	-.065	-.065	-.065
-8.	-.062	-.061	-.060	-.062	-.065	-.065	-.065
-4.	-.062	-.061	-.060	-.062	-.065	-.065	-.065
0.	-.062	-.061	-.060	-.062	-.065	-.065	-.065
4.	-.064	-.064	-.065	-.067	-.068	-.067	-.066
8.	-.066	-.067	-.068	-.068	-.068	-.067	-.066
12.	-.066	-.067	-.068	-.068	-.068	-.067	-.066
16.	-.064	-.063	-.062	-.063	-.065	-.065	-.065
20.	-.058	-.057	-.057	-.057	-.059	-.062	-.065
24.	-.050	-.050	-.050	-.047	-.047	-.050	-.055
28.	-.046	-.046	-.045	-.048	-.050	-.053	-.056
32.	-.046	-.048	-.050	-.055	-.060	-.060	-.060
36.	-.040	-.045	-.050	-.057	-.065	-.064	-.062
40.	-.042	-.046	-.050	-.047	-.047	-.050	-.055
44.	-.050	-.055	-.060	-.057	-.055	-.056	-.058
48.	-.054	-.062	-.070	-.070	-.070	-.066	-.063
52.	-.060	-.070	-.080	-.080	-.080	-.073	-.066
56.	-.062	-.076	-.090	-.090	-.090	-.080	-.070
60.	-.062	-.076	-.090	-.090	-.090	-.080	-.070

UNCLASSIFIED

(U) TABLE B16.- Continued (U)

(b) $|\beta| = 8^\circ$

ALPHA	MACH NUMBER						1.4	1.6
	0.2	0.4	0.6	0.8	0.9	1.0		
-12.	-.124	-.128	-.130	-.133	-.135	-.133	-.132	-.120
-8.	-.124	-.128	-.130	-.133	-.135	-.133	-.132	-.120
-4.	-.124	-.128	-.130	-.133	-.135	-.133	-.132	-.120
0.	-.124	-.128	-.130	-.133	-.135	-.133	-.132	-.120
4.	-.128	-.132	-.135	-.136	-.137	-.136	-.134	-.124
8.	-.132	-.136	-.140	-.138	-.137	-.136	-.136	-.130
12.	-.132	-.136	-.140	-.137	-.135	-.135	-.135	-.130
16.	-.128	-.129	-.130	-.130	-.130	-.132	-.134	-.135
20.	-.116	-.112	-.108	-.108	-.108	-.117	-.126	-.135
24.	-.100	-.095	-.090	-.085	-.080	-.092	-.104	-.115
28.	-.092	-.088	-.085	-.087	-.090	-.098	-.106	-.115
32.	-.092	-.091	-.090	-.095	-.110	-.112	-.114	-.115
36.	-.080	-.087	-.095	-.106	-.127	-.121	-.119	-.125
40.	-.093	-.092	-.090	-.090	-.090	-.098	-.106	-.115
44.	-.100	-.100	-.100	-.100	-.100	-.105	-.110	-.115
48.	-.108	-.114	-.110	-.112	-.115	-.115	-.115	-.125
52.	-.120	-.122	-.125	-.125	-.125	-.121	-.118	-.115
56.	-.124	-.130	-.135	-.135	-.135	-.127	-.121	-.125
60.	-.124	-.130	-.135	-.135	-.135	-.127	-.121	-.125

UNCLASSIFIED

UNCLASSIFIED

APPENDIX B

(U) TABLE B16.- Continued (U)

	(C) $ \beta = 120$						
	MACH NUMBER						
ALPHA	0.2	0.4	0.6	0.8	0.9	1.0	1.1
-12.	-0.185	-0.185	-0.185	-0.179	-0.173	-0.180	-0.187
-8.	-0.185	-0.185	-0.185	-0.179	-0.173	-0.180	-0.187
-4.	-0.185	-0.185	-0.185	-0.179	-0.173	-0.180	-0.187
0.	-0.185	-0.185	-0.185	-0.179	-0.173	-0.180	-0.187
4.	-0.191	-0.195	-0.200	-0.196	-0.192	-0.195	-0.197
8.	-0.196	-0.200	-0.205	-0.200	-0.196	-0.199	-0.192
12.	-0.194	-0.197	-0.200	-0.198	-0.196	-0.200	-0.205
16.	-0.187	-0.186	-0.185	-0.185	-0.185	-0.195	-0.205
20.	-0.170	-0.158	-0.146	-0.154	-0.162	-0.189	-0.206
24.	-0.149	-0.130	-0.120	-0.126	-0.133	-0.150	-0.167
28.	-0.138	-0.124	-0.110	-0.122	-0.135	-0.150	-0.167
32.	-0.136	-0.130	-0.125	-0.135	-0.145	-0.158	-0.171
36.	-0.121	-0.128	-0.135	-0.145	-0.155	-0.165	-0.175
40.	-0.134	-0.132	-0.130	-0.130	-0.130	-0.148	-0.166
44.	-0.141	-0.140	-0.140	-0.140	-0.140	-0.155	-0.170
48.	-0.154	-0.154	-0.155	-0.155	-0.155	-0.165	-0.175
52.	-0.167	-0.166	-0.165	-0.165	-0.165	-0.171	-0.177
56.	-0.169	-0.169	-0.170	-0.170	-0.170	-0.175	-0.180
60.	-0.167	-0.168	-0.170	-0.170	-0.170	-0.175	-0.180

UNCLASSIFIED

ORIGINAL PAGE IS
OF POOR QUALITY

UNCLASSIFIED

APPENDIX B

(U) TABLE B16.- Continued (U)

(d) $|B| = 160$

ALPHA	MACH NUMBER						APPENDIX B			
	0.2	0.4	0.6	0.8	0.9	1.0				
-12.	-.245	-.240	-.235	-.232	-.230	-.238	-.246	-.255	-.240	-.225
-8.	-.245	-.240	-.235	-.232	-.230	-.238	-.246	-.255	-.240	-.225
-4.	-.245	-.240	-.235	-.232	-.230	-.238	-.246	-.255	-.240	-.225
0.	-.245	-.240	-.235	-.232	-.230	-.238	-.246	-.255	-.240	-.225
4.	-.253	-.252	-.250	-.245	-.240	-.248	-.256	-.265	-.250	-.235
8.	-.258	-.259	-.260	-.254	-.248	-.257	-.264	-.270	-.260	-.250
12.	-.252	-.253	-.255	-.254	-.253	-.260	-.267	-.275	-.268	-.262
16.	-.241	-.238	-.235	-.242	-.250	-.262	-.273	-.285	-.277	-.270
20.	-.220	-.197	-.195	-.205	-.215	-.237	-.259	-.280	-.285	-.270
24.	-.197	-.185	-.175	-.177	-.180	-.232	-.234	-.235	-.245	-.270
28.	-.184	-.179	-.175	-.175	-.175	-.195	-.215	-.235	-.245	-.270
32.	-.178	-.177	-.175	-.180	-.185	-.201	-.218	-.235	-.245	-.270
36.	-.163	-.169	-.175	-.185	-.195	-.213	-.226	-.235	-.245	-.270
40.	-.172	-.169	-.165	-.167	-.170	-.192	-.212	-.235	-.245	-.270
44.	-.173	-.177	-.180	-.180	-.180	-.202	-.224	-.235	-.245	-.270
48.	-.192	-.192	-.192	-.192	-.192	-.206	-.220	-.235	-.245	-.270
52.	-.201	-.200	-.200	-.200	-.200	-.202	-.216	-.235	-.245	-.270
56.	-.197	-.198	-.200	-.200	-.200	-.202	-.216	-.235	-.245	-.270
60.	-.190	-.195	-.200	-.200	-.200	-.202	-.216	-.235	-.245	-.270

UNCLASSIFIED

(U) TABLE B16.- Continued (U)

(e) $|\beta| = 20^{\circ}$

ALPHA	MACH NUMBER							1.4	1.6
	0.2	0.4	0.6	0.8	0.9	1.0	1.1		
-12.	-.305	-.297	-.290	-.282	-.275	-.271	-.268	-.255	-.240
-8.	-.305	-.297	-.290	-.282	-.275	-.281	-.288	-.255	-.240
-4.	-.305	-.297	-.290	-.282	-.275	-.281	-.288	-.255	-.240
0.	-.305	-.297	-.290	-.282	-.275	-.281	-.288	-.255	-.240
4.	-.315	-.310	-.305	-.292	-.280	-.275	-.270	-.265	-.250
8.	-.320	-.323	-.325	-.310	-.295	-.280	-.275	-.270	-.260
12.	-.310	-.315	-.320	-.315	-.310	-.299	-.287	-.275	-.268
16.	-.295	-.285	-.275	-.292	-.310	-.310	-.293	-.285	-.277
20.	-.270	-.259	-.247	-.258	-.270	-.273	-.276	-.280	-.285
24.	-.245	-.245	-.240	-.240	-.235	-.235	-.235	-.235	-.245
28.	-.230	-.237	-.245	-.235	-.225	-.225	-.231	-.235	-.245
32.	-.220	-.227	-.235	-.232	-.230	-.232	-.233	-.235	-.245
36.	-.205	-.208	-.210	-.207	-.205	-.215	-.225	-.235	-.245
40.	-.210	-.209	-.207	-.208	-.210	-.218	-.226	-.235	-.245
44.	-.205	-.213	-.220	-.220	-.220	-.225	-.230	-.235	-.245
48.	-.230	-.225	-.220	-.220	-.220	-.225	-.230	-.235	-.245
52.	-.235	-.227	-.220	-.220	-.220	-.225	-.230	-.235	-.245
56.	-.225	-.222	-.220	-.220	-.220	-.225	-.230	-.235	-.245
60.	-.213	-.217	-.220	-.220	-.220	-.225	-.230	-.235	-.245

UNCLASSIFIED

(U) TABLE B16.- Continued (U)

(F) $|\beta| = 240$

ALPHA	MACH NUMBER						APPENDIX B			
	0.2	0.4	0.6	0.8	1.0	1.1				
-12.	-.365	-.350	-.335	-.325	-.315	-.295	-.275	-.255	-.240	-.225
-8.	-.365	-.350	-.335	-.325	-.315	-.295	-.275	-.255	-.240	-.225
-4.	-.365	-.350	-.335	-.325	-.315	-.295	-.275	-.255	-.240	-.225
0.	-.365	-.350	-.335	-.325	-.315	-.295	-.275	-.255	-.240	-.225
4.	-.357	-.353	-.350	-.340	-.330	-.310	-.287	-.265	-.250	-.235
8.	-.360	-.370	-.380	-.360	-.340	-.312	-.293	-.270	-.260	-.250
12.	-.356	-.358	-.370	-.362	-.355	-.327	-.302	-.275	-.268	-.262
16.	-.351	-.343	-.335	-.350	-.365	-.341	-.313	-.285	-.277	-.270
20.	-.332	-.320	-.312	-.321	-.330	-.313	-.296	-.280	-.285	-.270
24.	-.299	-.307	-.315	-.302	-.290	-.271	-.253	-.235	-.245	-.270
28.	-.293	-.296	-.310	-.292	-.275	-.261	-.248	-.235	-.245	-.270
32.	-.256	-.268	-.282	-.271	-.260	-.252	-.243	-.235	-.245	-.270
36.	-.241	-.243	-.245	-.242	-.240	-.238	-.236	-.235	-.245	-.270
40.	-.244	-.242	-.240	-.240	-.240	-.238	-.236	-.235	-.245	-.270
44.	-.243	-.246	-.250	-.250	-.250	-.245	-.240	-.236	-.245	-.270
48.	-.258	-.254	-.250	-.250	-.250	-.245	-.240	-.235	-.245	-.270
52.	-.265	-.257	-.250	-.250	-.250	-.245	-.240	-.235	-.245	-.270
56.	-.253	-.252	-.250	-.250	-.250	-.245	-.240	-.235	-.245	-.270
60.	-.242	-.246	-.250	-.250	-.250	-.245	-.245	-.235	-.245	-.270

UNCLASSIFIED

(U) TABLE B16.- Concluded (U)

(g) $|\beta| = 28^\circ$

MACH NUMBER

ALPHA	0.2	0.4	0.6	0.8	0.9	1.0	1.1	1.2	1.4	1.6
-12.	-•425	-•402	-•380	-•362	-•345	-•315	-•285	-•255	-•240	-•225
-8.	-•425	-•402	-•380	-•362	-•345	-•315	-•285	-•255	-•240	-•225
-4.	-•425	-•402	-•380	-•362	-•345	-•315	-•285	-•255	-•240	-•225
0.	-•425	-•402	-•380	-•362	-•345	-•315	-•285	-•255	-•240	-•225
4.	-•399	-•399	-•400	-•387	-•375	-•339	-•302	-•265	-•250	-•235
8.	-•400	-•412	-•425	-•405	-•385	-•346	-•308	-•270	-•260	-•250
12.	-•402	-•403	-•405	-•402	-•400	-•359	-•317	-•275	-•268	-•262
16.	-•407	-•393	-•380	-•405	-•430	-•382	-•333	-•285	-•277	-•270
20.	-•382	-•381	-•380	-•395	-•410	-•366	-•323	-•280	-•285	-•270
24.	-•353	-•364	-•375	-•367	-•360	-•318	-•276	-•235	-•245	-•270
28.	-•314	-•338	-•362	-•343	-•325	-•295	-•265	-•235	-•245	-•270
32.	-•292	-•314	-•335	-•327	-•320	-•292	-•263	-•235	-•245	-•270
36.	-•277	-•281	-•285	-•283	-•280	-•265	-•250	-•235	-•245	-•270
40.	-•278	-•279	-•280	-•280	-•280	-•265	-•250	-•235	-•245	-•270
44.	-•281	-•283	-•285	-•284	-•282	-•266	-•251	-•235	-•245	-•270
48.	-•286	-•285	-•285	-•283	-•282	-•266	-•251	-•235	-•245	-•270
52.	-•295	-•290	-•285	-•283	-•282	-•266	-•251	-•235	-•245	-•270
56.	-•281	-•283	-•285	-•283	-•282	-•266	-•251	-•235	-•245	-•270
60.	-•271	-•278	-•285	-•283	-•282	-•266	-•251	-•235	-•245	-•270

UNCLASSIFIED

APPENDIX B

UNCLASSIFIED

(U) TABLE B17.- CY,2 (U)

MACH	BETA	ALPHA					
		25	30	35	40	45	50
.2	-10.	.1150	.1150	.1050	.1100	.1250	.1450
.2	-5.	.0600	.0600	.0550	.0500	.0550	.0600
.2	0.	0.0000	0.0000	0.0000	-.0100	-.0200	-.0300
.2	5.	-.0600	-.0600	-.0550	-.0600	-.0750	-.0900
.2	10.	-.1150	-.1150	-.1050	-.1100	-.1250	-.1450
.6	-10.	.1010	.1030	.1170	.1090	.1230	.1400
.6	-5.	.0580	.0880	.0950	.0880	.1020	.1200
.6	0.	0.0000	0.0000	0.0000	0.0000	0.0000	0.0000
.6	5.	-.0560	-.0560	-.0610	-.0580	-.0720	-.0860
.6	10.	-.1010	-.1030	-.1170	-.1090	-.1230	-.1400

UNCLASSIFIED

(U) TABLE B18.- $C_{Y\delta_a}$ (PER DEGREE) (U)

ALPHA	MACH NUMBER							1.6
	0.2	0.4	0.6	0.8	0.9	1.0	1.2	
-12.	-0.00020	-0.00020	-0.00025	-0.00020	-0.00020	-0.00010	-0.00010	-0.00004
-6.	-0.00020	-0.00020	-0.00025	-0.00020	-0.00020	-0.00010	-0.00010	-0.00004
-4.	-0.00020	-0.00020	-0.00025	-0.00020	-0.00020	-0.00010	-0.00010	-0.00004
0.	-0.00020	-0.00020	-0.00025	-0.00020	-0.00020	-0.00010	-0.00008	-0.00003
4.	-0.00020	-0.00020	-0.00020	-0.00010	-0.00005	0.00000	0.00000	0.00000
b.	-0.00015	-0.00010	-0.00010	0.00000	0.00010	0.00007	0.00006	0.00000
12.	-0.00005	0.00005	0.00015	0.00015	0.00013	0.00010	0.00008	0.00001
16.	0.00005	0.00010	0.00020	0.00020	0.00015	0.00014	0.00014	0.00002
20.	0.00010	0.00010	0.00020	0.00030	0.00030	0.00020	0.00018	0.00010
24.	0.00010	0.00020	0.00030	0.00040	0.00040	0.00030	0.00020	0.00010
28.	0.00015	0.00035	0.00055	0.00060	0.00065	0.00040	0.00020	0.00010
32.	0.00030	0.00046	0.00062	0.00065	0.00065	0.00040	0.00020	0.00010
36.	0.00050	0.00050	0.00060	0.00060	0.00060	0.00040	0.00020	0.00010
40.	0.00070	0.00070	0.00068	0.00070	0.00070	0.00050	0.00030	0.00018
44.	0.00080	0.00080	0.00080	0.00080	0.00080	0.00060	0.00030	0.00018
48.	0.00065	0.00090	0.00090	0.00090	0.00087	0.00070	0.00040	0.00018
52.	0.00095	0.00095	0.00095	0.00090	0.00093	0.00070	0.00040	0.00018
56.	0.00105	0.00105	0.00105	0.00100	0.00102	0.00080	0.00050	0.00018
60.	0.00110	0.00110	0.00115	0.00110	0.00110	0.00080	0.00050	0.00018

UNCLASSIFIED

APPENDIX B

UNCLASSIFIED

ORIGINAL PAGE IS
OF POOR QUALITY

(U) TABLE B19.- $C_{Y\delta_D}$ (PER DEGREE) (U)

ALPHA	MACH NUMBER						1.4	1.6
	0.2	0.4	0.6	0.8	0.9	1.0		
-12.	-0.00100	-0.00110	-0.00120	-0.00120	-0.00130	-0.00100	-0.00080	-0.00060
-8.	-0.00100	-0.00110	-0.00120	-0.00120	-0.00130	-0.00100	-0.00080	-0.00060
-4.	-0.00100	-0.00110	-0.00120	-0.00120	-0.00130	-0.00100	-0.00080	-0.00060
0.	-0.00100	-0.00110	-0.00120	-0.00120	-0.00130	-0.00100	-0.00080	-0.00060
4.	-0.00120	-0.00130	-0.00140	-0.00140	-0.00140	-0.00130	-0.00120	-0.00100
8.	-0.00130	-0.00150	-0.00160	-0.00150	-0.00130	-0.00130	-0.00140	-0.00140
12.	-0.00110	-0.00140	-0.00170	-0.00150	-0.00130	-0.00140	-0.00150	-0.00160
16.	-0.00100	-0.00130	-0.00170	-0.00120	-0.00080	-0.00100	-0.00120	-0.00150
20.	-0.00080	-0.00080	-0.00070	-0.00050	-0.00020	-0.00050	-0.00090	-0.00120
24.	-0.00030	-0.00030	-0.00080	-0.00050	-0.00020	-0.00050	-0.00090	-0.00120
28.	0.00000	0.00040	0.00060	0.00100	0.00120	0.00040	-0.00040	-0.00120
32.	0.00000	0.00050	0.00090	0.00120	0.00160	0.00070	-0.00020	-0.00120
36.	0.00020	0.00050	0.00070	0.00110	0.00160	0.00070	-0.00020	-0.00120
40.	0.00060	0.00080	0.00110	0.00120	0.00130	0.00040	-0.00040	-0.00120
44.	0.00060	0.00100	0.00130	0.00130	0.00120	0.00040	-0.00040	-0.00120
48.	0.00110	0.00130	0.00150	0.00140	0.00140	0.00050	-0.00040	-0.00120
52.	0.00170	0.00190	0.00210	0.00200	0.00200	0.0100	-0.00010	-0.00120
56.	0.00220	0.00230	0.00250	0.00240	0.00230	0.0120	0.00010	-0.00120
60.	0.00230	0.00230	0.00220	0.00200	0.00100	0.00010	-0.00120	-0.00070

UNCLASSIFIED

UNCLASSIFIED

APPENDIX B

(U) TABLE B20.- $\Delta C_Y \delta_r$ (U)(a) $|\delta_r| = 100$

ALPHA	MACH NUMBER						1.4	1.6
	0.2	0.4	0.6	0.8	1.0	1.1		
-12.	.032	.032	.032	.032	.032	.032	.021	.015
-8.	.032	.032	.032	.032	.032	.032	.021	.015
-4.	.032	.032	.032	.032	.032	.032	.027	.017
0.	.032	.032	.032	.032	.032	.032	.027	.022
4.	.032	.032	.032	.033	.033	.033	.028	.023
8.	.032	.033	.035	.035	.035	.035	.029	.024
12.	.032	.034	.036	.035	.035	.034	.029	.024
16.	.029	.031	.034	.031	.029	.029	.019	.015
20.	.022	.025	.029	.024	.019	.017	.014	.018
24.	.016	.017	.018	.014	.010	.010	.010	.015
28.	.010	.010	.010	.007	.005	.006	.008	.012
32.	.007	.006	.005	.004	.003	.003	.005	.008
36.	.003	.003	.002	.003	.003	.003	.005	.008
40.	0.000	0.000	0.000	0.001	0.002	0.002	0.005	.007
44.	0.000	0.000	0.000	0.000	0.000	0.000	.003	.007
46.	0.000	0.000	0.000	0.000	0.000	0.000	.003	.007
52.	0.000	0.000	0.000	0.000	0.000	0.000	.003	.007
56.	0.000	0.000	0.000	0.000	0.000	0.000	.003	.007
60.	0.000	0.000	0.000	0.000	0.000	0.000	.003	.007

UNCLASSIFIED

(U) TABLE B20.- Continued (U)

	(b) $ \delta_r = 20^\circ$								
	MACH NUMBER								
ALPHA	0.4	0.6	0.8	0.9	1.0	1.1	1.2	1.4	1.6
-12.	.060	.055	.050	.050	.045	.040	.034	.032	.030
-8.	.060	.055	.050	.050	.045	.040	.034	.032	.030
-4.	.060	.055	.050	.050	.045	.040	.034	.032	.030
0.	.060	.055	.050	.050	.045	.040	.035	.030	.024
4.	.062	.060	.056	.050	.046	.042	.038	.030	.020
8.	.063	.060	.058	.050	.046	.042	.037	.030	.020
12.	.062	.060	.060	.050	.048	.045	.041	.037	.030
16.	.057	.056	.055	.050	.042	.040	.036	.030	.018
20.	.045	.044	.044	.040	.029	.027	.025	.023	.020
24.	.032	.030	.028	.020	.013	.015	.017	.018	.018
28.	.020	.018	.016	.010	.007	.011	.014	.018	.018
32.	.011	.010	.008	.006	.004	.009	.014	.016	.018
36.	.004	.004	.004	.004	.004	.009	.014	.018	.018
40.	.001	.001	.001	.002	.003	.008	.013	.018	.018
44.	0.000	0.000	0.000	0.000	0.000	0.008	0.013	0.018	0.016
48.	0.000	0.000	0.000	0.000	0.000	0.008	0.013	0.018	0.018
52.	0.000	0.000	0.000	0.000	0.000	0.008	0.013	0.018	0.016
56.	0.000	0.000	0.000	0.000	0.000	0.008	0.013	0.018	0.016
60.	0.000	0.000	0.000	0.000	0.000	0.008	0.013	0.018	0.016

UNCLASSIFIED

(U) TABLE B20.- Concluded (U)

(b) $|\delta_r| = 30^\circ$

ALPHA	MACH NUMBER						
	0.2	0.4	0.6	0.8	0.9	1.0	1.1
-12.	.052	.070	.060	.050	.045	.050	.050
-8.	.082	.070	.060	.050	.045	.050	.050
-4.	.082	.070	.060	.050	.045	.050	.045
0.	.082	.070	.060	.050	.045	.050	.050
4.	.085	.070	.060	.050	.045	.050	.045
8.	.087	.074	.060	.050	.045	.050	.050
12.	.087	.074	.060	.050	.045	.050	.050
16.	.080	.069	.058	.045	.032	.040	.047
20.	.065	.055	.045	.030	.016	.022	.028
24.	.047	.036	.025	.017	.008	.014	.020
28.	.030	.021	.013	.008	.003	.011	.019
32.	.018	.014	.010	.007	.003	.011	.019
36.	.008	.008	.008	.005	.003	.011	.019
40.	.003	.003	.003	.001	.000	.011	.019
44.	0.000	0.000	0.000	0.000	0.000	0.011	0.019
48.	0.000	0.000	0.000	0.000	0.000	0.011	0.019
52.	0.000	0.000	0.000	0.000	0.000	0.011	0.019
56.	0.000	0.000	0.000	0.000	0.000	0.011	0.019
60.	0.000	0.000	0.000	0.000	0.000	0.011	0.019

UNCLASSIFIED

UNCLASSIFIED

APPENDIX B

(U) TABLE B21.- $K\delta_r$ (U)

Mach number	$K\delta_r$
0.2	1.000
.4	.970
.6	.900
.8	.825
.9	.788
1.0	.752
1.1	.718
1.2	.686
1.4	.625
1.6	.570

(U) TABLE B22.- $C_{q,1}$ (U)(a) $|\beta| = 4^\circ$

ALPHA	MACH NUMBER						1.4	1.6
	0.2	0.4	0.6	0.8	0.9	1.0		
-12.	-0.0060	-0.0057	-0.0055	-0.0057	-0.0060	-0.0060	-0.0060	-0.0047
-8.	-0.0060	-0.0057	-0.0055	-0.0057	-0.0060	-0.0060	-0.0060	-0.0047
-4.	-0.0060	-0.0057	-0.0055	-0.0057	-0.0060	-0.0060	-0.0060	-0.0047
0.	-0.0060	-0.0057	-0.0055	-0.0057	-0.0060	-0.0060	-0.0060	-0.0047
4.	-0.0090	-0.0083	-0.0075	-0.0063	-0.0090	-0.0079	-0.0067	-0.0045
8.	-0.0100	-0.0095	-0.0090	-0.0103	-0.0115	-0.0094	-0.0072	-0.0050
12.	-0.0100	-0.0093	-0.0085	-0.0105	-0.0125	-0.0104	-0.0082	-0.0060
16.	-0.0100	-0.0102	-0.0105	-0.0110	-0.0115	-0.0110	-0.0105	-0.0100
20.	-0.0090	-0.0102	-0.0115	-0.0117	-0.0120	-0.0118	-0.0116	-0.0115
24.	-0.0090	-0.0112	-0.0135	-0.0142	-0.0150	-0.0140	-0.0130	-0.0120
28.	-0.0100	-0.0101	-0.0102	-0.0110	-0.0120	-0.0120	-0.0120	-0.0092
32.	-0.0110	-0.0102	-0.0095	-0.0090	-0.0085	-0.0097	-0.0109	-0.0120
36.	-0.0110	-0.0110	-0.0110	-0.0100	-0.0095	-0.0103	-0.0111	-0.0120
40.	-0.0130	-0.0120	-0.0110	-0.0110	-0.0110	-0.0113	-0.0117	-0.0120
44.	-0.0120	-0.0120	-0.0110	-0.0110	-0.0105	-0.0110	-0.0115	-0.0120
48.	-0.0090	-0.0080	-0.0060	-0.0060	-0.0065	-0.0083	-0.0100	-0.0120
52.	-0.0080	-0.0070	-0.0060	-0.0060	-0.0052	-0.0075	-0.0090	-0.0120
56.	-0.0090	-0.0090	-0.0100	-0.0090	-0.0080	-0.0093	-0.0107	-0.0120
60.	-0.0100	-0.0100	-0.0100	-0.0090	-0.0080	-0.0093	-0.0107	-0.0120

UNCLASSIFIED

(U) TABLE B22.- Continued (U)

(b) $|\beta| = 80$

ALPHA	MACH NUMBER						1.4	1.6
	0.2	0.4	0.6	0.8	0.9	1.0		
-12.	-.0100	-.0102	-.0105	-.0107	-.0115	-.0111	-.0108	-.0090
-8.	-.0100	-.0102	-.0105	-.0107	-.0115	-.0111	-.0108	-.0090
-4.	-.0100	-.0102	-.0105	-.0107	-.0115	-.0111	-.0108	-.0090
0.	-.0100	-.0102	-.0105	-.0107	-.0115	-.0111	-.0108	-.0090
4.	-.0150	-.0145	-.0140	-.0145	-.0150	-.0132	-.0115	-.0098
8.	-.0180	-.0182	-.0185	-.0182	-.0180	-.0152	-.0124	-.0096
12.	-.0180	-.0180	-.0180	-.0195	-.0210	-.0177	-.0144	-.0109
16.	-.0180	-.0180	-.0180	-.0200	-.0220	-.0210	-.0200	-.0190
20.	-.0190	-.0201	-.0213	-.0219	-.0225	-.0216	-.0208	-.0200
24.	-.0190	-.0223	-.0255	-.0265	-.0275	-.0260	-.0245	-.0230
28.	-.0170	-.0200	-.0230	-.0222	-.0215	-.0220	-.0225	-.0230
32.	-.0190	-.0187	-.0185	-.0175	-.0165	-.0187	-.0209	-.0230
36.	-.0200	-.0211	-.0222	-.0209	-.0195	-.0207	-.0217	-.0230
40.	-.0230	-.0230	-.0235	-.0232	-.0230	-.0230	-.0230	-.0230
44.	-.0220	-.0220	-.0215	-.0210	-.0205	-.0213	-.0221	-.0230
48.	-.0170	-.0190	-.0210	-.0187	-.0175	-.0193	-.0212	-.0230
52.	-.0160	-.0160	-.0160	-.0160	-.0160	-.0183	-.0207	-.0230
56.	-.0170	-.0170	-.0165	-.0165	-.0165	-.0187	-.0209	-.0230
60.	-.0190	-.0180	-.0165	-.0165	-.0165	-.0187	-.0209	-.0230

UNCLASSIFIED

UNCLASSIFIED

APPENDIX B

(U) TABLE B22.- Continued (U)

(c) $|\beta| = 120^\circ$

ALPHA	MACH NUMBER						
	0.2	0.4	0.6	0.8	0.9	1.0	1.1
-12.	-0.0150	-0.0147	-0.0145	-0.0150	-0.0155	-0.0157	-0.0158
-8.	-0.0150	-0.0147	-0.0145	-0.0150	-0.0155	-0.0157	-0.0158
-4.	-0.0150	-0.0147	-0.0145	-0.0150	-0.0155	-0.0157	-0.0158
0.	-0.0150	-0.0147	-0.0145	-0.0150	-0.0155	-0.0157	-0.0158
4.	-0.0210	-0.0210	-0.0205	-0.0200	-0.0185	-0.0170	-0.0155
8.	-0.0260	-0.0270	-0.0280	-0.0260	-0.0240	-0.0212	-0.0183
12.	-0.0270	-0.0275	-0.0280	-0.0272	-0.0265	-0.0240	-0.0215
16.	-0.0260	-0.0267	-0.0265	-0.0270	-0.0275	-0.0271	-0.0268
20.	-0.0290	-0.0285	-0.0280	-0.0290	-0.0300	-0.0291	-0.0282
24.	-0.0300	-0.0310	-0.0320	-0.0342	-0.0365	-0.0344	-0.0322
28.	-0.0260	-0.0287	-0.0315	-0.0320	-0.0325	-0.0316	-0.0308
32.	-0.0270	-0.0285	-0.0300	-0.0282	-0.0265	-0.0277	-0.0288
36.	-0.0290	-0.0302	-0.0315	-0.0285	-0.0255	-0.0270	-0.0285
40.	-0.0310	-0.0315	-0.0320	-0.0320	-0.0320	-0.0314	-0.0307
44.	-0.0300	-0.0270	-0.0245	-0.0260	-0.0215	-0.0296	-0.0298
48.	-0.0260	-0.0250	-0.0242	-0.0252	-0.0260	-0.0273	-0.0286
52.	-0.0250	-0.0250	-0.0250	-0.0250	-0.0250	-0.0267	-0.0283
56.	-0.0260	-0.0257	-0.0255	-0.0255	-0.0255	-0.0270	-0.0285
60.	-0.0280	-0.0267	-0.0255	-0.0255	-0.0255	-0.0270	-0.0283

UNCLASSIFIED

(U) TABLE B22.- Continued (U)

(d) $|\beta| = 160$

ALPHA	MACH NUMBER						1.4	1.6
	0.2	0.4	0.6	0.8	0.9	1.0		
-12.	-0.0200	-0.0185	-0.0170	-0.0175	-0.0180	-0.0187	-0.0194	-0.0195
-8.	-0.0200	-0.0185	-0.0170	-0.0175	-0.0180	-0.0187	-0.0194	-0.0195
-4.	-0.0200	-0.0185	-0.0170	-0.0175	-0.0180	-0.0187	-0.0194	-0.0195
0.	-0.0200	-0.0185	-0.0170	-0.0175	-0.0180	-0.0187	-0.0194	-0.0195
4.	-0.0280	-0.0257	-0.0235	-0.0237	-0.0230	-0.0215	-0.0199	-0.0195
8.	-0.0350	-0.0335	-0.0320	-0.0300	-0.0280	-0.0247	-0.0216	-0.0183
12.	-0.0390	-0.0355	-0.0320	-0.0315	-0.0310	-0.0277	-0.0246	-0.0199
16.	-0.0350	-0.0327	-0.0305	-0.0307	-0.0310	-0.0310	-0.0310	-0.0180
20.	-0.0380	-0.0350	-0.0320	-0.0332	-0.0345	-0.0331	-0.0338	-0.0180
24.	-0.0400	-0.0380	-0.0375	-0.0412	-0.0450	-0.0420	-0.0390	-0.0175
28.	-0.0380	-0.0385	-0.0442	-0.0500	-0.0453	-0.0407	-0.0360	-0.0175
32.	-0.0360	-0.0380	-0.0400	-0.0432	-0.0465	-0.0428	-0.0394	-0.0175
36.	-0.0360	-0.0397	-0.0435	-0.0442	-0.0350	-0.0353	-0.0356	-0.0175
40.	-0.0390	-0.0390	-0.0395	-0.0392	-0.0390	-0.0380	-0.0370	-0.0175
44.	-0.0390	-0.0385	-0.0380	-0.0377	-0.0375	-0.0370	-0.0365	-0.0175
48.	-0.0350	-0.0350	-0.0347	-0.0347	-0.0347	-0.0351	-0.0355	-0.0175
52.	-0.0350	-0.0350	-0.0345	-0.0347	-0.0350	-0.0353	-0.0356	-0.0175
56.	-0.0360	-0.0360	-0.0360	-0.0358	-0.0357	-0.0358	-0.0359	-0.0175
60.	-0.0380	-0.0370	-0.0360	-0.0359	-0.0357	-0.0358	-0.0359	-0.0175

UNCLASSIFIED

(U) TABLE B22.- Continued (U)

(e) $|\beta| = 20^\circ$

ALPHA	MACH NUMBER						1.4	1.6
	0.2	0.4	0.6	0.8	1.0	1.1		
-12.	-0.0250	-0.0212	-0.0175	-0.0187	-0.0200	-0.0200	-0.0200	-0.0195
-8.	-0.0250	-0.0212	-0.0175	-0.0187	-0.0200	-0.0200	-0.0200	-0.0190
-4.	-0.0250	-0.0212	-0.0175	-0.0187	-0.0200	-0.0200	-0.0200	-0.0190
0.	-0.0250	-0.0212	-0.0175	-0.0187	-0.0200	-0.0200	-0.0200	-0.0190
4.	-0.0350	-0.0312	-0.0275	-0.0250	-0.0230	-0.0215	-0.0199	-0.0178
8.	-0.0440	-0.0395	-0.0350	-0.0320	-0.0290	-0.0255	-0.0220	-0.0185
12.	-0.0480	-0.0420	-0.0360	-0.0350	-0.0340	-0.0299	-0.0257	-0.0215
16.	-0.0440	-0.0358	-0.0330	-0.0340	-0.0350	-0.0336	-0.0323	-0.0310
20.	-0.0470	-0.0415	-0.0360	-0.0380	-0.0400	-0.0338	-0.0337	-0.0335
24.	-0.0500	-0.0490	-0.0480	-0.0540	-0.0600	-0.0520	-0.0440	-0.0360
28.	-0.0500	-0.0475	-0.0450	-0.0550	-0.0650	-0.0553	-0.0457	-0.0360
32.	-0.0440	-0.0430	-0.0420	-0.0532	-0.0645	-0.0551	-0.0455	-0.0360
36.	-0.0440	-0.0427	-0.0412	-0.0480	-0.0550	-0.0486	-0.0423	-0.0360
40.	-0.0460	-0.0459	-0.0457	-0.0464	-0.0470	-0.0432	-0.0396	-0.0360
44.	-0.0460	-0.0457	-0.0455	-0.0452	-0.0450	-0.0420	-0.0390	-0.0360
48.	-0.0450	-0.0450	-0.0455	-0.0452	-0.0450	-0.0420	-0.0390	-0.0360
52.	-0.0450	-0.0450	-0.0455	-0.0452	-0.0450	-0.0420	-0.0390	-0.0360
56.	-0.0470	-0.0460	-0.0455	-0.0452	-0.0450	-0.0420	-0.0390	-0.0360
60.	-0.0480	-0.0470	-0.0455	-0.0452	-0.0450	-0.0420	-0.0390	-0.0360

UNCLASSIFIED

(U) TABLE B22.- Continued (U)

(F) $|\beta| = 24^\circ$

ALPHA	MACH NUMBER					
	0.2	0.4	0.6	0.8	0.9	1.0
-12.	-0.0250	-0.0210	-0.0170	-0.0190	-0.0210	-0.0206
-8.	-0.0250	-0.0210	-0.0170	-0.0190	-0.0210	-0.0203
-4.	-0.0250	-0.0210	-0.0170	-0.0190	-0.0210	-0.0203
0.	-0.0250	-0.0210	-0.0170	-0.0190	-0.0210	-0.0206
4.	-0.0370	-0.0320	-0.0260	-0.0250	-0.0240	-0.0220
8.	-0.0460	-0.0425	-0.0390	-0.0355	-0.0320	-0.0275
12.	-0.0520	-0.0470	-0.0420	-0.0405	-0.0390	-0.0335
16.	-0.0520	-0.0455	-0.0390	-0.0400	-0.0410	-0.0376
20.	-0.0560	-0.0490	-0.0420	-0.0440	-0.0460	-0.0422
24.	-0.0620	-0.0595	-0.0570	-0.0620	-0.0670	-0.0566
28.	-0.0570	-0.0580	-0.0590	-0.0680	-0.0770	-0.0640
32.	-0.0540	-0.0537	-0.0535	-0.0642	-0.0750	-0.0650
36.	-0.0530	-0.0525	-0.0520	-0.0565	-0.0650	-0.0550
40.	-0.0530	-0.0535	-0.0540	-0.0540	-0.0540	-0.0480
44.	-0.0540	-0.0535	-0.0530	-0.0530	-0.0530	-0.0474
48.	-0.0530	-0.0530	-0.0530	-0.0530	-0.0530	-0.0474
52.	-0.0530	-0.0530	-0.0530	-0.0530	-0.0530	-0.0474
56.	-0.0550	-0.0540	-0.0530	-0.0530	-0.0530	-0.0474
60.	-0.0560	-0.0545	-0.0530	-0.0530	-0.0530	-0.0474

UNCLASSIFIED

(U) TABLE B22.- Concluded (U)

(g) $|\beta| = 28^\circ$

ALPHA	MACH NUMBER						1.4	1.6
	0.2	0.4	0.6	0.8	0.9	1.0		
-12.	-.0250	-.0210	-.0170	-.0190	-.0210	-.0206	-.0203	-.0195
-8.	-.0250	-.0210	-.0170	-.0190	-.0210	-.0206	-.0203	-.0195
-4.	-.0250	-.0210	-.0170	-.0190	-.0210	-.0206	-.0203	-.0195
0.	-.0250	-.0210	-.0170	-.0190	-.0210	-.0206	-.0203	-.0195
4.	-.0380	-.0320	-.0260	-.0250	-.0240	-.0220	-.0200	-.0180
8.	-.0480	-.0435	-.0390	-.0370	-.0350	-.0295	-.0240	-.0180
12.	-.0550	-.0515	-.0480	-.0455	-.0430	-.0357	-.0285	-.0215
16.	-.0590	-.0530	-.0470	-.0460	-.0450	-.0405	-.0356	-.0310
20.	-.0650	-.0660	-.0670	-.0695	-.0520	-.0459	-.0397	-.0335
24.	-.0730	-.0700	-.0680	-.0770	-.0800	-.0610	-.0505	-.0360
28.	-.0640	-.0660	-.0670	-.0770	-.0870	-.0600	-.0430	-.0360
32.	-.0630	-.0630	-.0630	-.0735	-.0840	-.0680	-.0520	-.0360
36.	-.0620	-.0620	-.0620	-.0690	-.0730	-.0606	-.0483	-.0360
40.	-.0610	-.0610	-.0610	-.0610	-.0610	-.0530	-.0440	-.0360
44.	-.0600	-.0600	-.0600	-.0600	-.0600	-.0520	-.0440	-.0360
48.	-.0600	-.0600	-.0600	-.0600	-.0600	-.0520	-.0440	-.0360
52.	-.0610	-.0600	-.0600	-.0600	-.0600	-.0520	-.0440	-.0360
56.	-.0630	-.0620	-.0600	-.0600	-.0600	-.0520	-.0440	-.0360
60.	-.0650	-.0630	-.0600	-.0600	-.0600	-.0520	-.0440	-.0360

UNCLASSIFIED

(U) TABLE B23.- $C_{\lambda,2}$ (U)

MACH	BETA	ALPHA					
		25	30	35	40	45	50
.2	-10.	.0200	.0220	.0340	.0290	.0250	.0200
.2	-5.	.0150	.0150	-.0100	.0160	.0130	.0100
.2	0.	0.0000	.0080	-.0100	.0070	.0020	0.0000
.2	5.	-.0080	-.0070	.0050	-.0150	-.0130	-.0100
.2	10.	-.0200	-.0170	-.0120	-.0290	-.0250	-.0200
.6	-10.	.0300	.0245	.0262	.0278	.0220	.0206
.6	-5.	.0171	.0116	.0136	.0141	.0130	.0076
.6	0.	0.0000	0.0000	0.0000	0.0000	0.0000	0.0000
.6	5.	-.0171	-.0116	-.0136	-.0141	-.0130	-.0076
.6	10.	-.0300	-.0245	-.0262	-.0278	-.0220	-.0206

UNCLASSIFIED

APPENDIX B

(U) TABLE B24.- C_{λ_p} (PER RADIANS) (U)

	MACH NUMBER						
ALPHA	0.2	0.4	0.6	0.8	0.9	1.0	1.1
-12.	-.29	-.25	-.23	-.21	-.20	-.20	-.23
-8.	-.29	-.25	-.23	-.21	-.20	-.20	-.23
-4.	-.29	-.25	-.23	-.25	-.20	-.20	-.23
0.	-.29	-.25	-.23	-.21	-.20	-.20	-.23
4.	-.26	-.25	-.23	-.21	-.20	-.20	-.23
8.	-.27	-.25	-.23	-.21	-.20	-.20	-.23
12.	-.29	-.25	-.23	-.21	-.20	-.20	-.22
16.	-.24	-.25	-.23	-.21	-.20	-.20	-.22
20.	-.28	-.25	-.23	-.21	-.20	-.20	-.22
24.	-.35	-.25	-.16	-.18	-.19	-.19	-.21
28.	-.36	-.30	-.22	-.23	-.23	-.22	-.21
32.	-.40	-.39	-.38	-.38	-.38	-.32	-.26
36.	-.52	-.52	-.51	-.51	-.40	-.30	-.20
40.	-.55	-.55	-.55	-.54	-.43	-.30	-.20
44.	-.42	-.42	-.42	-.41	-.34	-.27	-.20
48.	-.32	-.37	-.42	-.41	-.34	-.27	-.20
52.	-.31	-.37	-.42	-.41	-.34	-.27	-.20
56.	-.33	-.37	-.42	-.41	-.34	-.27	-.20
60.	-.32	-.37	-.42	-.41	-.34	-.27	-.20

UNCLASSIFIED

(U) TABLE B25.- C_{x_r} (PER RADIAN) (U)

ALPHA	MACH NUMBER						1.4	1.6
	0.2	0.4	0.6	0.8	0.9	1.0		
-12.	.100	.100	.100	.100	.080	.060	.037	.035
-8.	.100	.100	.100	.100	.080	.060	.037	.035
-4.	.100	.100	.100	.100	.080	.060	.037	.035
0.	.100	.100	.100	.100	.080	.060	.037	.035
4.	.140	.140	.140	.140	.120	.100	.080	.070
8.	.210	.210	.210	.210	.180	.150	.122	.110
12.	.310	.310	.310	.310	.260	.210	.166	.140
16.	.420	.420	.420	.420	.350	.280	.211	.180
20.	.420	.420	.420	.420	.360	.300	.242	.200
24.	.500	.500	.500	.500	.410	.320	.242	.200
28.	.580	.580	.580	.580	.470	.360	.242	.200
32.	.550	.550	.550	.550	.450	.350	.242	.200
36.	.510	.510	.510	.510	.400	.320	.242	.200
40.	.500	.500	.500	.500	.410	.320	.242	.200
44.	.150	.150	.150	.150	.180	.210	.242	.200
48.	.070	.070	.070	.070	.130	.190	.242	.200
52.	.070	.070	.070	.070	.130	.190	.242	.200
56.	.060	.060	.060	.060	.120	.180	.242	.200
60.	.020	.020	.020	.020	.090	.160	.242	.200

UNCLASSIFIED

UNCLASSIFIED

APPENDIX B

(U) TABLE B26.- C_{δ_a} (PER DEGREE) (U)

ALPHA	MACH NUMBER						
	0.2	0.4	0.6	0.8	0.9	1.0	1.2
-12.	.00086	.00080	.00066	.00060	.00045	.00040	.00030
-8.	.00086	.00080	.00066	.00060	.00045	.00040	.00030
-4.	.00066	.00080	.00066	.00060	.00045	.00040	.00030
0.	.00066	.00080	.00066	.00060	.00045	.00040	.00030
4.	.00086	.00080	.00066	.00060	.00046	.00040	.00030
8.	.00088	.00080	.00064	.00060	.00046	.00040	.00036
12.	.00065	.00050	.00042	.00043	.00044	.00044	.00035
16.	.00043	.00043	.00035	.00037	.00039	.00032	.00024
20.	.00037	.00036	.00035	.00034	.00032	.00028	.00025
24.	.00029	.00032	.00035	.00030	.00024	.00023	.00023
28.	.00028	.00027	.00026	.00022	.00018	.00019	.00021
32.	.00030	.00025	.00020	.00020	.00019	.00023	.00021
36.	.00029	.00026	.00022	.00024	.00028	.00026	.00024
40.	.00025	.00025	.00024	.00024	.00025	.00024	.00023
44.	.00020	.00020	.00020	.00020	.00021	.00021	.00024
48.	.00017	.00018	.00018	.00018	.00018	.00019	.00019
52.	.00016	.00016	.00016	.00017	.00017	.00017	.00019
56.	.00016	.00016	.00016	.00016	.00016	.00018	.00020
60.	.00016	.00016	.00016	.00016	.00016	.00018	.00020

UNCLASSIFIED

(U) TABLE B27.- $C_{\delta D}$ (PER DEGREE) (U)

ALPHA	MACH NUMBER						1.4	1.6
	0.2	0.4	0.6	0.8	0.9	1.0		
-12.	.00075	.00075	.00075	.00072	.00070	.00072	.00073	.00075
-8.	.00075	.00075	.00075	.00072	.00070	.00072	.00073	.00075
-4.	.00075	.00075	.00075	.00072	.00070	.00072	.00073	.00075
0.	.00075	.00075	.00075	.00072	.00070	.00072	.00073	.00075
4.	.00070	.00072	.00075	.00072	.00070	.00072	.00070	.00070
8.	.00075	.00072	.00075	.00072	.00070	.00061	.00053	.00045
12.	.00080	.00072	.00065	.00067	.00070	.00063	.00056	.00050
16.	.00085	.00067	.00060	.00067	.00075	.00068	.00061	.00055
20.	.00090	.00083	.00077	.00078	.00080	.00071	.00063	.00055
24.	.00092	.00088	.00085	.00083	.00082	.00073	.00064	.00055
28.	.00095	.00097	.00100	.00120	.00125	.00100	.00076	.00055
32.	.00105	.00097	.00099	.00087	.00075	.00068	.00060	.00055
36.	.00107	.00098	.00090	.00087	.00075	.00068	.00061	.00055
40.	.00107	.00108	.00110	.00110	.00110	.00091	.00073	.00055
44.	.00100	.00098	.00097	.00098	.00100	.00085	.00070	.00055
48.	.00097	.00091	.00085	.00085	.00085	.00075	.00065	.00055
52.	.00092	.00086	.00080	.00080	.00080	.00071	.00063	.00055
56.	.00087	.00082	.00075	.00075	.00075	.00068	.00061	.00055
60.	.00082	.00077	.00072	.00073	.00075	.00068	.00061	.00055

UNCLASSIFIED

UNCLASSIFIED

APPENDIX B

(U) TABLE B28.- $\Delta C_{\lambda \delta_r}$ (U)(a) $|\delta_r| = 10^\circ$

ALPHA	MACH NUMBER							1.4	1.6
	0.2	0.4	0.6	0.8	0.9	1.0	1.1		
-12.	.00200	.00170	.00130	.00100	.00080	.00085	.00090	.00095	.00100
-8.	.00200	.00170	.00130	.00100	.00080	.00085	.00090	.00095	.00100
-4.	.00200	.00170	.00130	.00100	.00080	.00085	.00090	.00095	.00100
0.	.00200	.00170	.00130	.00100	.00080	.00087	.00093	.00100	.00100
4.	.00150	.00140	.00120	.00090	.00070	.00083	.00097	.00110	.00100
8.	.00100	.00090	.00080	.00040	.00020	.00050	.00090	.00120	.00090
12.	.00100	.00060	.00020	.00010	0.00000	.00040	.00080	.00110	.00090
16.	.00080	.00050	.00020	.00010	0.00000	.00030	.00060	.00080	.00070
20.	.00020	0.00000	.00020	.00010	0.00000	.00020	.00040	.00060	.00070
24.	0.00000	.00010	.00030	.00010	0.00000	.00010	.00030	.00040	.00060
28.	.00040	.00060	.00080	.00040	.00030	.00030	.00040	.00040	.00080
32.	.00100	.00100	.00100	.00080	.00070	.00060	.00050	.00040	.00060
36.	.00120	.00110	.00100	.00080	.00070	.00060	.00050	.00040	.00060
40.	.00090	.00090	.00080	.00080	.00090	.00070	.00055	.00040	.00060
44.	.00010	.00010	.00010	.00010	.00010	.00020	.00030	.00040	.00060
48.	0.00000	0.00000	0.00000	0.00000	0.00000	0.00000	0.00020	.00030	.00040
52.	0.00000	0.00000	0.00000	0.00000	0.00000	0.00000	0.00020	.00030	.00040
56.	0.00000	0.00000	0.00000	0.00000	0.00000	0.00000	0.00020	.00030	.00040
60.	0.00000	0.00000	0.00000	0.00000	0.00000	0.00020	.00030	.00040	.00060

UNCLASSIFIED

APPENDIX B

UNCLASSIFIED

(U) TABLE B28.- Continued (U)

(b) $|\delta_r| = 20^\circ$

ALPHA	MACH NUMBER						1.4	1.6
	0.2	0.4	0.6	0.8	0.9	1.0		
-12.	.00400	.00300	.00210	.00170	.00160	.00180	.00200	.00190
-8.	.00400	.00300	.00210	.00170	.00160	.00180	.00200	.00190
-4.	.00400	.00300	.00210	.00170	.00160	.00180	.00200	.00195
0.	.00400	.00300	.00210	.00170	.00160	.00180	.00200	.00200
4.	.00280	.00240	.00190	.00140	.00120	.00150	.00190	.00210
8.	.00190	.00170	.00140	.00070	.00040	.00100	.00170	.00230
12.	.000200	.00130	.00050	.00010	.00000	.00070	.00140	.00210
16.	.000120	.00080	.00040	.00010	.00000	.00050	.00100	.00150
20.	-.000040	0.00000	.00040	.00010	0.00000	.00040	.00080	.00120
24.	-.00010	.00040	.00080	.00020	0.00000	.00030	.00060	.00100
28.	.00090	.00120	.00150	.00090	.00060	.00060	.00120	.00160
32.	.00200	.00200	.00200	.00160	.00140	.00110	.00090	.00120
36.	.00240	.00220	.00200	.00160	.00140	.00110	.00090	.00110
40.	.00170	.00170	.00170	.00180	.00140	.00110	.00100	.00110
44.	.00020	.00020	.00020	.00030	.00030	.00040	.00050	.00060
48.	0.00000	0.00000	0.00000	0.00000	0.00000	0.00020	0.00040	0.00060
52.	0.00000	0.00000	0.00000	0.00000	0.00000	0.00020	0.00040	0.00060
56.	0.00000	0.00000	0.00000	0.00000	0.00000	0.00020	0.00040	0.00060
60.	0.00000	0.00000	0.00000	0.00000	0.00000	0.00020	0.00040	0.00060

UNCLASSIFIED

(U) TABLE B28.- Concluded (U)

	(C) $ \delta_r = 30^\circ$						
	MACH NUMBER						
ALPHA	0.2	0.4	0.6	0.8	0.9	1.0	1.1
-12.	.00520	.00380	.00250	.00220	.00200	.00240	.00270
-8.	.00520	.00380	.00250	.00220	.00200	.00240	.00270
-4.	.00520	.00380	.00250	.00220	.00200	.00240	.00270
0.	.00520	.00380	.00250	.00220	.00200	.00240	.00270
4.	.00370	.00300	.00230	.00180	.00150	.00210	.00270
8.	.00260	.00220	.00170	.00090	.00050	.00150	.00250
12.	.00250	.00150	.00060	.00020	.00010	.00120	.00230
16.	.00180	.00120	.00050	.00020	.00000	.00070	.00140
20.	-.00050	0.00000	.00050	.00020	.00000	.00060	.00120
24.	-.00020	.00050	.00120	.00050	.00010	.00050	.00090
28.	.00100	.00160	.00220	.00140	.00100	.00100	.00100
32.	.00310	.00300	.00300	.00240	.00210	.00180	.00130
36.	.00370	.00330	.00300	.00250	.00220	.00180	.00140
40.	.00260	.00260	.00270	.00260	.00260	.00210	.00150
44.	.00030	.00030	.00040	.00040	.00040	.00060	.00080
48.	0.00000	0.00000	0.00000	0.00000	0.00000	0.00000	0.00000
52.	0.00000	0.00000	0.00000	0.00000	0.00000	0.00000	0.00000
56.	0.00000	0.00000	0.00000	0.00000	0.00000	0.00000	0.00000
60.	0.00000	0.00000	0.00000	0.00000	0.00000	0.00000	0.00000

UNCLASSIFIED

APPENDIX B

ORIGINAL PAGE IS
OF POOR QUALITY

UNCLASSIFIED

APPENDIX B

(U) TABLE B29.- $K_{\delta_{rl}}$ (U)

Mach number	$K_{\delta_{rl}}$
0.2	1.000
.4	.960
.6	.835
.8	.721
.9	.670
1.0	.623
1.1	.577
1.2	.531
1.4	.434
1.6	.325

UNCLASSIFIED

(U) TABLE B30.- $\Delta C_{L, sb}$ (U)(a) $|\beta| = 4^\circ$

ALPHA	MACH NUMBER						1.4	1.6
	0.2	0.4	0.6	0.8	0.9	1.0		
-12.	0.0000	0.0000	0.0000	0.0000	0.0010	0.0030	0.0050	0.0040
-8.	0.0000	0.0000	0.0000	0.0000	0.0010	0.0030	0.0050	0.0040
-4.	0.0000	0.0000	0.0000	0.0000	0.0010	0.0030	0.0050	0.0040
0.	0.0000	0.0000	0.0000	0.0000	0.0010	0.0030	0.0050	0.0040
4.	0.0000	0.0000	0.0000	0.0000	0.0010	0.0020	0.0030	0.0020
8.	0.0000	0.0000	0.0000	0.0000	0.0010	0.0010	0.0010	0.0000
12.	0.0000	0.0000	0.0000	0.0010	0.0020	0.0020	0.0020	0.0000
16.	-0.0010	-0.0010	-0.0020	0.0000	0.0010	0.0020	0.0020	0.0000
20.	-0.0020	-0.0020	-0.0020	0.0010	0.0040	0.0030	0.0010	0.0000
24.	0.0040	0.0030	0.0020	0.0020	0.0020	0.0020	0.0010	0.0000
28.	0.0050	0.0030	0.0010	0.0005	0.0000	0.0000	0.0010	0.0000
32.	0.0020	0.0010	0.0000	0.0000	0.0000	0.0000	0.0000	0.0000
36.	0.0000	0.0000	0.0000	0.0000	0.0000	0.0000	0.0000	0.0000
40.	0.0000	0.0000	0.0000	0.0000	0.0000	0.0000	0.0000	0.0000
44.	0.0000	0.0000	0.0000	0.0000	0.0000	0.0000	0.0000	0.0000
48.	0.0000	0.0000	0.0000	0.0000	0.0000	0.0000	0.0000	0.0000
52.	0.0000	0.0000	0.0000	0.0000	0.0000	0.0000	0.0000	0.0000
56.	0.0000	0.0000	0.0000	0.0000	0.0000	0.0000	0.0000	0.0000
60.	0.0000	0.0000	0.0000	0.0000	0.0000	0.0000	0.0000	0.0000

UNCLASSIFIED

(U) TABLE B30.- Continued (U)

(b) $|\beta| = 8^\circ$

ALPHA	MACH NUMBER						1.4	1.6
	0.2	0.4	0.6	0.8	0.9	1.0		
-12.	.0020	.0020	.0020	.0020	.0025	.0050	.0075	.0100
-8.	.0020	.0020	.0020	.0020	.0025	.0050	.0075	.0100
-4.	.0020	.0020	.0020	.0020	.0025	.0050	.0075	.0100
0.	.0020	.0020	.0020	.0020	.0025	.0050	.0075	.0100
4.	.0020	.0020	.0020	.0020	.0025	.0050	.0075	.0100
8.	.0020	.0020	.0020	.0020	.0025	.0050	.0075	.0100
12.	.0020	.0020	.0020	.0020	.0025	.0050	.0075	.0100
16.	-.0020	-.0020	-.0020	0.0000	.0025	.0050	.0075	.0100
20.	-.0030	-.0020	0.0000	.0000	.0030	.0060	.0090	.0120
24.	.0125	.0030	.0040	.0040	.0050	.0080	.0110	.0140
28.	.0125	.0020	.0030	.0030	.0040	.0070	.0100	.0130
32.	.0020	.0010	.0010	.0010	.0015	.0030	.0050	.0070
36.	0.0000	0.0000	0.0000	0.0000	0.0000	0.0000	0.0000	0.0000
40.	0.0000	0.0000	0.0000	0.0000	0.0000	0.0000	0.0000	0.0000
44.	0.0000	0.0000	0.0000	0.0000	0.0000	0.0000	0.0000	0.0000
48.	0.0000	0.0000	0.0000	0.0000	0.0000	0.0000	0.0000	0.0000
52.	0.0000	0.0000	0.0000	0.0000	0.0000	0.0000	0.0000	0.0000
56.	0.0000	0.0000	0.0000	0.0000	0.0000	0.0000	0.0000	0.0000
60.	0.0000	0.0000	0.0000	0.0000	0.0000	0.0000	0.0000	0.0000

UNCLASSIFIED

(U) TABLE B30.- Continued (U)

(C) $|\beta| = 12^\circ$

ALPHA	MACH NUMBER						1.4	1.6
	0.4	0.6	0.8	0.9	1.0	1.1		
-12.	.0025	.0025	.0025	.0030	.0035	.0070	.0100	.0130
-8.	.0025	.0025	.0025	.0030	.0035	.0070	.0100	.0130
-4.	.0025	.0025	.0025	.0030	.0035	.0070	.0100	.0130
0.	.0025	.0025	.0025	.0030	.0035	.0070	.0100	.0125
4.	.0025	.0025	.0025	.0030	.0035	.0045	.0055	.0065
8.	.0025	.0025	.0025	.0030	.0030	.0030	.0040	.0020
12.	.0025	.0025	.0025	.0030	.0035	.0040	.0040	.0045
16.	.0010	.0010	.0010	.0020	.0035	.0050	.0060	.0070
20.	.0010	.0010	.0020	.0020	.0030	.0030	.0040	.0040
24.	.0150	.0110	.0070	.0100	.0120	.0080	.0040	.0000
28.	.0150	.0100	.0050	.0050	.0040	.0030	.0010	.0000
32.	.0030	.0020	.0020	.0020	.0015	.0010	.0005	.0000
36.	0.0000	0.0000	0.0000	0.0000	0.0000	0.0000	0.0000	0.0000
40.	0.0000	0.0000	0.0000	0.0000	0.0000	0.0000	0.0000	0.0000
44.	0.0000	0.0000	0.0000	0.0000	0.0000	0.0000	0.0000	0.0000
48.	0.0000	0.0000	0.0000	0.0000	0.0000	0.0000	0.0000	0.0000
52.	0.0000	0.0000	0.0000	0.0000	0.0000	0.0000	0.0000	0.0000
56.	0.0000	0.0000	0.0000	0.0000	0.0000	0.0000	0.0000	0.0000
60.	0.0000	0.0000	0.0000	0.0000	0.0000	0.0000	0.0000	0.0000

UNCLASSIFIED

(U) TABLE B30.- Concluded (U)

	(d)	$ \beta = 16^\circ$	MACH NUMBER							
ALPHA			0.6	0.8	0.9	1.0	1.1	1.2	1.4	1.6
-12.	.0030	.0030	.0030	.0030	.0035	.0070	.0100	.0130	.0060	.0000
-8.	.0030	.0030	.0030	.0030	.0035	.0070	.0100	.0130	.0060	.0000
-4.	.0030	.0030	.0030	.0030	.0035	.0070	.0100	.0130	.0060	.0000
0.	.0030	.0030	.0030	.0030	.0035	.0070	.0100	.0125	.0060	.0000
4.	.0030	.0030	.0030	.0030	.0035	.0045	.0055	.0065	.0030	.0000
8.	.0030	.0030	.0030	.0030	.0030	.0030	.0040	.0040	.0020	.0000
12.	.0030	.0030	.0030	.0030	.0035	.0040	.0040	.0045	.0020	.0000
16.	.0015	.0015	.0015	.0015	.0055	.0060	.0060	.0070	.0030	.0000
20.	.0010	.0020	.0030	.0030	.0030	.0030	.0030	.0040	.0020	.0000
24.	.0150	.0110	.0080	.0110	.0140	.0100	.0050	.0000	.0000	.0000
28.	.0150	.0100	.0050	.0050	.0055	.0040	.0020	.0000	.0000	.0000
32.	.0030	.0020	.0020	.0020	.0025	.0020	.0010	.0000	.0000	.0000
36.	0.0000	0.0000	0.0000	0.0000	0.0000	0.0000	0.0000	0.0000	0.0000	0.0000
40.	0.0000	0.0000	0.0000	0.0000	0.0000	0.0000	0.0000	0.0000	0.0000	0.0000
44.	0.0000	0.0000	0.0000	0.0000	0.0000	0.0000	0.0000	0.0000	0.0000	0.0000
48.	0.0000	0.0000	0.0000	0.0000	0.0000	0.0000	0.0000	0.0000	0.0000	0.0000
52.	0.0000	0.0000	0.0000	0.0000	0.0000	0.0000	0.0000	0.0000	0.0000	0.0000
56.	0.0000	0.0000	0.0000	0.0000	0.0000	0.0000	0.0000	0.0000	0.0000	0.0000
60.	0.0000	0.0000	0.0000	0.0000	0.0000	0.0000	0.0000	0.0000	0.0000	0.0000

UNCLASSIFIED

(U) TABLE B31.- $C_{n,1}$ (U)(a) $|\beta| = 40$

ALPHA	MACH NUMBER						1.4	1.6
	0.2	0.4	0.6	0.8	0.9	1.0		
-12.	.0120	.0113	.0115	.0120	.0125	.0117	.0110	.0069 .0035
-8.	.0120	.0113	.0115	.0120	.0125	.0117	.0110	.0069 .0035
-4.	.0120	.0113	.0115	.0120	.0125	.0117	.0110	.0069 .0035
0.	.0120	.0113	.0115	.0120	.0125	.0117	.0110	.0069 .0035
4.	.0100	.0095	.0090	.0095	.0100	.0100	.0100	.0098 .0035
8.	.0090	.0082	.0075	.0072	.0070	.0073	.0076	.0080 .0047 .0015
12.	.0060	.0057	.0055	.0041	.0030	.0031	.0033	.0034 .0020 .0005
16.	.0030	.0025	.0020	.0000	-.0020	-.0015	-.0011	-.0070 -.0030 .0010
20.	-.0010	-.0015	-.0020	-.0045	-.0070	-.0080	-.0100	-.0110 -.0060 .0010
24.	-.0070	-.0067	-.0065	-.0063	-.0060	-.0078	-.0096	-.0115 -.0058 .0010
28.	-.0100	-.0052	-.0045	-.0050	-.0055	-.0075	-.0095	-.0115 -.0058 .0010
32.	-.0040	-.0050	-.0060	-.0067	-.0075	-.0098	-.0111	-.0115 -.0058 .0010
36.	-.0050	-.0072	-.0095	-.0095	-.0102	-.0109	-.0115	-.0115 -.0058 .0010
40.	-.0050	-.0080	-.0100	-.0100	-.0100	-.0105	-.0110	-.0115 -.0058 .0010
44.	-.0100	-.0100	-.0100	-.0100	-.0100	-.0105	-.0110	-.0115 -.0058 .0010
48.	-.0090	-.0100	-.0100	-.0100	-.0100	-.0105	-.0110	-.0115 -.0058 .0010
52.	-.0090	-.0100	-.0100	-.0100	-.0100	-.0105	-.0110	-.0115 -.0058 .0010
56.	-.0100	-.0100	-.0100	-.0100	-.0100	-.0105	-.0110	-.0115 -.0058 .0010
60.	-.0100	-.0100	-.0100	-.0100	-.0105	-.0110	-.0115	-.0058 .0010

UNCLASSIFIED

(U) TABLE B31.- Continued (U)

(b) $|\beta| = 8^\circ$

ALPHA	MACH NUMBER							1.6
	0.2	0.4	0.6	0.8	0.9	1.0	1.1	
-12.	.0230	.0225	.0220	.0222	.0225	.0215	.0205	.0195
-8.	.0230	.0225	.0220	.0222	.0225	.0215	.0205	.0195
-4.	.0230	.0225	.0220	.0222	.0225	.0215	.0205	.0195
0.	.0230	.0225	.0220	.0222	.0225	.0215	.0205	.0195
4.	.0210	.0190	.0180	.0180	.0190	.0189	.0188	.0185
8.	.0180	.0160	.0138	.0137	.0135	.0143	.0152	.0160
12.	.0130	.0115	.0100	.0085	.0070	.0085	.0100	.0115
16.	.0060	.0055	.0050	-.0030	-.0065	-.0044	-.0022	0.0000
20.	-.0020	-.0032	-.0045	-.0090	-.0135	-.0140	-.0145	-.0150
24.	-.0130	-.0130	-.0130	-.0120	-.0110	-.0123	-.0135	-.0150
28.	-.0190	-.0155	-.0115	-.0117	-.0120	-.0130	-.0140	-.0150
32.	-.0200	-.0187	-.0175	-.0175	-.0175	-.0183	-.0191	-.0150
36.	-.0280	-.0293	-.0305	-.0280	-.0255	-.0220	-.0183	-.0150
40.	-.0220	-.0220	-.0210	-.0213	-.0215	-.0194	-.0172	-.0150
44.	-.0210	-.0210	-.0210	-.0213	-.0215	-.0194	-.0172	-.0150
48.	-.0180	-.0195	-.0210	-.0213	-.0215	-.0194	-.0172	-.0150
52.	-.0180	-.0195	-.0210	-.0213	-.0215	-.0194	-.0172	-.0150
56.	-.0200	-.0205	-.0210	-.0213	-.0215	-.0194	-.0172	-.0150
60.	-.0200	-.0205	-.0210	-.0213	-.0215	-.0194	-.0172	-.0150

UNCLASSIFIED

(U) TABLE B31.- Continued (U)

	(c) $ \beta = 120$									
	MACH NUMBER									
ALPHA	0.2	0.4	0.6	0.8	0.9	1.0	1.1	1.2	1.4	1.6
-12.	.0320	.0300	.0290	.0270	.0250	.0248	.0246	.0245	.0152	.0060
-8.	.0320	.0300	.0290	.0270	.0250	.0248	.0246	.0245	.0152	.0060
-4.	.0320	.0300	.0290	.0270	.0250	.0248	.0246	.0245	.0152	.0060
0.	.0320	.0300	.0290	.0270	.0250	.0248	.0246	.0245	.0152	.0060
4.	.0270	.0250	.0240	.0230	.0220	.0223	.0226	.0230	.0140	.0050
8.	.0220	.0200	.0180	.0170	.0160	.0173	.0187	.0200	.0117	.0035
12.	.0140	.0140	.0130	.0105	.0080	.0097	.0114	.0130	.0080	.0030
16.	.0050	.0060	.0060	.0037	.0070	.0037	.0010	.0010	.0030	.0030
20.	-.0060	-.0046	-.0075	-.0120	-.0150	-.0137	-.0125	-.0115	-.0042	.0030
24.	-.0200	-.0210	-.0220	-.0195	-.0170	-.0210	-.0250	-.0300	-.0135	.0030
28.	-.0280	-.0270	-.0270	-.0237	-.0205	-.0235	-.0267	-.0300	-.0135	.0030
32.	-.0280	-.0280	-.0280	-.0280	-.0280	-.0287	-.0295	-.0300	-.0135	.0030
36.	-.0360	-.0370	-.0375	-.0375	-.0375	-.0350	-.0325	-.0300	-.0135	.0030
40.	-.0330	-.0330	-.0330	-.0330	-.0330	-.0320	-.0310	-.0300	-.0135	.0030
44.	-.0300	-.0320	-.0330	-.0330	-.0330	-.0320	-.0310	-.0300	-.0135	.0030
48.	-.0270	-.0300	-.0330	-.0330	-.0330	-.0320	-.0310	-.0300	-.0135	.0030
52.	-.0260	-.0290	-.0330	-.0330	-.0330	-.0320	-.0310	-.0300	-.0135	.0030
56.	-.0270	-.0300	-.0330	-.0330	-.0330	-.0320	-.0310	-.0300	-.0135	.0030
60.	-.0260	-.0300	-.0330	-.0330	-.0330	-.0320	-.0310	-.0300	-.0135	.0030

UNCLASSIFIED

(U) TABLE B31 - Continued (U)

(d) $|\beta| = 160$

ALPHA	MACH NUMBER					
	0.2	0.4	0.6	0.8	1.0	1.2
-12.	.0370	.0340	.0310	.0258	.0215	.0225
-8.	.0370	.0340	.0310	.0258	.0215	.0225
-4.	.0370	.0340	.0310	.0258	.0215	.0225
0.	.0370	.0340	.0310	.0258	.0215	.0225
4.	.0300	.0270	.0250	.0220	.0190	.0205
8.	.0230	.0210	.0190	.0162	.0135	.0157
12.	.0130	.0120	.0120	.0095	.0070	.0092
16.	-.0020	0.0000	.0030	-.0040	-.0080	-.0050
20.	-.0150	-.0140	-.0130	-.0155	-.0180	-.0170
24.	-.0290	-.0300	-.0300	-.0295	-.0290	-.0246
28.	-.0390	-.0420	-.0460	-.0420	-.0380	-.0312
32.	-.0410	-.0420	-.0430	-.0423	-.0415	-.0330
36.	-.0430	-.0440	-.0455	-.0452	-.0450	-.0354
40.	-.0400	-.0400	-.0395	-.0397	-.0400	-.0320
44.	-.0390	-.0387	-.0395	-.0397	-.0397	-.0400
48.	-.0340	-.0370	-.0395	-.0397	-.0400	-.0320
52.	-.0320	-.0357	-.0395	-.0397	-.0400	-.0320
56.	-.0300	-.0347	-.0395	-.0397	-.0400	-.0320
60.	-.0270	-.0332	-.0395	-.0397	-.0400	-.0320

UNCLASSIFIED

UNCLASSIFIED

APPENDIX B

(U) TABLE B31.- Continued (U)

(e) $|\beta| = 20^\circ$ ORIGINAL PAGE IS
OF POOR QUALITY

ALPHA	MACH NUMBER						1.4	1.6
	0.2	0.4	0.6	0.8	0.9	1.0		
-12.	.0420	.0380	.0330	.0255	.0180	.0202	.0224	.0245
-8.	.0420	.0380	.0330	.0255	.0180	.0202	.0224	.0245
-4.	.0420	.0380	.0330	.0255	.0180	.0202	.0224	.0245
0.	.0420	.0380	.0330	.0255	.0180	.0202	.0224	.0245
4.	.0330	.0290	.0260	.0205	.0150	.0178	.0206	.0235
8.	.0230	.0190	.0160	.0135	.0120	.0147	.0174	.0200
12.	.0130	.0110	.0090	.0060	.0030	.0065	.0100	.0135
16.	-.0080	-.0050	-.0020	-.0040	-.0060	-.0036	-.0013	.0010
20.	-.0230	-.0210	-.0200	-.0210	-.0220	-.0200	-.0180	-.0160
24.	-.0380	-.0390	-.0400	-.0400	-.0410	-.0326	-.0243	-.0160
28.	-.0500	-.0500	-.0510	-.0515	-.0520	-.0400	-.0280	-.0160
32.	-.0540	-.0540	-.0540	-.0540	-.0540	-.0413	-.0287	-.0160
36.	-.0500	-.0520	-.0530	-.0530	-.0530	-.0407	-.0283	-.0160
40.	-.0470	-.0470	-.0470	-.0470	-.0460	-.0360	-.0260	-.0160
44.	-.0460	-.0460	-.0470	-.0470	-.0460	-.0360	-.0260	-.0160
48.	-.0420	-.0450	-.0470	-.0470	-.0460	-.0360	-.0260	-.0160
52.	-.0380	-.0430	-.0470	-.0470	-.0460	-.0360	-.0260	-.0160
56.	-.0330	-.0400	-.0470	-.0470	-.0460	-.0360	-.0260	-.0160
60.	-.0280	-.0380	-.0470	-.0470	-.0460	-.0360	-.0260	-.0160

UNCLASSIFIED

(U) TABLE B31.- Continued (U)

(F) $|\beta| = 24^\circ$

ALPHA	MACH NUMBER						1.6			
	0.2	0.4	0.6	0.8	0.9	1.0				
-12.	.0380	.0340	.0310	.0225	.0140	.0175	.0210	.0245	.0146	.0047
-8.	.0380	.0340	.0310	.0225	.0140	.0175	.0210	.0245	.0146	.0047
-4.	.0380	.0340	.0310	.0225	.0140	.0175	.0210	.0245	.0146	.0047
0.	.0380	.0340	.0310	.0225	.0140	.0175	.0210	.0245	.0146	.0047
4.	.0310	.0270	.0230	.0180	.0120	.0158	.0196	.0235	.0140	.0045
8.	.0220	.0180	.0150	.0115	.0080	.0120	.0160	.0200	.0118	.0037
12.	.0130	.0100	.0070	.0040	.0010	.0050	.0099	.0135	.0062	.0030
16.	-.0070	-.0060	-.0060	-.0095	-.0130	-.0084	-.0037	.0010	.0025	.0025
20.	-.0240	-.0250	-.0260	-.0270	-.0280	-.0240	-.0200	-.0160	-.0070	.0025
24.	-.0510	-.0480	-.0450	-.0460	-.0470	-.0306	-.0203	-.0160	-.0070	.0025
28.	-.0590	-.0590	-.0600	-.0600	-.0600	-.0453	-.0307	-.0160	-.0070	.0025
32.	-.0680	-.0660	-.0640	-.0650	-.0670	-.0400	-.0330	-.0160	-.0070	.0025
36.	-.0640	-.0640	-.0645	-.0660	-.0690	-.0410	-.0240	-.0160	-.0070	.0025
40.	-.0600	-.0600	-.0600	-.0570	-.0550	-.0420	-.0290	-.0160	-.0070	.0025
44.	-.0540	-.0570	-.0600	-.0570	-.0550	-.0420	-.0290	-.0160	-.0070	.0025
48.	-.0490	-.0550	-.0600	-.0570	-.0550	-.0420	-.0290	-.0160	-.0070	.0025
52.	-.0460	-.0530	-.0600	-.0570	-.0550	-.0420	-.0290	-.0160	-.0070	.0025
56.	-.0430	-.0520	-.0600	-.0570	-.0550	-.0420	-.0290	-.0160	-.0070	.0025
60.	-.0300	-.0450	-.0600	-.0570	-.0550	-.0420	-.0290	-.0160	-.0070	.0025

UNCLASSIFIED

UNCLASSIFIED

APPENDIX B

(U) TABLE B31.- Concluded (U)

(g) $|\beta| = 28^\circ$

ALPHA	MACH NUMBER						1.4	1.6
	0.2	0.4	0.6	0.8	0.9	1.0		
-12.	.0330	.0290	.0250	.0180	.0100	.0148	.0197	.0245
-8.	.0330	.0290	.0250	.0180	.0100	.0148	.0197	.0245
-4.	.0330	.0290	.0250	.0180	.0100	.0148	.0197	.0245
0.	.0330	.0290	.0250	.0180	.0100	.0148	.0197	.0245
4.	.0280	.0230	.0190	.0140	.0090	.0138	.0177	.0235
8.	.0210	.0160	.0120	.0090	.0060	.0107	.0143	.0200
12.	.0120	.0090	.0050	.0020	-.0010	.0038	.0086	.0135
16.	-.0060	-.0070	-.0090	-.0115	-.0140	.0003	.0047	.0010
20.	-.0250	-.0280	-.0310	-.0305	-.0300	-.0253	-.0206	-.0160
24.	-.0640	-.0570	-.0500	-.0505	-.0510	-.0393	-.0277	-.0160
28.	-.0680	-.0680	-.0690	-.0685	-.0680	-.0507	-.0333	-.0160
32.	-.0810	-.0810	-.0810	-.0810	-.0860	-.0627	-.0393	-.0160
36.	-.0790	-.0820	-.0860	-.0860	-.0860	-.0593	-.0377	-.0160
40.	-.0680	-.0710	-.0730	-.0730	-.0730	-.0540	-.0350	-.0160
44.	-.0610	-.0670	-.0730	-.0730	-.0730	-.0540	-.0350	-.0160
48.	-.0560	-.0670	-.0730	-.0730	-.0730	-.0540	-.0350	-.0160
52.	-.0530	-.0670	-.0730	-.0730	-.0730	-.0540	-.0350	-.0160
56.	-.0530	-.0670	-.0730	-.0730	-.0730	-.0540	-.0350	-.0160
60.	-.0320	-.0670	-.0730	-.0730	-.0730	-.0540	-.0350	-.0160

UNCLASSIFIED

(U) TABLE B32.- C_{n,2} (U)

MACH	BETA	ALPHA					
		25	30	35	40	45	50
.2	-10.	.0240	.0200	.0320	.0290	.0250	.0240
.2	-5.	.0120	.0100	.0160	.0130	.0050	-.0110
.2	0.	0.0000	0.0000	0.0000	0.0000	-.0030	-.0140
.2	5.	-.0120	-.0100	-.0120	-.0130	-.0090	-.0150
.2	10.	-.0250	-.0200	-.0320	-.0290	-.0260	-.0230
.6	-10.	.0194	.0190	.0300	.0270	.0270	.0270
.6	-5.	.0089	.0064	.0128	.0129	.0126	.0128
.6	0.	0.0000	0.0000	0.0000	0.0000	0.0000	0.0000
.6	5.	-.0089	-.0064	-.0128	-.0128	-.0128	-.0128
.6	10.	-.0194	-.0190	-.0300	-.0270	-.0270	-.0270

UNCLASSIFIED

(U) TABLE B33.- C_{n_p} (PER RADIAN) (U)

ALPHA	MACH NUMBER						1.4	1.6
	0.2	0.4	0.6	0.8	1.0	1.1		
-12.	0.000	0.000	0.000	0.000	0.000	0.000	0.000	0.000
-8.	0.000	0.000	0.000	0.000	0.000	0.000	0.000	0.000
-4.	0.000	0.000	0.000	0.000	0.000	0.000	0.000	0.000
0.	0.000	0.000	0.000	0.000	0.000	0.000	0.000	0.000
4.	-0.025	-0.050	-0.070	-0.050	-0.040	-0.040	-0.035	-0.006
8.	-0.035	-0.040	-0.040	-0.010	0.000	-0.010	-0.020	-0.004
12.	-0.030	-0.025	-0.020	-0.020	-0.025	-0.010	-0.010	.002
16.	-0.065	-0.040	-0.010	0.000	-0.010	0.006	-0.006	.003
20.	-0.110	-0.090	-0.070	-0.045	-0.035	-0.020	-0.004	.010
24.	-0.120	-0.120	-0.100	-0.090	-0.060	-0.030	0.000	0.000
28.	-0.110	-0.110	-0.110	-0.110	-0.080	-0.040	0.000	0.000
32.	-0.070	-0.070	-0.070	-0.070	-0.040	-0.030	0.000	0.000
36.	-0.010	-0.010	-0.010	-0.010	0.000	0.000	0.000	0.000
40.	0.000	0.000	0.000	0.000	0.000	0.000	0.000	0.000
44.	0.000	0.000	0.000	0.000	0.000	0.000	0.000	0.000
48.	0.000	0.000	0.000	0.000	0.000	0.000	0.000	0.000
52.	0.000	0.000	0.000	0.000	0.000	0.000	0.000	0.000
56.	0.000	0.000	0.000	0.000	0.000	0.000	0.000	0.000
60.	0.000	0.000	0.000	0.000	0.000	0.000	0.000	0.000

UNCLASSIFIED

123

(U) TABLE B34.- C_{n_r} (PER RADIAN) (U)

ALPHA	MACH NUMBER						1.6				
	0.2	0.4	0.6	0.8	0.9	1.0					
-12.	-.370	-.370	-.370	-.370	-.370	-.351	-.332	-.313	-.270	-.230	
-8.	-.370	-.370	-.370	-.370	-.370	-.351	-.332	-.313	-.270	-.230	
-4.	-.370	-.370	-.370	-.370	-.370	-.351	-.332	-.313	-.270	-.230	
0.	-.370	-.370	-.370	-.370	-.370	-.351	-.332	-.313	-.250	-.230	
4.	-.400	-.400	-.400	-.400	-.400	-.370	-.340	-.315	-.270	-.230	
8.	-.430	-.430	-.430	-.430	-.430	-.390	-.350	-.318	-.280	-.235	
12.	-.455	-.455	-.455	-.455	-.455	-.405	-.355	-.313	-.280	-.245	
16.	-.475	-.475	-.475	-.475	-.475	-.390	-.310	-.230	-.260	-.290	
20.	-.455	-.455	-.455	-.455	-.455	-.360	-.270	-.175	-.230	-.290	
24.	-.450	-.450	-.450	-.450	-.450	-.360	-.270	-.175	-.230	-.290	
28.	-.390	-.390	-.390	-.390	-.390	-.380	-.280	-.175	-.230	-.290	
32.	-.210	-.210	-.210	-.210	-.210	-.200	-.190	-.175	-.230	-.290	
36.	-.300	-.300	-.300	-.300	-.300	-.260	-.210	-.175	-.230	-.290	
40.	-.480	-.480	-.480	-.480	-.480	-.480	-.380	-.280	-.175	-.230	-.290
44.	-.400	-.400	-.400	-.400	-.400	-.400	-.330	-.270	-.175	-.230	-.290
48.	-.310	-.310	-.310	-.310	-.310	-.310	-.270	-.230	-.175	-.230	-.290
52.	-.220	-.220	-.220	-.220	-.220	-.220	-.200	-.190	-.175	-.130	-.290
56.	-.150	-.150	-.150	-.150	-.150	-.160	-.160	-.170	-.175	-.130	-.290
60.	-.160	-.160	-.160	-.160	-.160	-.170	-.170	-.170	-.175	-.130	-.290

UNCLASSIFIED

(U) TABLE B35.- $C_{n\delta_a}$ (PER DEGREE) (U)

ALPHA	MACH NUMBER						1.4	1.6
	0.2	0.4	0.6	0.8	1.0	1.1		
-12.	.00010	.00009	.00008	.00006	.00005	.00004	.00003	.00002
-8.	.00113	.0009	.0008	.0006	.0005	.0004	.0003	.0002
-4.	.00010	.00009	.00008	.00006	.00005	.00004	.00003	.00002
0.	.00010	.00009	.00008	.00006	.00005	.00004	.00003	.00002
4.	.00010	.00009	.00007	.00005	.00004	.00003	.00002	.00001
8.	.00006	.00006	.00005	.00004	.00003	.00002	.00001	.00000
12.	0.00000	0.00000	0.00000	0.00000	0.00001	0.00000	-0.00001	-0.00000
16.	-0.00007	-0.00006	-0.00005	-0.00004	-0.00003	-0.00002	-0.00001	-0.00000
20.	-0.00008	-0.00009	-0.00009	-0.00006	-0.00004	-0.00003	-0.00002	-0.00001
24.	-0.00007	-0.00009	-0.00010	-0.00010	-0.00012	-0.00011	-0.00009	-0.00008
28.	-0.00009	-0.00010	-0.00012	-0.00016	-0.00013	-0.00015	-0.00013	-0.00012
32.	-0.00010	-0.00011	-0.00013	-0.00015	-0.00016	-0.00014	-0.00012	-0.00010
36.	-0.00010	-0.00010	-0.00010	-0.00010	-0.00010	-0.00010	-0.00010	-0.00009
40.	-0.00013	-0.00012	-0.00012	-0.00012	-0.00011	-0.00011	-0.00010	-0.00009
44.	-0.00012	-0.00012	-0.00012	-0.00012	-0.00011	-0.00011	-0.00010	-0.00009
48.	-0.00007	-0.00008	-0.00008	-0.00008	-0.00008	-0.00009	-0.00009	-0.00008
52.	-0.00001	0.00000	0.00000	0.00000	0.00000	-0.00003	-0.00007	-0.00010
56.	0.00006	0.00005	0.00004	0.00004	0.00004	0.00000	-0.00005	-0.00010
60.	0.00016	0.00005	0.00004	0.00004	0.00004	0.00000	-0.00005	-0.00010

UNCLASSIFIED

APPENDIX B

UNCLASSIFIED

(U) TABLE B36.- $C_{n\delta_D}$ (PER DEGREE) (U)

ALPHA	MACH NUMBER						
	0.2	0.4	0.6	0.8	0.9	1.0	1.1
-12.	.00055	.00052	.00050	.00052	.00055	.00046	.00036
-8.	.00055	.00052	.00050	.00052	.00053	.00046	.00038
-4.	.00055	.00052	.00050	.00052	.00055	.00046	.00038
0.	.00055	.00052	.00050	.00052	.00055	.00046	.00038
4.	.00060	.00060	.00060	.00057	.00055	.00053	.00052
8.	.00060	.00062	.00065	.00057	.00050	.00058	.00066
12.	.00060	.00062	.00065	.00055	.00045	.00067	.00059
16.	.00055	.00055	.00055	.00040	.00025	.00050	.00075
20.	.00045	.00035	.00025	.00017	.00010	.00040	.00070
24.	.00030	.00010	-.00010	-.00005	0.00000	.00030	.00100
28.	.00025	.00005	-.00015	-.00015	-.00015	-.00007	.00070
32.	.00015	0.00000	-.00020	-.00030	-.00040	0.00000	.00090
36.	.00015	-.00005	-.00025	-.00045	-.00060	-.00010	.00010
40.	.00012	0.00000	-.00020	-.00012	-.00010	.00020	.00050
44.	0.00000	-.000020	-.00030	-.00030	-.00030	.00010	.00050
48.	-.00017	-.00031	-.00045	-.00045	-.00045	0.00000	.00045
52.	-.00030	-.00042	-.00055	-.00052	-.00050	-.00030	.00043
56.	-.00047	-.00051	-.00055	-.00055	-.00055	-.00007	.00041
60.	-.00051	-.00057	-.00060	-.00060	-.00060	-.00010	.00040

UNCLASSIFIED

(U) TABLE B37.- $C_{n\delta_r}$ (PER DEGREE) (U)(a) $|\beta| \leq 10^\circ$

MACH NUMBER

ALPHA	0.2	0.4	0.6	0.8	0.9	1.0	1.1	1.2	1.4	1.6
-12.	-.00155	-.00140	-.00130	-.00130	-.00130	-.00120	-.00110	-.00103	-.00085	-.00068
-6.	-.00155	-.00140	-.00130	-.00130	-.00130	-.00120	-.00110	-.00103	-.00085	-.00068
-4.	-.00155	-.00140	-.00130	-.00130	-.00130	-.00120	-.00110	-.00101	-.00084	-.00067
0.	-.00155	-.00140	-.00130	-.00130	-.00130	-.00120	-.00110	-.00100	-.00080	-.00061
4.	-.00157	-.00143	-.00130	-.00130	-.00125	-.00120	-.00110	-.00098	-.00075	-.00056
8.	-.00160	-.00145	-.00130	-.00120	-.00120	-.00110	-.00100	-.00094	-.00070	-.00053
12.	-.00160	-.00145	-.00130	-.00120	-.00115	-.00110	-.00100	-.00088	-.00070	-.00050
16.	-.00145	-.00130	-.00120	-.00100	-.00095	-.00090	-.00090	-.00081	-.00060	-.00044
20.	-.00105	-.00095	-.00075	-.00065	-.00063	-.00070	-.00070	-.00075	-.00060	-.00039
24.	-.00075	-.00060	-.00045	-.00040	-.00040	-.00050	-.00050	-.00063	-.00050	-.00038
28.	-.00050	-.00040	-.00038	-.00030	-.00028	-.00040	-.00050	-.00060	-.00050	-.00038
32.	-.00035	-.00035	-.00035	-.00025	-.00020	-.00030	-.00050	-.00060	-.00050	-.00038
36.	-.00020	-.00025	-.00033	-.00030	-.00023	-.00030	-.00050	-.00060	-.00050	-.00038
40.	-.00016	-.00030	-.00030	-.00030	-.00030	-.00030	-.00050	-.00060	-.00050	-.00038
44.	-.00025	-.00025	-.00025	-.00025	-.00025	-.00025	-.00030	-.00050	-.00060	-.00050
48.	-.00018	-.00018	-.00018	-.00018	-.00018	-.00018	-.00030	-.00050	-.00060	-.00050
52.	-.00015	-.00015	-.00015	-.00015	-.00015	-.00015	-.00030	-.00050	-.00060	-.00050
56.	-.00016	-.00018	-.00018	-.00018	-.00018	-.00018	-.00030	-.00050	-.00060	-.00050
60.	-.00025	-.00025	-.00025	-.00025	-.00025	-.00025	-.00030	-.00050	-.00060	-.00050

UNCLASSIFIED

UNCLASSIFIED

(U) TABLE B37.- Continued (U)

(b) $|\beta| = 200$

MACH NUMBER

ALPHA	0.2	0.4	0.6	0.8	0.9	1.0	1.1	1.2	1.4	1.6
-12.	-0.00098	-0.00090	-0.00080	-0.00080	-0.00080	-0.00087	-0.00094	-0.00103	-0.00085	-0.00068
-8.	-0.00098	-0.00090	-0.00080	-0.00080	-0.00080	-0.00087	-0.00094	-0.00103	-0.00085	-0.00068
-4.	-0.00098	-0.00090	-0.00080	-0.00080	-0.00080	-0.00087	-0.00094	-0.00101	-0.00084	-0.00067
0.	-0.00098	-0.00090	-0.00080	-0.00080	-0.00080	-0.00087	-0.00094	-0.00100	-0.00080	-0.00061
4.	-0.00110	-0.00100	-0.00100	-0.00090	-0.00085	-0.00090	-0.00094	-0.00098	-0.00075	-0.00056
8.	-0.00120	-0.00110	-0.00105	-0.00095	-0.00090	-0.00090	-0.00094	-0.00094	-0.00070	-0.00053
12.	-0.00110	-0.00100	-0.00090	-0.00083	-0.00078	-0.00081	-0.00085	-0.00088	-0.00070	-0.00050
16.	-0.00065	-0.00075	-0.00065	-0.00060	-0.00060	-0.00067	-0.00074	-0.00081	-0.00065	-0.00044
20.	-0.00060	-0.00055	-0.00053	-0.00040	-0.00035	-0.00050	-0.00063	-0.00075	-0.00060	-0.00039
24.	-0.00055	-0.00050	-0.00040	-0.00035	-0.00033	-0.00043	-0.00053	-0.00063	-0.00050	-0.00038
26.	-0.00050	-0.00040	-0.00035	-0.00033	-0.00033	-0.00042	-0.00051	-0.00060	-0.00050	-0.00038
32.	-0.00043	-0.00040	-0.00035	-0.00033	-0.00033	-0.00042	-0.00051	-0.00060	-0.00050	-0.00038
36.	-0.00035	-0.00031	-0.00028	-0.00028	-0.00028	-0.00033	-0.00040	-0.00050	-0.00060	-0.00050
40.	-0.00020	-0.00020	-0.00020	-0.00020	-0.00020	-0.00020	-0.00034	-0.00048	-0.00060	-0.00050
44.	-0.00018	-0.00018	-0.00018	-0.00018	-0.00018	-0.00025	-0.00032	-0.00046	-0.00060	-0.00050
48.	-0.00020	-0.00020	-0.00020	-0.00020	-0.00020	-0.00020	-0.00032	-0.00046	-0.00060	-0.00050
52.	-0.00025	-0.00025	-0.00025	-0.00025	-0.00025	-0.00025	-0.00032	-0.00046	-0.00060	-0.00050
56.	-0.00030	-0.00030	-0.00030	-0.00030	-0.00030	-0.00030	-0.00032	-0.00046	-0.00060	-0.00050
60.	-0.00030	-0.00030	-0.00030	-0.00030	-0.00030	-0.00032	-0.00032	-0.00046	-0.00060	-0.00050

UNCLASSIFIED

APPENDIX B

(U) TABLE B37.- Concluded (U)

(C) $|\beta| = 30^\circ$

ALPHA	MACH NUMBER						
	0.2	0.4	0.6	0.8	0.9	1.0	1.1
-12.	-0.00049	-0.00044	-0.00040	-0.00040	-0.00040	-0.00060	-0.00080
-8.	-0.00048	-0.00044	-0.00040	-0.00040	-0.00040	-0.00060	-0.00080
-4.	-0.00046	-0.00044	-0.00040	-0.00040	-0.00040	-0.00060	-0.00080
0.	-0.00048	-0.00044	-0.00040	-0.00040	-0.00040	-0.00063	-0.00080
4.	-0.00070	-0.00065	-0.00060	-0.00060	-0.00055	-0.00060	-0.00074
8.	-0.00063	-0.00060	-0.00075	-0.00070	-0.00070	-0.00078	-0.00081
12.	-0.00078	-0.00071	-0.00065	-0.00060	-0.00055	-0.00066	-0.00077
16.	-0.00063	-0.00057	-0.00050	-0.00055	-0.00040	-0.00055	-0.00068
20.	-0.00048	-0.00045	-0.00043	-0.00035	-0.00030	-0.00045	-0.00060
24.	-0.00043	-0.00040	-0.00040	-0.00040	-0.00035	-0.00044	-0.00054
28.	-0.00040	-0.00040	-0.00040	-0.00040	-0.00035	-0.00043	-0.00051
32.	-0.00035	-0.00035	-0.00035	-0.00030	-0.00025	-0.00037	-0.00049
36.	-0.00028	-0.00028	-0.00028	-0.00025	-0.00023	-0.00035	-0.00047
40.	-0.00025	-0.00025	-0.00025	-0.00025	-0.00023	-0.00035	-0.00047
44.	-0.00028	-0.00028	-0.00028	-0.00028	-0.00028	-0.00035	-0.00047
48.	-0.00026	-0.00028	-0.00028	-0.00028	-0.00028	-0.00035	-0.00047
52.	-0.00028	-0.00026	-0.00028	-0.00028	-0.00028	-0.00035	-0.00047
56.	-0.00026	-0.00028	-0.00028	-0.00028	-0.00028	-0.00035	-0.00047
60.	-0.00028	-0.00028	-0.00028	-0.00028	-0.00028	-0.00035	-0.00047

UNCLASSIFIED

(U) TABLE B38.- $\Delta C_{\eta, \text{sb}}$ (U)(a) $|\beta| = 4^\circ$

ALPHA	MACH NUMBER					
	0.2	0.4	0.6	0.8	0.9	1.0
-12.	-0.0010	-0.0010	-0.0010	-0.0030	-0.0040	-0.0060
-8.	-0.0010	-0.0010	-0.0010	-0.0030	-0.0040	-0.0060
-4.	-0.0010	-0.0010	-0.0010	-0.0030	-0.0040	-0.0060
0.	-0.0010	-0.0010	-0.0010	-0.0030	-0.0035	-0.0060
4.	-0.0010	-0.0010	-0.0010	-0.0020	-0.0030	-0.0040
8.	-0.0010	-0.0010	-0.0010	-0.0020	-0.0025	-0.0040
12.	-0.0010	-0.0010	-0.0010	-0.0020	-0.0030	-0.0050
16.	-0.0015	-0.0015	-0.0015	-0.0015	-0.0015	-0.0040
20.	0.0000	0.0000	0.0000	0.0000	0.0010	0.0010
24.	0.0000	0.0000	0.0000	0.0010	0.0030	0.0020
28.	0.0020	0.0020	0.0020	0.0010	0.0030	0.0040
32.	0.0000	0.0000	0.0000	0.0000	0.0010	0.0000
36.	0.0000	0.0000	0.0000	0.0000	0.0000	0.0000
40.	0.0000	0.0000	0.0000	0.0000	0.0000	0.0000
44.	0.0000	0.0000	0.0000	0.0000	0.0000	0.0000
48.	0.0000	0.0000	0.0000	0.0000	0.0000	0.0000
52.	0.0000	0.0000	0.0000	0.0000	0.0000	0.0000
56.	0.0000	0.0000	0.0000	0.0000	0.0000	0.0000
60.	0.0000	0.0000	0.0000	0.0000	0.0000	0.0000

UNCLASSIFIED

UNCLASSIFIED

APPENDIX B

(U) TABLE B38.- Continued (U)

(b) $|\beta| = 8^\circ$

ALPHA	MACH NUMBER						1.4	1.6
	0.2	0.4	0.6	0.8	0.9	1.0		
-12.	-0.0055	-0.0055	-0.0055	-0.0090	-0.0110	-0.0110	-0.0120	-0.0096
-8.	-0.0055	-0.0055	-0.0055	-0.0090	-0.0110	-0.0110	-0.0120	-0.0096
-4.	-0.0055	-0.0055	-0.0055	-0.0090	-0.0110	-0.0110	-0.0120	-0.0096
0.	-0.0055	-0.0055	-0.0055	-0.0090	-0.0110	-0.0110	-0.0120	-0.0096
4.	-0.0055	-0.0055	-0.0055	-0.0060	-0.0060	-0.0060	-0.0070	-0.0050
8.	-0.0055	-0.0055	-0.0055	-0.0060	-0.0060	-0.0060	-0.0060	-0.0070
12.	-0.0050	-0.0050	-0.0050	-0.0060	-0.0060	-0.0060	-0.0050	-0.0020
16.	-0.0035	-0.0035	-0.0035	-0.0030	-0.0030	0.0000	0.0030	0.0000
20.	0.0000	0.0000	0.0000	0.0010	0.0020	0.0020	0.0040	0.0020
24.	0.0000	0.0000	0.0000	0.0010	0.0010	0.0010	0.0000	0.0000
28.	-0.0080	-0.0080	-0.0080	-0.0030	0.0115	0.0010	0.0000	0.0000
32.	-0.0080	-0.0080	-0.0080	-0.0030	0.0110	0.0000	0.0000	0.0000
36.	0.0000	0.0000	0.0000	0.0000	0.0000	0.0000	0.0000	0.0000
40.	0.0000	0.0000	0.0000	0.0000	0.0000	0.0000	0.0000	0.0000
44.	0.0000	0.0000	0.0000	0.0000	0.0000	0.0000	0.0000	0.0000
48.	0.0000	0.0000	0.0000	0.0000	0.0000	0.0000	0.0000	0.0000
52.	0.0000	0.0000	0.0000	0.0000	0.0000	0.0000	0.0000	0.0000
56.	0.0000	0.0000	0.0000	0.0000	0.0000	0.0000	0.0000	0.0000
60.	0.0000	0.0000	0.0000	0.0000	0.0000	0.0000	0.0000	0.0000

UNCLASSIFIED

(U) TABLE B38.- Continued (U)

(C) $|\beta| = 120$

ALPHA	MACH NUMBER						1.4	1.6
	0.2	0.4	0.6	0.8	1.0	1.1		
-12.	-0.0095	-0.0095	-0.0095	-0.0110	-0.0130	-0.0130	-0.0125	-0.0090
-8.	-0.0095	-0.0095	-0.0095	-0.0110	-0.0130	-0.0130	-0.0125	-0.0090
-4.	-0.0095	-0.0095	-0.0095	-0.0110	-0.0130	-0.0130	-0.0125	-0.0090
0.	-0.0095	-0.0095	-0.0095	-0.0110	-0.0130	-0.0130	-0.0125	-0.0090
4.	-0.0095	-0.0095	-0.0095	-0.0100	-0.0110	-0.0110	-0.0110	-0.0070
8.	-0.0095	-0.0095	-0.0095	-0.0090	-0.0090	-0.0090	-0.0095	-0.0050
12.	-0.0080	-0.0080	-0.0080	-0.0080	-0.0090	-0.0090	-0.0080	-0.0040
16.	-0.0070	-0.0070	-0.0070	-0.0080	-0.0090	-0.0090	-0.0040	-0.0010
20.	-0.0060	-0.0060	-0.0060	-0.0040	-0.0015	-0.0005	0.0010	0.0000
24.	-0.0030	-0.0030	-0.0030	-0.0050	-0.0070	-0.0050	-0.0020	0.0000
28.	-0.0070	-0.0070	-0.0070	-0.0030	0.0020	0.0010	0.0000	0.0000
32.	-0.0070	-0.0070	-0.0070	-0.0030	0.0000	0.0000	0.0000	0.0000
36.	0.0000	0.0000	0.0000	0.0000	0.0000	0.0000	0.0000	0.0000
40.	0.0000	0.0000	0.0000	0.0000	0.0000	0.0000	0.0000	0.0000
44.	0.0000	0.0000	0.0000	0.0000	0.0000	0.0000	0.0000	0.0000
48.	0.0000	0.0000	0.0000	0.0000	0.0000	0.0000	0.0000	0.0000
52.	0.0000	0.0000	0.0000	0.0000	0.0000	0.0000	0.0000	0.0000
56.	0.0000	0.0000	0.0000	0.0000	0.0000	0.0000	0.0000	0.0000
60.	0.0000	0.0000	0.0000	0.0000	0.0000	0.0000	0.0000	0.0000

UNCLASSIFIED

(U) TABLE B38.- Concluded (U)

	(d) $ \beta = 16^\circ$									
	MACH NUMBER									
ALPHA	0.2	0.4	0.6	0.8	0.9	1.0	1.1	1.2	1.4	1.6
-12.	-0.0095	-0.0095	-0.0095	-0.0110	-0.0130	-0.0130	-0.0130	-0.0125	-0.0090	-0.0060
-8.	-0.0095	-0.0095	-0.0095	-0.0110	-0.0130	-0.0130	-0.0130	-0.0125	-0.0090	-0.0060
-4.	-0.0095	-0.0095	-0.0095	-0.0110	-0.0130	-0.0130	-0.0130	-0.0125	-0.0090	-0.0060
0.	-0.0095	-0.0095	-0.0095	-0.0110	-0.0130	-0.0130	-0.0130	-0.0125	-0.0090	-0.0060
4.	-0.0095	-0.0095	-0.0095	-0.0110	-0.0110	-0.0110	-0.0110	-0.0110	-0.0070	-0.0033
8.	-0.0095	-0.0095	-0.0095	-0.0090	-0.0090	-0.0090	-0.0090	-0.0095	-0.0050	-0.0007
12.	-0.0080	-0.0080	-0.0080	-0.0090	-0.0090	-0.0090	-0.0090	-0.0080	-0.0040	0.0000
16.	-0.0080	-0.0080	-0.0080	-0.0090	-0.0095	-0.0060	-0.0040	-0.0015	-0.0010	0.0000
20.	-0.0080	-0.0080	-0.0080	-0.0060	-0.0040	-0.0020	0.0000	0.0110	0.0000	0.0000
24.	-0.0080	-0.0080	-0.0080	-0.0080	-0.0090	-0.0060	-0.0030	0.0000	0.0000	0.0000
28.	-0.0090	-0.0090	-0.0090	-0.0030	0.0030	0.0020	0.0110	0.0000	0.0000	0.0000
32.	-0.0090	-0.0090	-0.0090	0.0000	0.0000	0.0000	0.0000	0.0000	0.0000	0.0000
36.	0.0000	0.0000	0.0000	0.0000	0.0000	0.0000	0.0000	0.0000	0.0000	0.0000
40.	0.0000	0.0000	0.0000	0.0000	0.0000	0.0000	0.0000	0.0000	0.0000	0.0000
44.	0.0000	0.0000	0.0000	0.0000	0.0000	0.0000	0.0000	0.0000	0.0000	0.0000
48.	0.0000	0.0000	0.0000	0.0000	0.0000	0.0000	0.0000	0.0000	0.0000	0.0000
52.	0.0000	0.0000	0.0000	0.0000	0.0000	0.0000	0.0000	0.0000	0.0000	0.0000
56.	0.0000	0.0000	0.0000	0.0000	0.0000	0.0000	0.0000	0.0000	0.0000	0.0000
60.	0.0000	0.0000	0.0000	0.0000	0.0000	0.0000	0.0000	0.0000	0.0000	0.0000

UNCLASSIFIED

UNCLASSIFIED

APPENDIX C

(U) SIMULATED FLIGHT CONTROL SYSTEM (U)

(U) The F-15 flight controls (refs. 20 and 21) simulated were stabilator, ailerons, and rudder, plus speed brakes for the basic airplane and thrust vectoring/reversing for the modified airplane.

(U) Stabilator (U)

(U) The stabilator was commanded by two separate systems in both pitch and roll, as shown in figure C1. A hydromechanical system commanded by stick displacement supplied pitch and roll commands δ_{pitch} and δ_{roll} to provide basic flying qualities. An electrical command augmentation system (CAS) commanded by stick force modified the surface deflections within its authority to provide comfortable forces and rapid response. Net symmetric tail deflection δ_h and differential tail deflection δ_D were obtained from the right and left surface deflections by

$$\delta_h = \frac{1}{2}(\delta_{h,L} + \delta_{h,R})$$

$$\delta_D = \delta_{h,L} - \delta_{h,R}$$

88

In figure C1 and subsequent control-system block diagrams, a limiter following an integrator denotes the integrator output limited to the values shown.

(U) Longitudinal Mechanical System Model (U)

(U) A block diagram of the hydromechanical portion of the longitudinal flight-control-system model is shown in figure C2. The stick displacement signal δ_{long} (in inches) is multiplied by the pitch-ratio changer actuator to supply part of the symmetric tail-deflection command δ_{pitch} . The stick displacement is also interpreted as an incremental load-factor command ($\pm 3.75g$ maximum) and summed with the output of the pitch-ratio adjust device. This signal is modified by the pitch trim compensator and also contributes to the δ_{pitch} command.

(U) The load-factor increment due to thrust vectoring $a_{n,vect}$ is subtracted from the incremental load factor ($a_n - 1$) so the simulated airplane would have the same flight-control-system response with and without thrust vectoring.

(U) The pitch-ratio actuator changer is scheduled as a function of total and static pressures, as indicated by functions F1 and F2 in the block diagram. These functions are defined in table C1.

UNCLASSIFIED

APPENDIX C

(U) TABLE C1.- PITCH-RATIO MULTIPLYING FACTORS (U)

p_T/p_s	F1	$p_T - p_s$		F2
		N/m ²	lb/ft ²	
1.0	1.0	0	0	6.0
1.65	1.0	9 576	200	6.0
1.8	1.8	24 900	520	1.9
2.2	5.4	32 560	680	1.44
2.45	6.3	47 880	1 000	1.1
3.05	7.3	77 570	1 620	.7
9.0	11.2	153 220	3 200	.5

(U) Function F3 determines the pitch trim compensator positive limit K_1 as a function of Δz_1 , an integral function of the pitch-ratio changer actuator position, where K_1 is given by

$$\begin{aligned} K_1 &= \Delta z_1 && (2.5^\circ < \Delta z_1 < 5.5^\circ) \\ &= 2.5^\circ && (2.5^\circ \geq \Delta z_1) \\ &= 5.5^\circ && (\Delta z_1 \geq 5.5^\circ) \end{aligned}$$

(U) Pitch CAS (U)

(U) Figure C3 shows a block diagram of the simulated pitch CAS.

(U) In flight, stick force and stick displacement would be sensed simultaneously. In the simulator, the stick displacement δ_{long} was sensed, and then the corresponding dual gradient spring force was computed (function F4), summed with feedback forces, and then transmitted to the force feel system in the DMS hardware. The spring gradient force F4 was computed as

$$\begin{aligned} F4 &= 8.5\delta_{long} && (-1. \leq \delta_{long} \leq 1.) \\ &= 4.5 + 4\delta_{long} && (\delta_{long} > 1.) \\ &= -4.5 + 4\delta_{long} && (\delta_{long} < -1.) \end{aligned}$$

UNCLASSIFIED

APPENDIX C

(U) The total stick force was converted to an incremental normal acceleration command by function F5, defined in table C2.

(U) TABLE C2.- INCREMENTAL NORMAL ACCELERATION COMMAND (U)

Longitudinal force input	F5, g units
-50.0	-8.0
-20.5	-8.0
-9.64	-2.57
9.64	2.57
20.5	8.0
50.0	8.0

(U) With pitch CAS engaged (on), the CAS authority was limited between K_2 and $+10^\circ$, where

$$K_2 = F6 \quad (F6 < 0)$$

$$K_2 = 0 \quad (F6 \geq 0)$$

$$F6 = -10^\circ \quad (\delta_h \geq -18.6^\circ)$$

$$F6 = -28.6^\circ - \delta_h \quad (\delta_h < -18.6^\circ)$$

(U) Lateral Mechanical System Model (U)

(U) Figure C4 shows a block diagram of the simulated lateral hydromechanical control system and the simulation of lateral stick force. The roll command δ_{roll} is limited by Mach number and airspeed (function F7) and by the mechanical stabilator command (function F8). The input to the roll calibrated airspeed servo is F7, defined by

$$F7 = 3.875 \quad (M < 1.0)$$

$$F7 = 2.208 - 0.02208 Krcs \quad (M > 1.0)$$

where

$$Krcs = 0 \quad (V_{cas} \leq 700 \text{ knots})$$

UNCLASSIFIED

APPENDIX C

$$K_{rcs} = 100 \quad (V_{cas} \geq 800)$$

$$K_{rcs} = V_{cas} - 100 \quad (700 < V_{cas} < 800)$$

(U) The differential-tail-deflection limit F8 is defined in table C3.

(U) TABLE C3.- DIFFERENTIAL-TAIL-DEFLECTION LIMIT (U)

δ_h , deg	F8
-25	1.25
-10	1.25
-3	5.0
2	5.0
10	.833
15	.833

(U) Function F9 is a dual gradient spring with breakout, as shown in figure C5.

(U) Roll CAS (U)

(U) Figure C6 shows a block diagram of the simulated roll CAS. The lateral stick force, after limiting to a value F_r , is scaled by function F12 to command roll rate in degrees per second. The difference between commanded and actual roll rate is limited to $\pm K_3$ deg/sec as the roll CAS command.

$$K_3 = 0 \quad (\text{Roll CAS is off})$$

if the roll CAS is on, K_3 is determined by function F10 and F11, where

$$F10 = 5.0 \quad (V_{cas} \leq 545 \text{ knots})$$

$$F10 = 1.2 \quad (V_{cas} \geq 800)$$

$$F10 = 3.3(800/V_{cas})^2 - 2.1 \quad (545 < V_{cas} < 800)$$

$$F11 = 5. \quad (\alpha < -1.^\circ)$$

$$F11 = 0 \quad (-1.^\circ \leq \alpha \leq 7.^\circ)$$

UNCLASSIFIED

APPENDIX C

$F_{11} = 0.376(\alpha - 7^\circ)$	$(7^\circ < \alpha < 20.3^\circ)$
$F_{11} = 5$	$(20.3^\circ \leq \alpha)$
$F_{12} = 0$	$(F_r \leq 3)$
$F_{12} = K_4(F_r - 3)$	$(F_r > 3.)$
$F_{12} = K_4(F_r + 3)$	$(F_r < -3.)$
$K_4 = 14.7$	$(M \leq 1.5)$
$K_4 = 8.3$	$(M > 1.5)$

(U) Aileron (U)

(U) The signal from the lateral hydromechanical system which commands differential-tail deflection (fig. C4) also commands aileron deflection. Figure C7 is a block diagram of the aileron simulation.

(U) Rudder (U)

(U) The rudder deflection command was simulated as the sum of three signals: (1) a mechanical signal from the pedals with $\pm 15^\circ$ maximum authority; (2) a signal from the yaw CAS with $\pm 15^\circ$ maximum authority; and (3) a stabilator/aileron-rudder interconnect. Figure C8 is a block diagram of the rudder simulation.

(U) Speed Brake (U)

(U) The pilot in the basic F-15 controlled the speed brake with an extend/hold/retract switch on the throttle lever. The speed brake was automatically retracted at $\alpha > 15^\circ$. Maximum deflection was limited to K_7 , the smaller of 45° or F_{13} , where $F_{13} = 45 K_8 / \bar{q}_S \Delta C_{D, sb}$ and $K_8 = 55\,600 \text{ N}$ ($12\,500 \text{ lb}$). Figure C9 is a block diagram of the speed-brake simulation.

(U) Thrust Vectoring (U)

(U) Figure C10 is a block diagram of the thrust-vectoring simulation. A manual vectoring mode and an automatic vectoring mode were simulated.

(U) The manual mode was controlled by a center-loaded thumb wheel on the control stick. When the pilot deflected the thumb wheel aft, the vector angle increased at 15 deg/sec to the limit K_9 , resulting in a positive lift force and a nose-down pitching moment. When the thumb wheel was released, the vector angle returned to zero. Manual vectoring was only available at subsonic speeds.

UNCLASSIFIED

APPENDIX C

(U) Because of the high deflection rate, the vector angle in the manual mode was usually zero or near the maximum available. This was consistent with reference 16 which showed that pilots tended to operate near zero or full vectoring, even though intermediate deflections were available. With the pitching moment balanced by the simulated canard, manual thrust vectoring was essentially direct lift control. It gave the pilot an immediate change in load factor without an attitude change.

(U) Automatic thrust vectoring was commanded by the computer. The commanded vector angle varied linearly with angle of attack between $\alpha = 5^\circ$ and $\alpha = 20^\circ$ to provide improved excess power (lift-drag ratio) within this range. At $\alpha > 20^\circ$, full vectoring ($\theta_j = 15^\circ$) was commanded. Figure 7 compares the specific excess power of the basic airplane and the modified airplane with automatic thrust vectoring.

(U) The maximum mechanical vector angle θ_j was limited to K_9 , the minimum of 15° or $F14$, where $F14 = (K_{10}\bar{q})/T_{gross}$ and $K_{10} = 250.2 \text{ deg-m}^2$ (2693 deg-ft^2). This limit is based on the canard characteristics assumed for the simulation. It results from the maximum canard pitching moment available to balance the moment due to thrust vectoring.

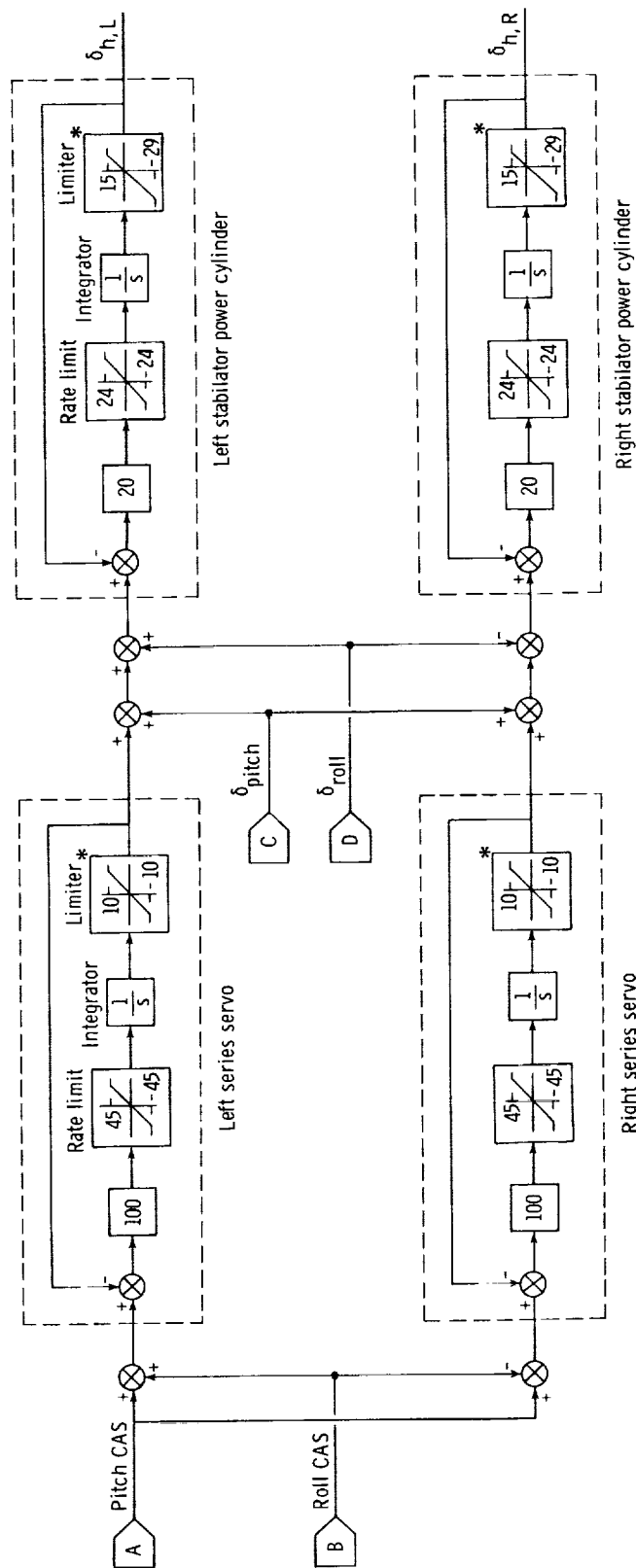
(U) Two vector angles are shown in figure C10, the mechanical (physical) angle θ_j and the effective angle δ_v . Experimental tests have indicated that the aerodynamic effects of vectoring are consistent with a larger angle than the physical deflection. The effective vector angle δ_v reflects this phenomenon, and $\delta_v = 1.16\theta_j$ was used in the force and moment calculations.

(U) Thrust Reversing (U)

(U) Thrust reversing was given lower priority than thrust vectoring. That is, the pilot could command in-flight thrust reversing, using the speed-brake switch, only when $\theta_j = 0$. If the engine was in afterburner when the pilot commanded thrust reversing, the control system would command military thrust and then initiate deployment when the engine reached military thrust. Full deployment (or retraction) occurred in 1 sec.

UNCLASSIFIED

APPENDIX C

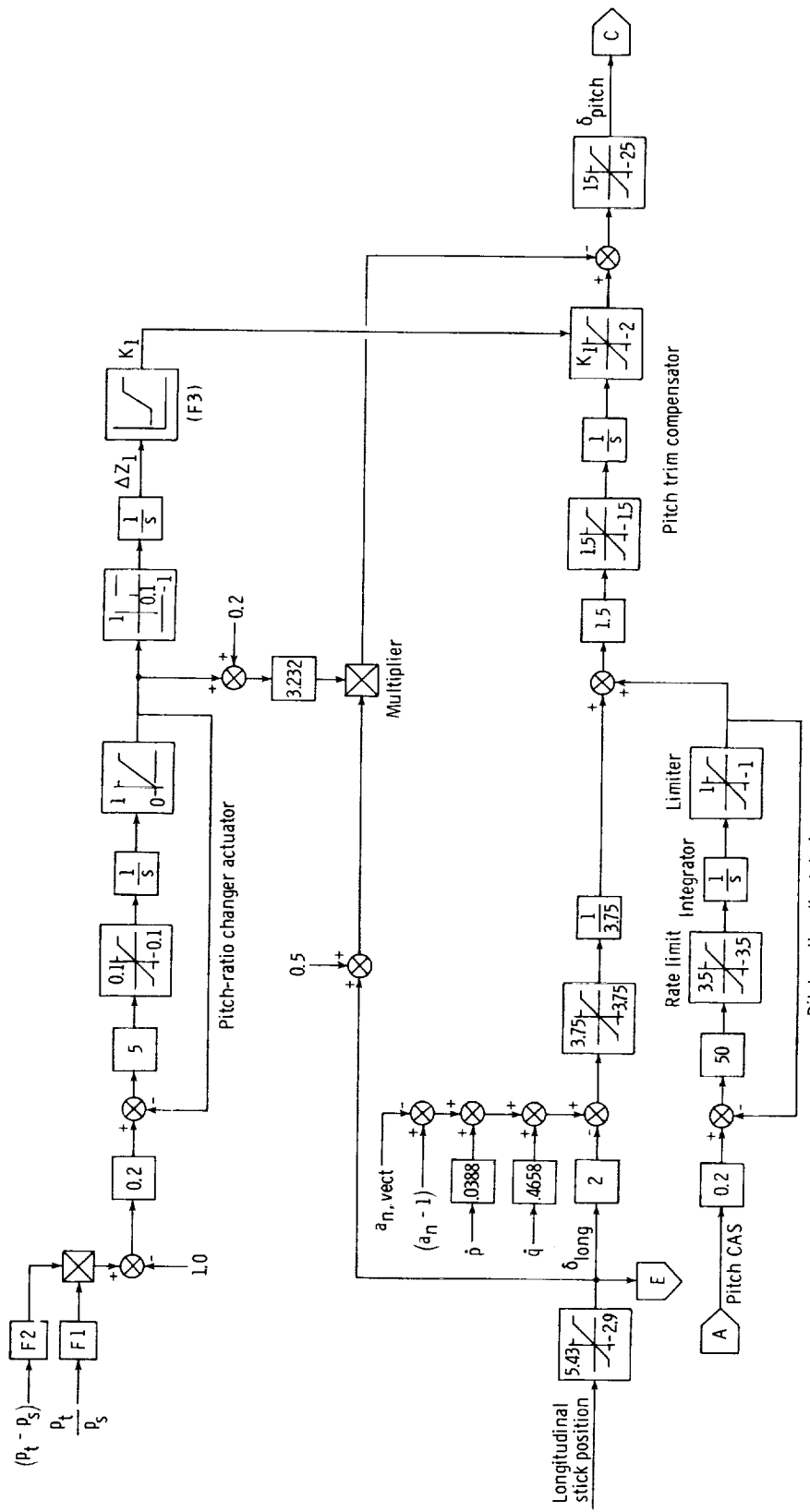


* Limits apply to the output of the preceding integrator

(U) Figure C1.- Block diagram of stabilator simulation. (U)

UNCLASSIFIED

APPENDIX C

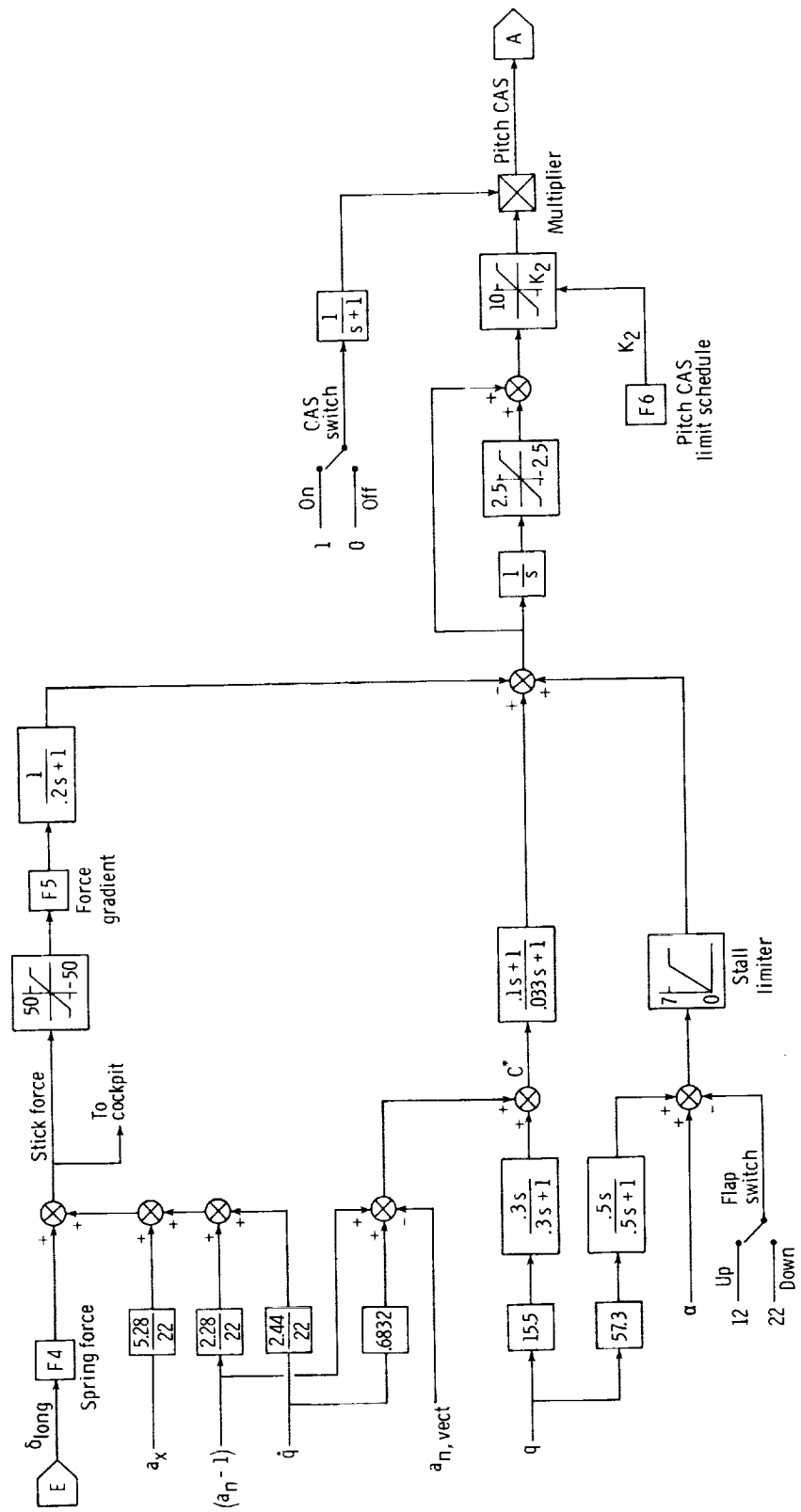


(U) Figure C2.— Block diagram of longitudinal hydromechanical control system. (U)

UNCLASSIFIED

UNCLASSIFIED

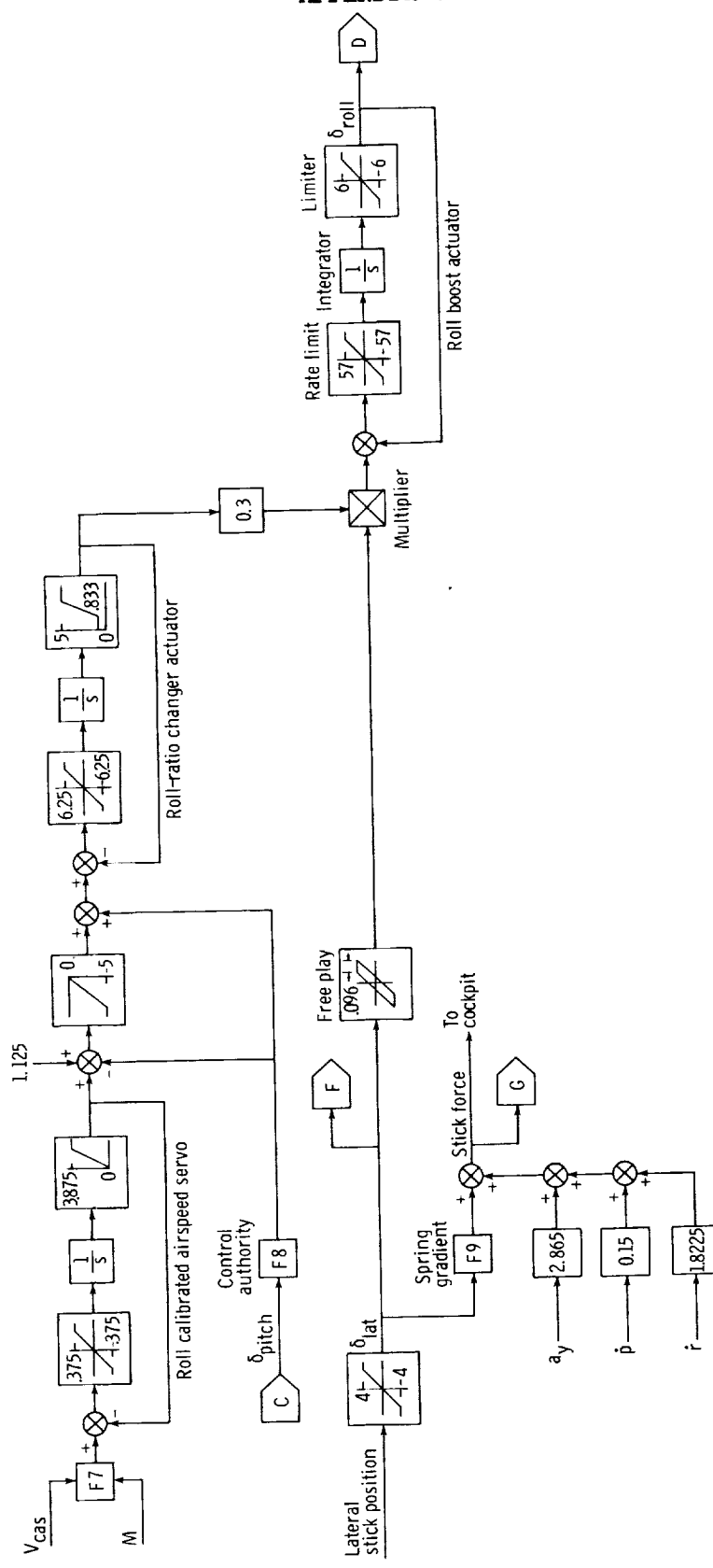
APPENDIX C



(U) Figure C3.- Block diagram of longitudinal command augmentation system. (U)

UNCLASSIFIED

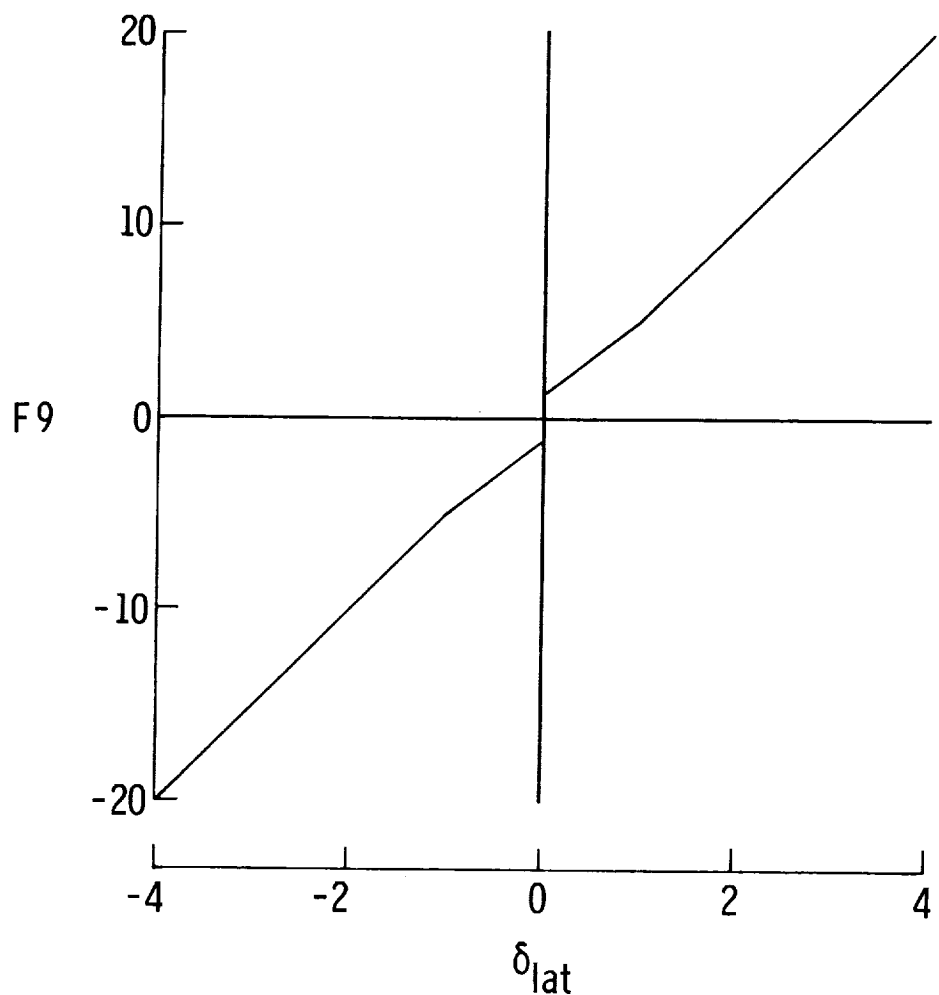
APPENDIX C



(U) Figure C4.- Block diagram of lateral hydromechanical control system. (U)

UNCLASSIFIED

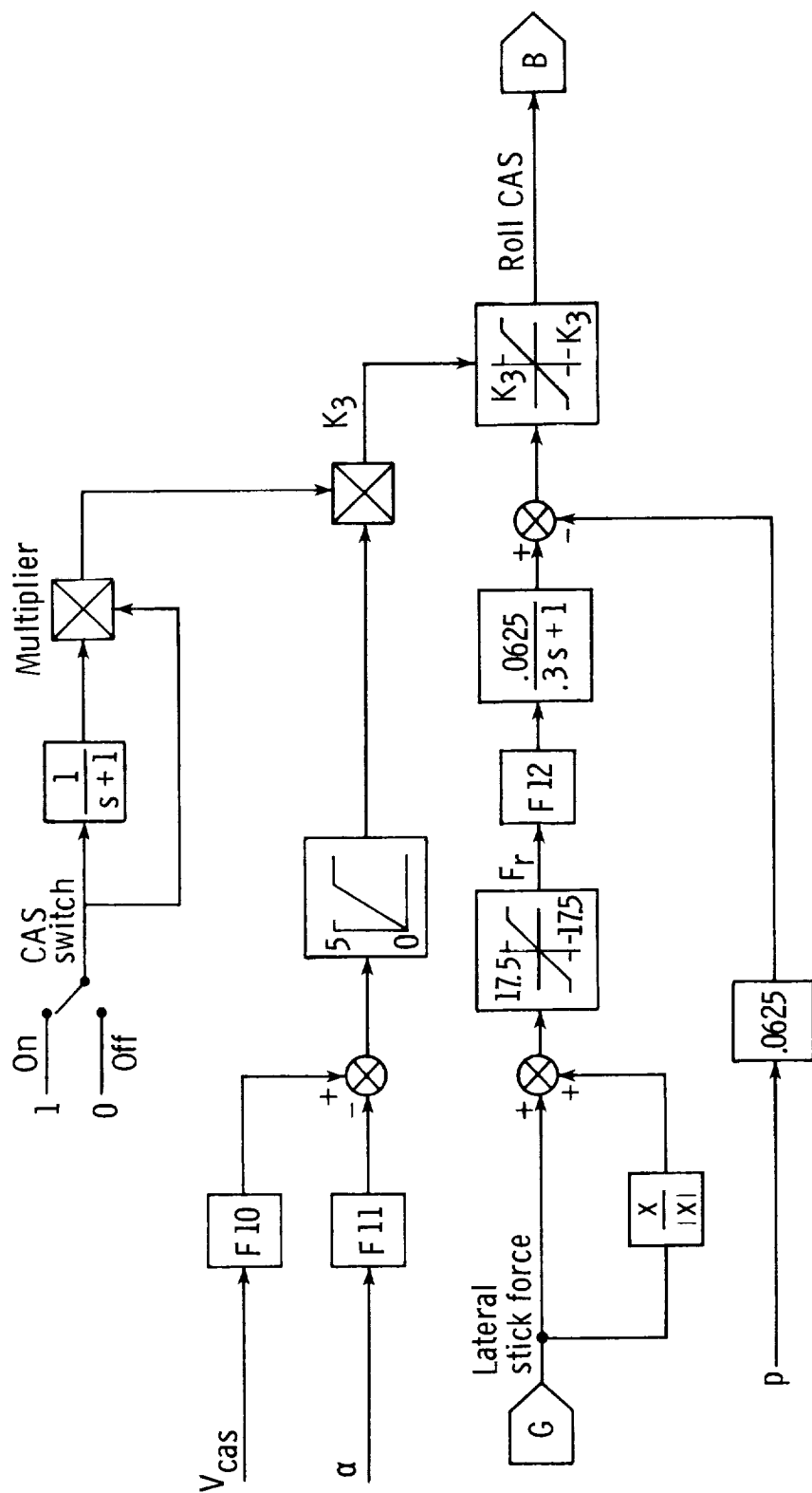
APPENDIX C



(U) Figure C5.- Lateral stick spring force function. (U)

UNCLASSIFIED

APPENDIX C

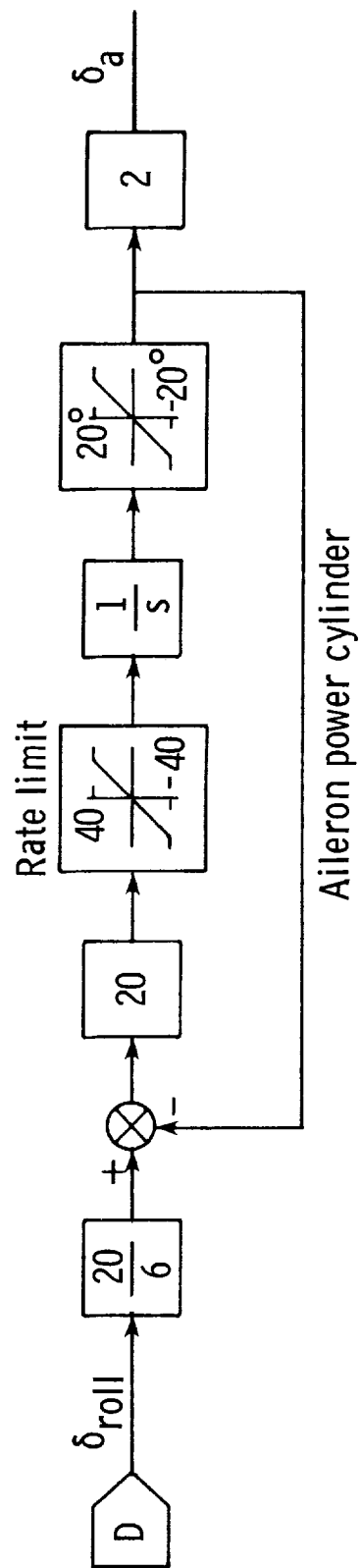


(U) Figure C6.- Block diagram of simulated roll CAS. (U)

UNCLASSIFIED

UNCLASSIFIED

APPENDIX C

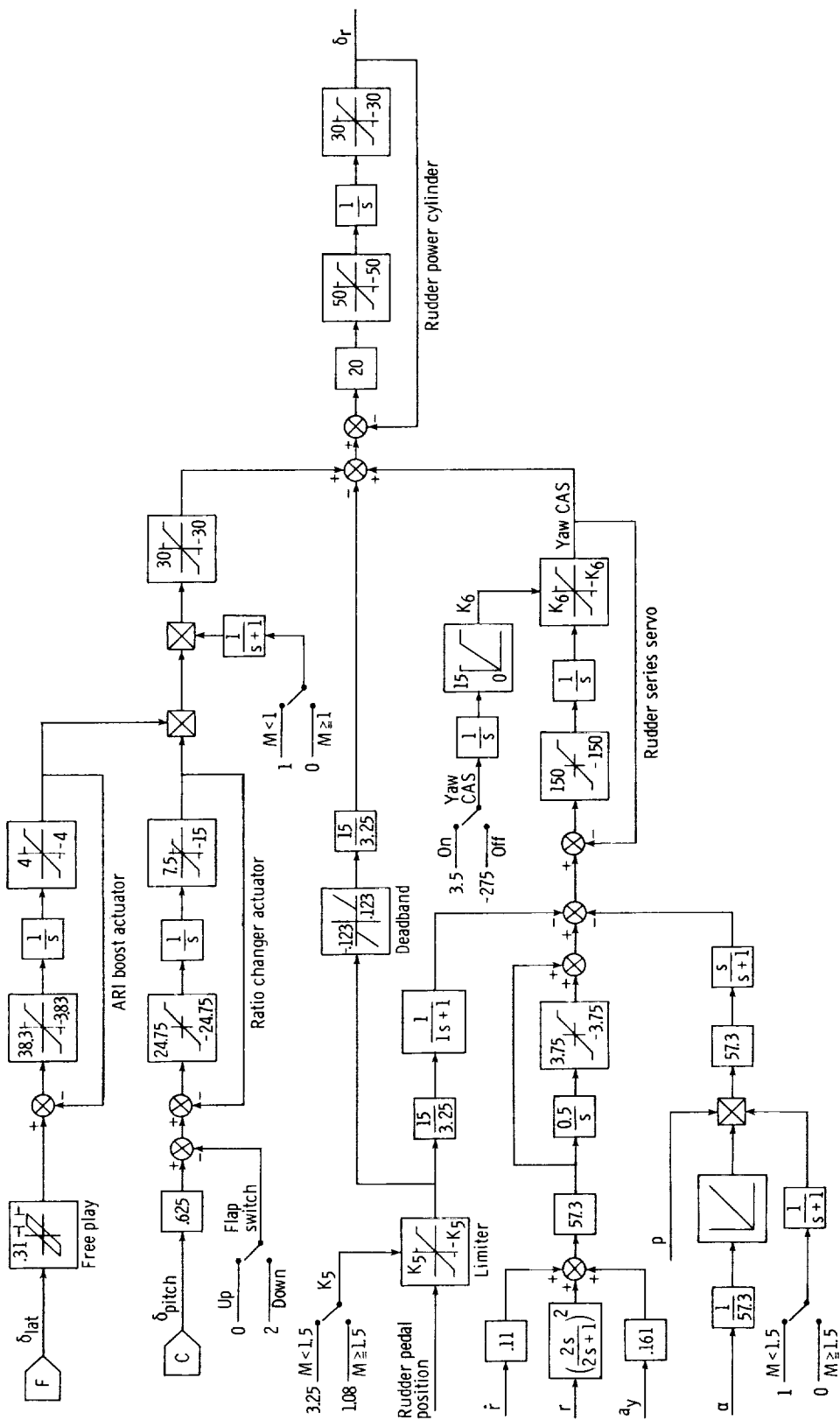


Aileron power cylinder

(U) Figure C7.- Block diagram of aileron simulation. (U)

UNCLASSIFIED

APPENDIX C



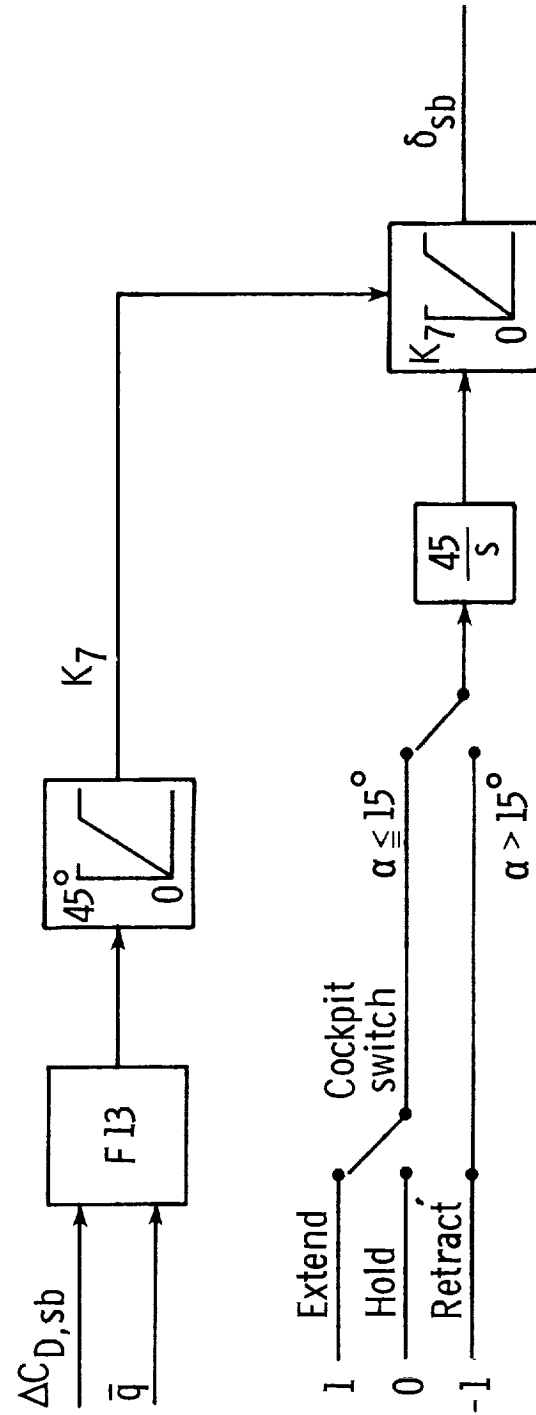
(U) Figure C8.- Block diagram of rudder simulation. (U)

UNCLASSIFIED

147

UNCLASSIFIED

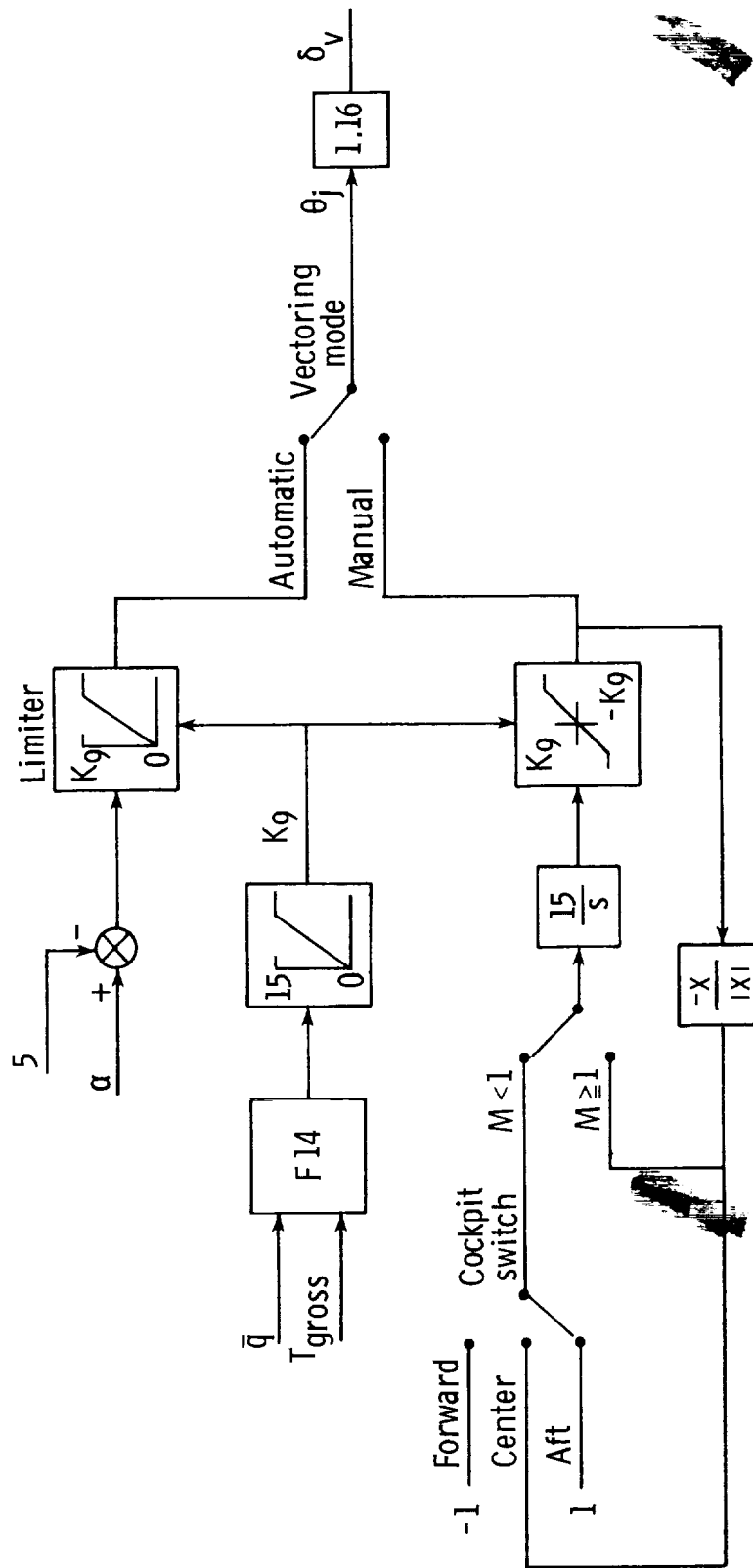
APPENDIX C



(U) Figure C9.—Block diagram of speed-brake simulation. (U)

UNCLASSIFIED

APPENDIX C



(U) Figure C10.- Block diagram of thrust-vectoring simulation. (U)

UNCLASSIFIED

APPENDIX D

FLYING QUALITIES AND PERFORMANCE (U)

(U) This appendix describes the tests conducted to document the flying qualities and performance of the simulated F-15 and to compare with available F-15 flight test data (refs. 22 and 23).

(U) Static Longitudinal Stability (U)

(U) Static longitudinal stability was tested by making level flight accelerations and decelerations at the flight conditions shown in table D1. The simulated airplane did not require a change in stick force or displacement as airspeed changed. This zero-speed stability is a characteristic of the F-15 (refs. 22 and 23). All tests were made with CAS on.

(U) TABLE D1.- TEST CONDITIONS FOR STATIC LONGITUDINAL

STABILITY CHECKS (U)

Altitude		Mach number range	Weight		Center-of-gravity position	Figure
m	ft		kg	lb		
3 048	10 000	0.5 to 1.1	15 876	35 000	0.28 \bar{c}	D1(a)
6 096	20 000	.6 to 1.3	15 876	35 000	.28 \bar{c}	D1(b)
10 668	35 000	.9 to 1.6	15 422	34 000	.30 \bar{c}	D1(c)

(U) Angle of attack and symmetric stabilator deflection are shown in figure D1. Angle of attack was in good agreement between the simulator and flight test. The flight test required more positive (nose down) stabilator to trim at supersonic speeds.

Dynamic Longitudinal Stability (U)

(U) Dynamic longitudinal stability tests were conducted to determine the short-period characteristics of the simulated airplane. Tests were made at $W = 15\ 422\ kg$ (34 000 lb), center of gravity = 0.24 \bar{c} , with roll CAS and yaw CAS on, with pitch CAS on and off, and at various flight conditions. Longitudinal oscillations were initiated by a 44-N (10-lb) doublet applied to the longitudinal stick force.

(C) Table D2 shows the test conditions and the natural frequency, damping ratio, and time to half amplitude that were found. Figure D2 shows the natural

APPENDIX D

frequency and damping ratio for the free airframe (pitch CAS off). Figure D2 also shows flight test results from reference 22. The data in figure D2 show that the simulated airplane with pitch CAS off had a higher damping ratio than the flight test airplane and had good agreement with the natural frequency.

TABLE D2.- LONGITUDINAL SHORT-PERIOD RESPONSE (U)

Mach	Dynamic pressure		Pitch CAS on			Pitch CAS off		
	N/m ²	lb/ft ²	ζ	ω_n	$t_{1/2}$	ζ	ω_n	$t_{1/2}$
0.4	4 790	100	0.65	1.52	0.71	0.54	1.70	0.76
.6	9 580	200	.70	1.77	.56	.51	2.18	.63
.79			.45	1.83	.85	.35	2.03	.99
.91			.37	2.06	.92	.21	2.15	1.56
.93			.35	2.17	.93	.28	2.33	1.06
.97			.31	2.52	.88	.22	2.71	1.18
.60	19 150	400	.71	2.78	.35	.63	3.42	.32
.79			.58	2.81	.43	.46	3.08	.49
.90			.53	3.08	.42	.41	3.21	.52
.94			.49	3.44	.41	.37	3.45	.54
1.20			.44	5.10	.31	.20	5.81	.59
.80	38 300	800	.73	4.50	.21	.54	4.76	.27
.9			.70	4.77	.21	.54	5.61	.23
.96			.64	5.43	.20	.37	6.12	.31
1.22			.50	6.20	.22	.28	8.49	.29

(U) Maneuvering Longitudinal Stability (U)

(U) Maneuvering longitudinal stability was evaluated at the flight conditions shown in table D3, for the basic airplane at a weight of 15 876 kg (35 000 lb) and 0.28 \bar{c} center-of-gravity position. The variation of symmetric stabilator deflection and angle of attack with normal load factor is shown in figure D3 and compared with flight test data from reference 23. The simulator and flight data were in good agreement at subsonic speeds. At M = 1.2 (fig. D3(d)), the flight data showed more positive (nose down) stabilator required.

STATIC LATERAL-DIRECTIONAL STABILITY (U)

(U) Static lateral-directional stability tests were accomplished to compare the dihedral effect of the simulated F-15 with flight data from reference 23. Steady heading sideslips were accomplished with CAS on at a weight of 15 876 kg (35 000 lb) and 0.28 \bar{c} center-of-gravity position at the flight conditions shown in table D4.

APPENDIX D

(U) TABLE D3.- TEST CONDITIONS FOR MANEUVERING LONGITUDINAL
STABILITY CHECKS (U)

Dynamic pressure		Mach number	Altitude		Figure
			m	ft	
N/m ²	lb/ft ²				
9 576	200	0.6	7 556	24 790	D3(a)
19 152	400	.6	2 362	7 750	D3(a)
9 576	200	.8	11 384	37 350	D3(b)
19 152	400	.8	6 720	22 047	D3(b)
9 576	200	.9	12 884	42 269	D3(c)
19 152	400	.9	8 374	27 473	D3(c)
19 152	400	1.2	12 133	39 808	D3(d)

(U) TABLE D4.- TEST CONDITIONS FOR STATIC LATERAL-DIRECTIONAL
STABILITY CHECKS (U)

Dynamic pressure		Mach number	Altitude		Figure
			m	ft	
N/m ²	lb/ft ²				
4 788	100	0.6	12 070	39 600	D4(a)
9 576	200	.6	7 556	24 790	D4(b)
19 152	400	.6	2 362	7 750	D4(c)

(U) Lateral stick deflection δ_{lat} and control surface deflections are shown in figure D4 as functions of sideslip angle. Simulated rudder deflection agreed well with flight data. Larger aileron deflection was required in the simulator, suggesting lower aileron effectiveness or larger dihedral effect in the simulated F-15.

(U) Dynamic Lateral-Directional Stability (U)

(U) Dynamic lateral-directional stability tests were conducted to determine the dutch roll characteristics of the simulated airplane. Tests were made at $W = 15\ 422\ kg$ (34 000 lb), center of gravity = $0.24\bar{c}$, with pitch CAS on, and

APPENDIX D

with roll and yaw CAS either both on or both off. Tests were initiated by applying a doublet to the rudder pedal force.

(U) Table D5 shows the test conditions and the natural frequency, damping ratio, and time to half amplitude that were found.

(C) TABLE D5.- DUTCH ROLL RESPONSE (U)

Mach	Dynamic pressure		CAS on			CAS off		
	N/m ²	lb/ft ²	ζ	ω_n	$t_{1/2}$	ζ	ω_n	$t_{1/2}$
0.4	4 790	100	0.52	1.56	0.85	0.22	2.10	1.48
.6	9 580	200	.56	2.19	.56	.17	2.57	1.61
.79			.47	2.34	.64	.13	2.64	2.04
.91			.39	2.51	.70	.11	2.73	2.34
.93			.43	2.50	.64	.11	2.71	2.40
.97			.39	2.58	.69	.10	2.71	2.48
.6	19 150	400	.73	3.10	.31	.22	3.40	.93
.79			.65	3.26	.33	.18	3.52	1.11
.90			.59	3.43	.34	.16	3.64	1.22
.94			.58	3.47	.34	.15	3.63	1.27
1.2			.46	3.30	.46	.13	3.42	1.60
.8	38 300	800	.72	4.56	.21	.23	4.92	.61
.9			.67	4.70	.22	.21	5.06	.66
.96			.63	4.64	.24	.20	4.97	.70
1.22			.56	4.87	.25	.17	4.64	.88

(U) Lateral Control Characteristics (U)

(U) Lateral control tests were performed to determine the roll performance and roll characteristics of the simulated F-15. Two tests were made, as shown in table D6. One was made at fixed speed with angle of attack varied from 0° to 20°. The other test was made in 1g flight with Mach number varied from 0.4 to 1.2.

(U) Roll response in the simulator did not agree well with the flight data (fig. D5). The simulated airplane had higher roll response at the higher dynamic pressure, and lower response at the lower pressure. Figure D6 shows that the roll response decreased drastically as speed increased above M = 0.9.

(U) Pilots participating in the validation checks noted that the unsatisfactory supersonic roll response was not representative of the F-15. Therefore, an effort was made to obtain more accurate data for the simulation. An updated

UNCLASSIFIED

APPENDIX D

(U) TABLE D6.- TEST CONDITIONS FOR LATERAL CONTROL CHECKS (U)

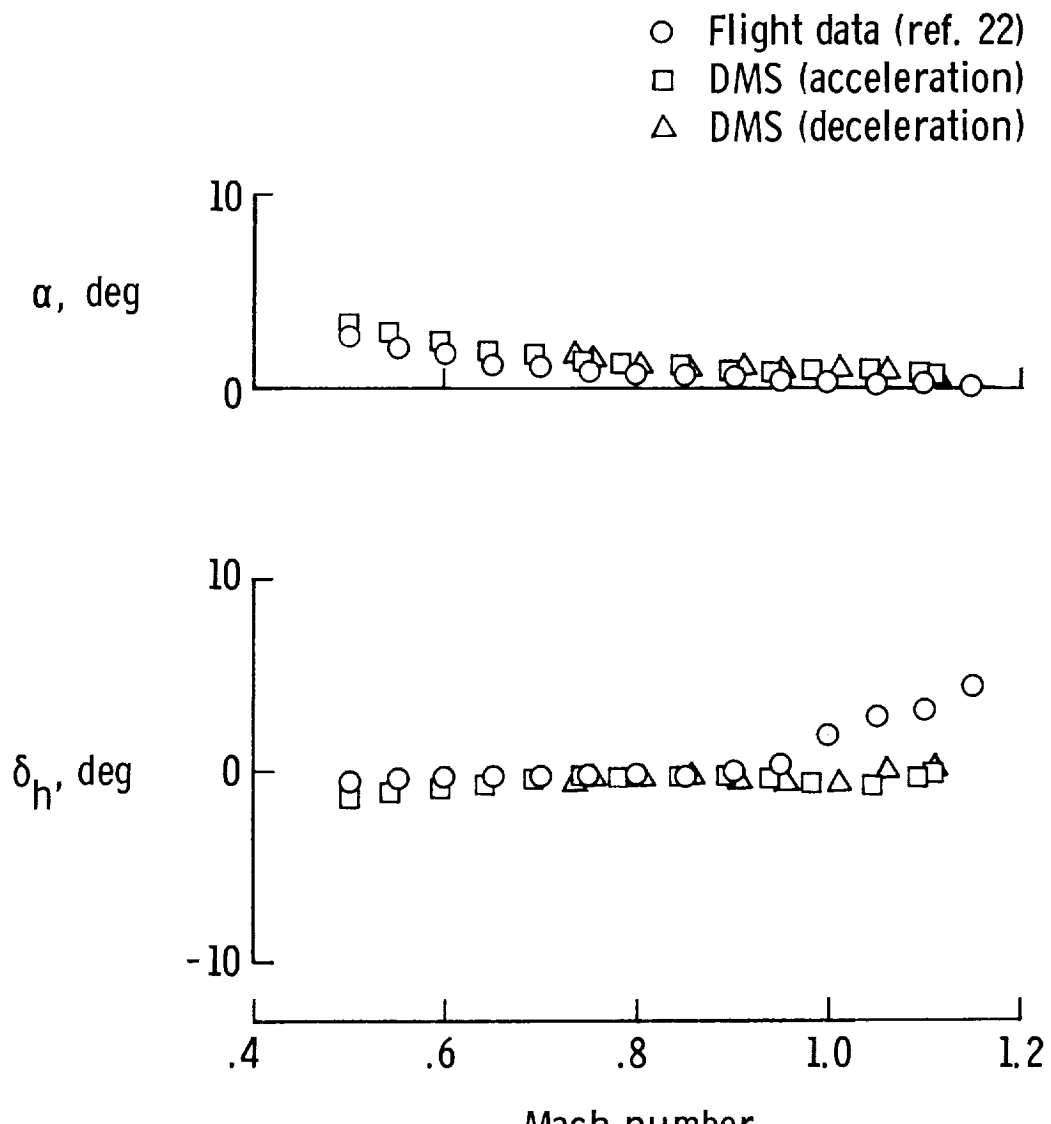
Mach number	Angle of attack	Dynamic pressure		Altitude		Figure
		N/m ²	lb/ft ²	m	ft	
0.4	0 to 20°	9 576	200	4 237	13 900	D5
.8	0 to 20°	19 152	400	6 720	22 047	D5
.4 - 1.2	1g to trim			9 144	30 000	D6

aerodynamic data package, based on flight test results, was being prepared at the time, but it was not available until after the DMS simulation was completed. The data presented in appendix B do not include this later data.

(U) Fortunately, this error did not significantly affect the simulation results. Simulated engagements were characterized by hard maneuvering at subsonic speeds. Therefore, the region of unrealistic lateral characteristics was beyond the resulting combat arena.

UNCLASSIFIED

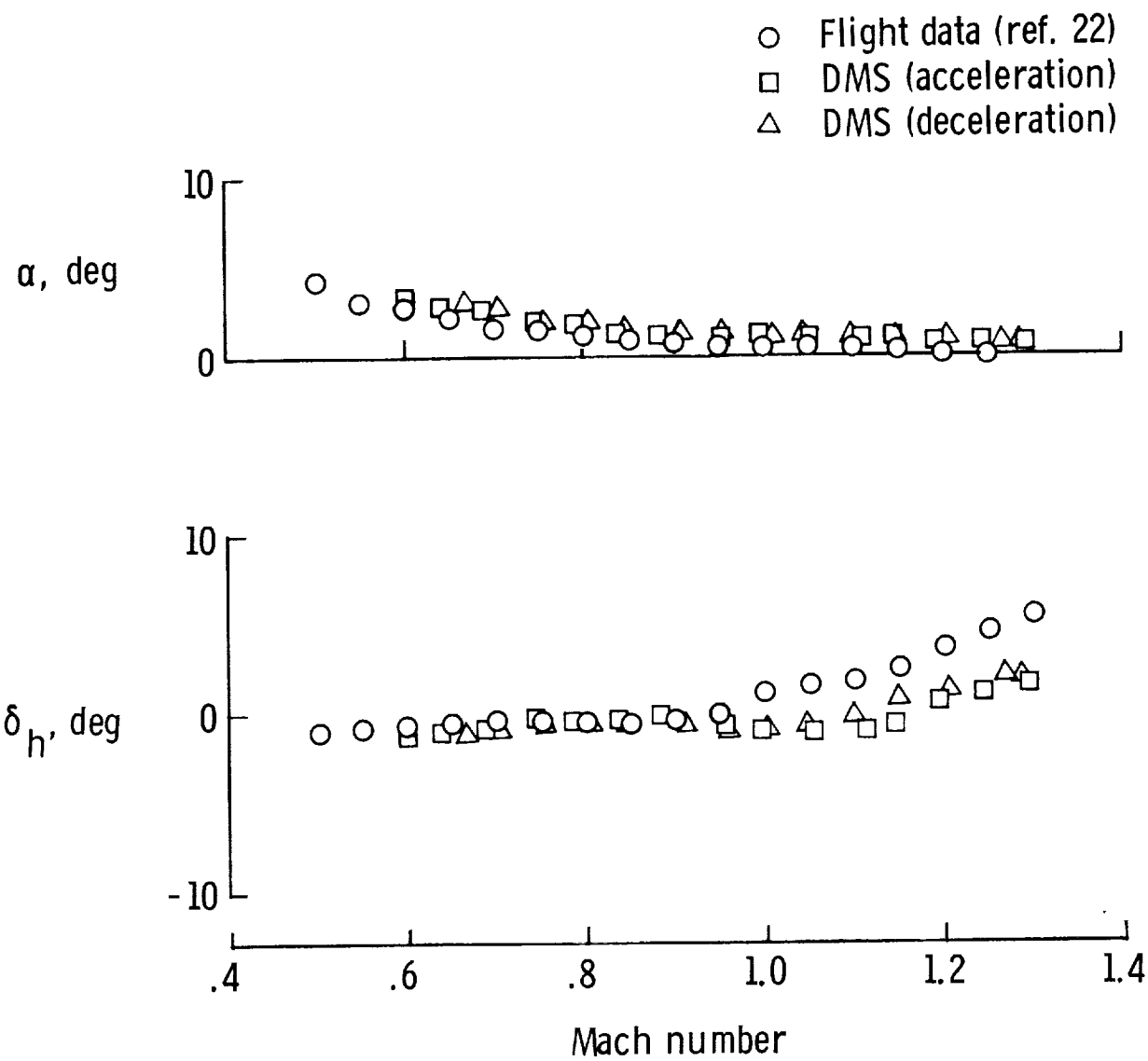
APPENDIX D

(a) $h = 3048 \text{ m} (10\,000 \text{ ft})$.

(U) Figure D1.- Static longitudinal stability. (U)

UNCLASSIFIED

APPENDIX D

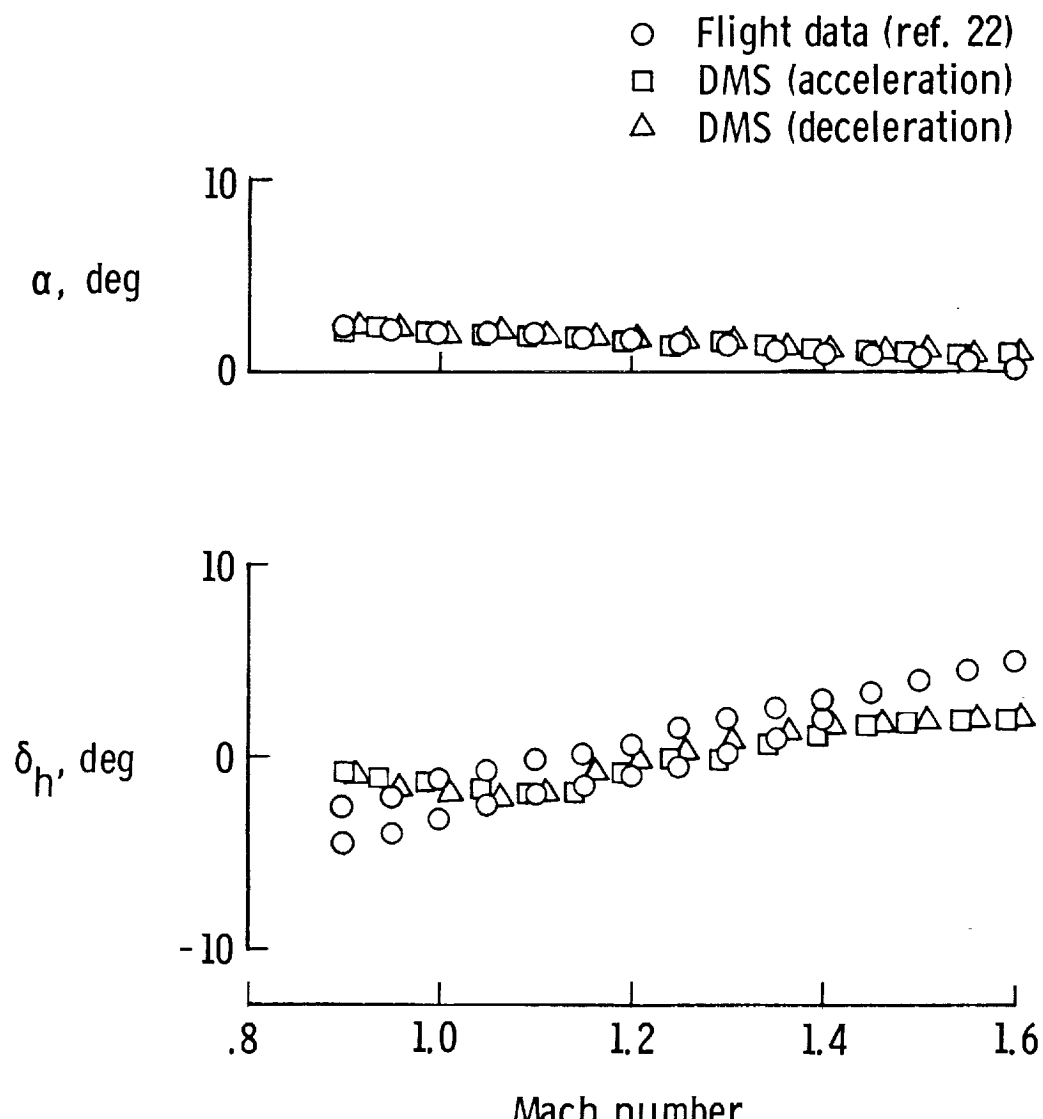


(b) h = 6096 m (20 000 ft).

(U) Figure D1.- Continued. (U)

UNCLASSIFIED

APPENDIX D



(c) h = 10 668 m (35 000 ft).

(U) Figure D1.- Concluded. (U)

APPENDIX D

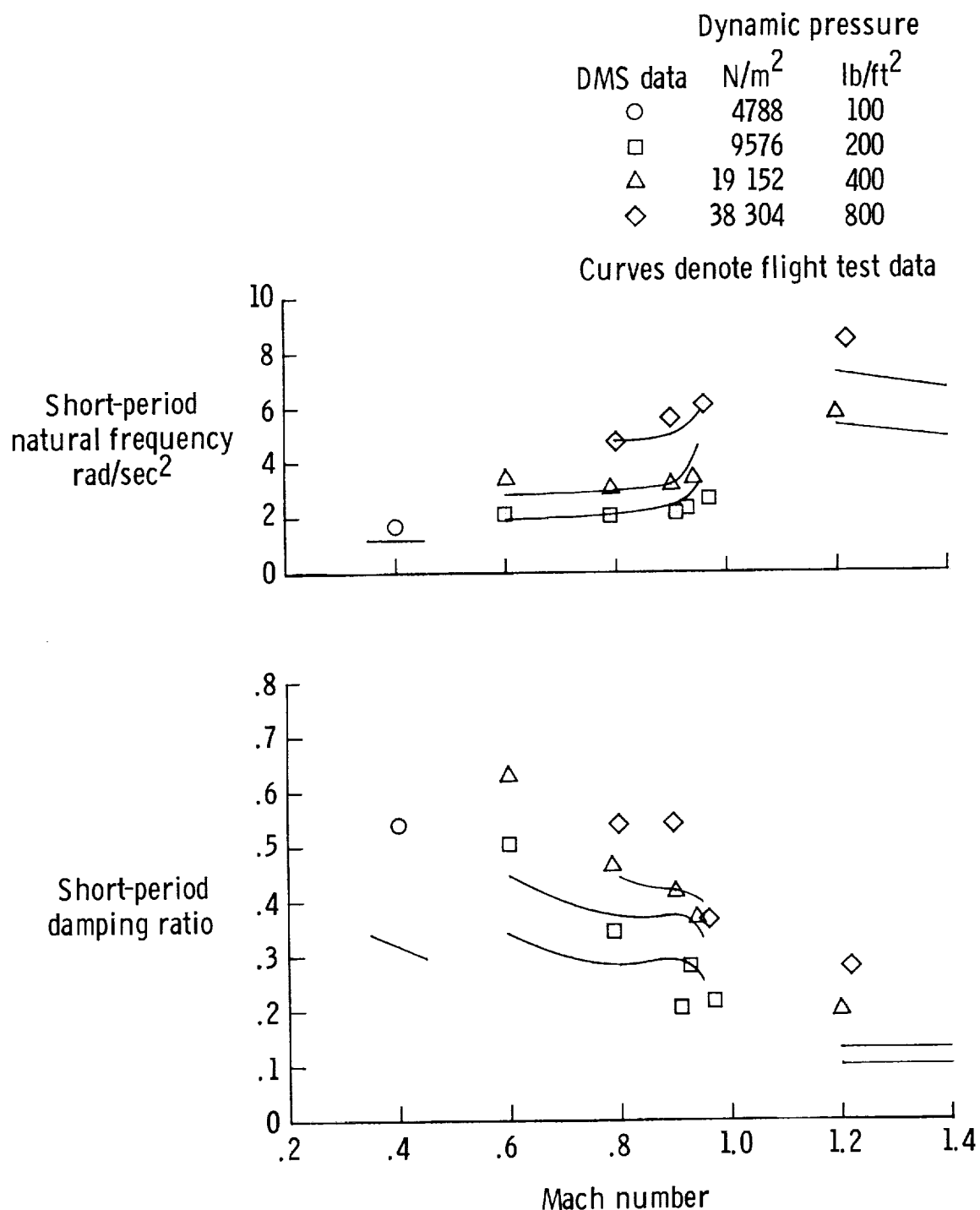
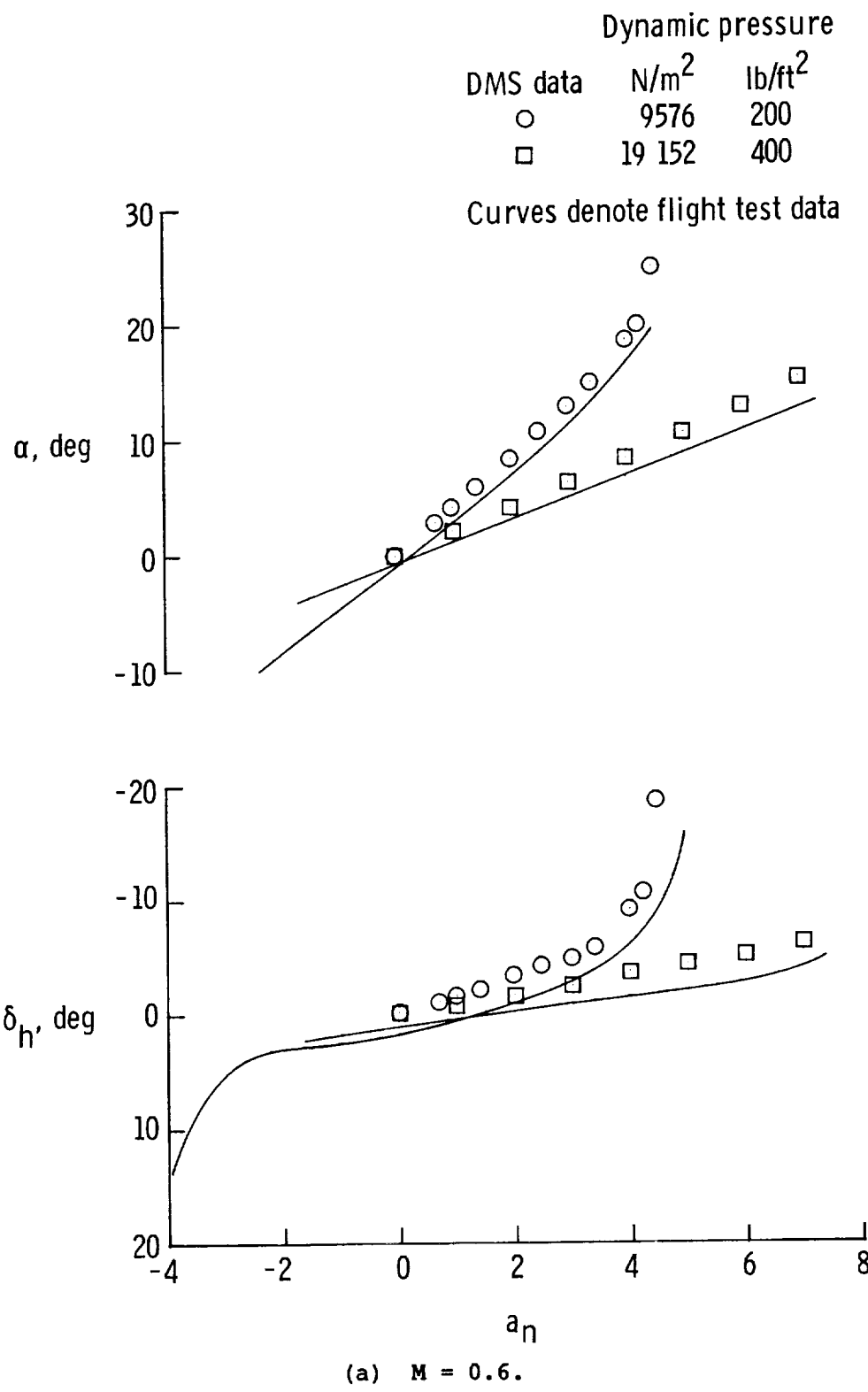


Figure D2.- Dynamic longitudinal stability with pitch CAS off. (U)

UNCLASSIFIED

APPENDIX D



(U) Figure D3.- Maneuvering longitudinal stability. (U)

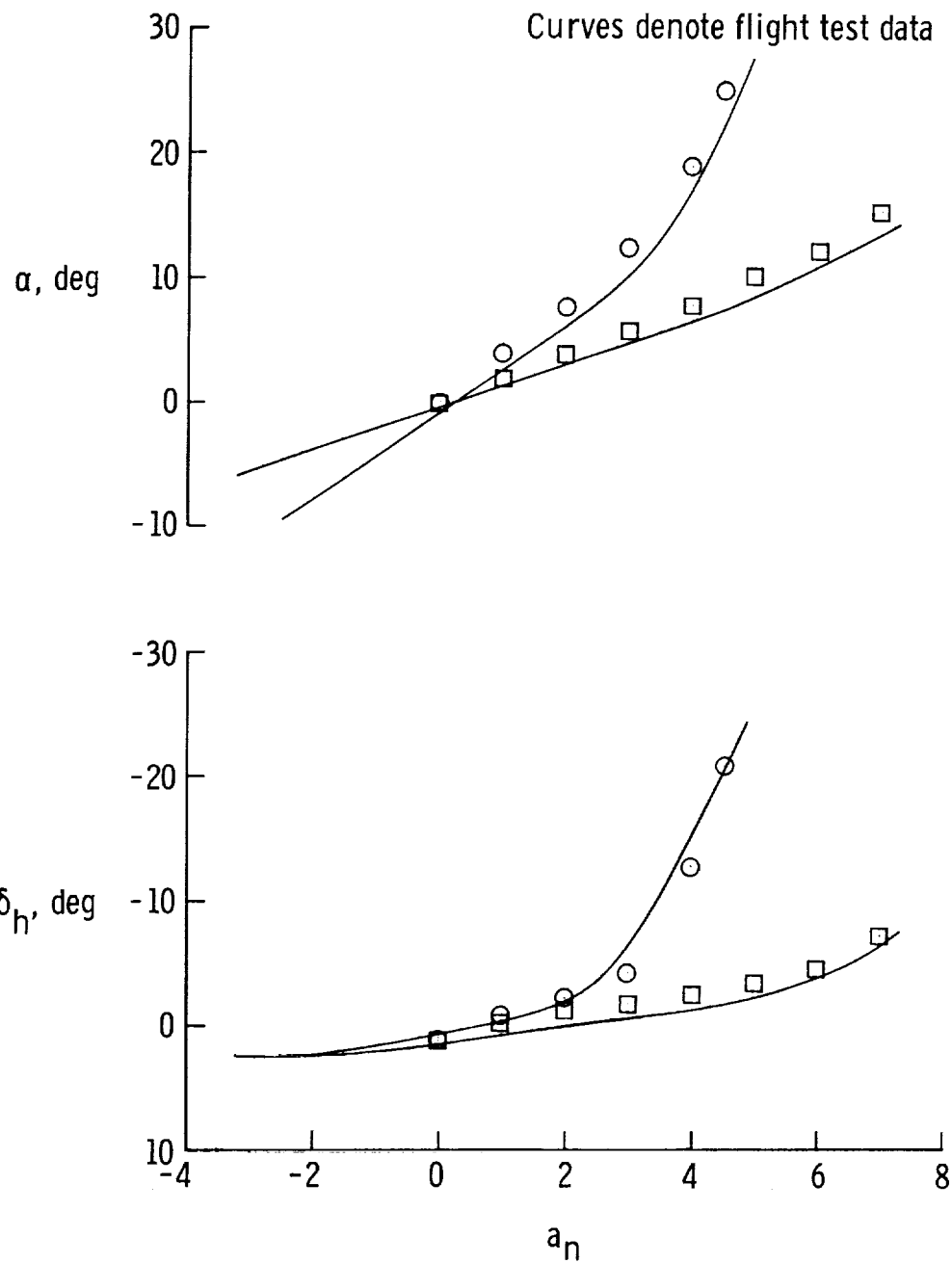
UNCLASSIFIED

UNCLASSIFIED

APPENDIX D

Dynamic pressure

DMS data	N/m ²	lb/ft ²
○	9576	200
□	19 152	400



(b) M = 0.8.

(U) Figure D3.- Continued. (U)

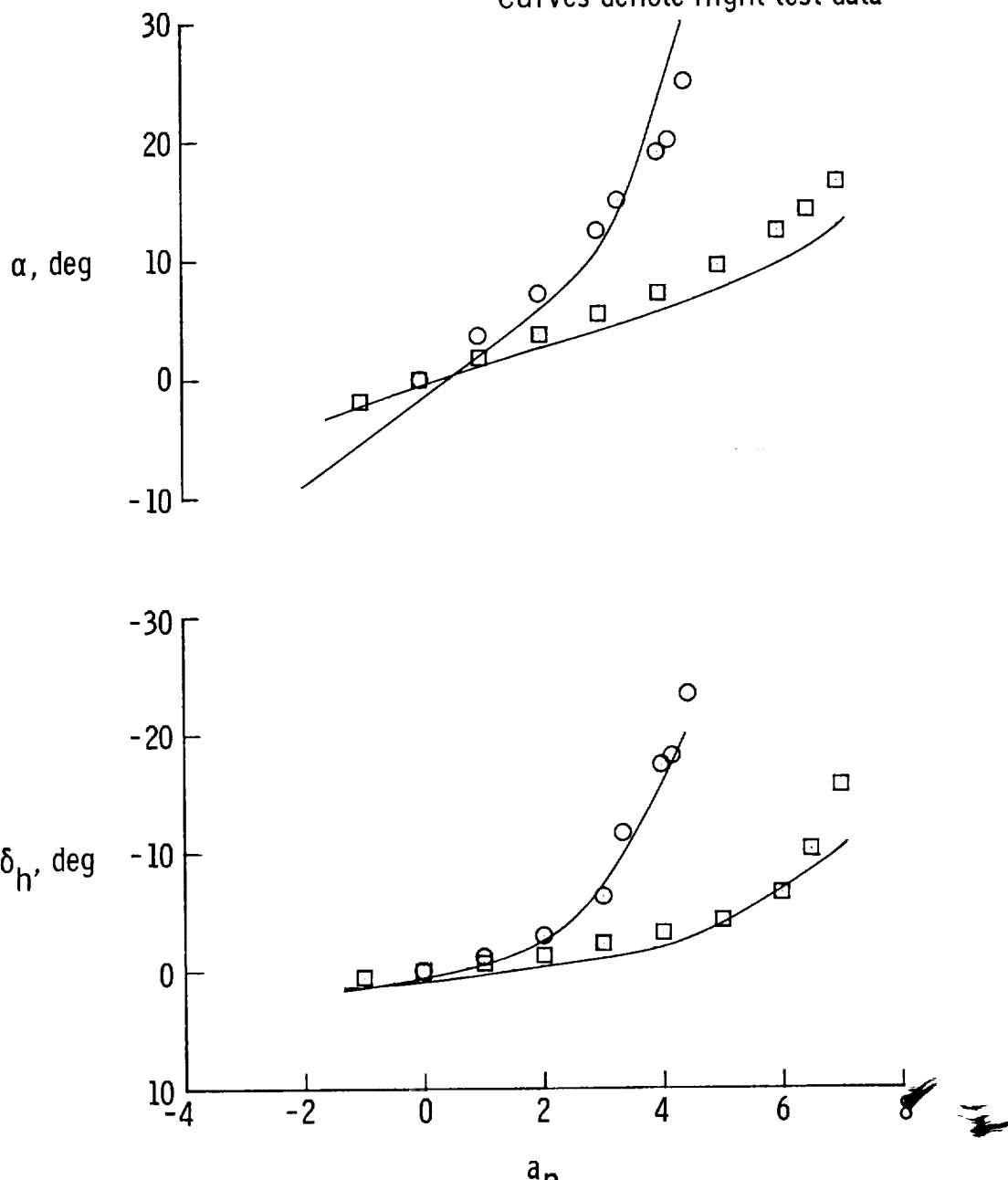
UNCLASSIFIED

APPENDIX D

Dynamic pressure

DMS data	N/m ²	lb/ft ²
○	9576	200
□	19 152	400

Curves denote flight test data



(c) M = 0.9.

(U) Figure D3.- Continued. (U)

UNCLASSIFIED

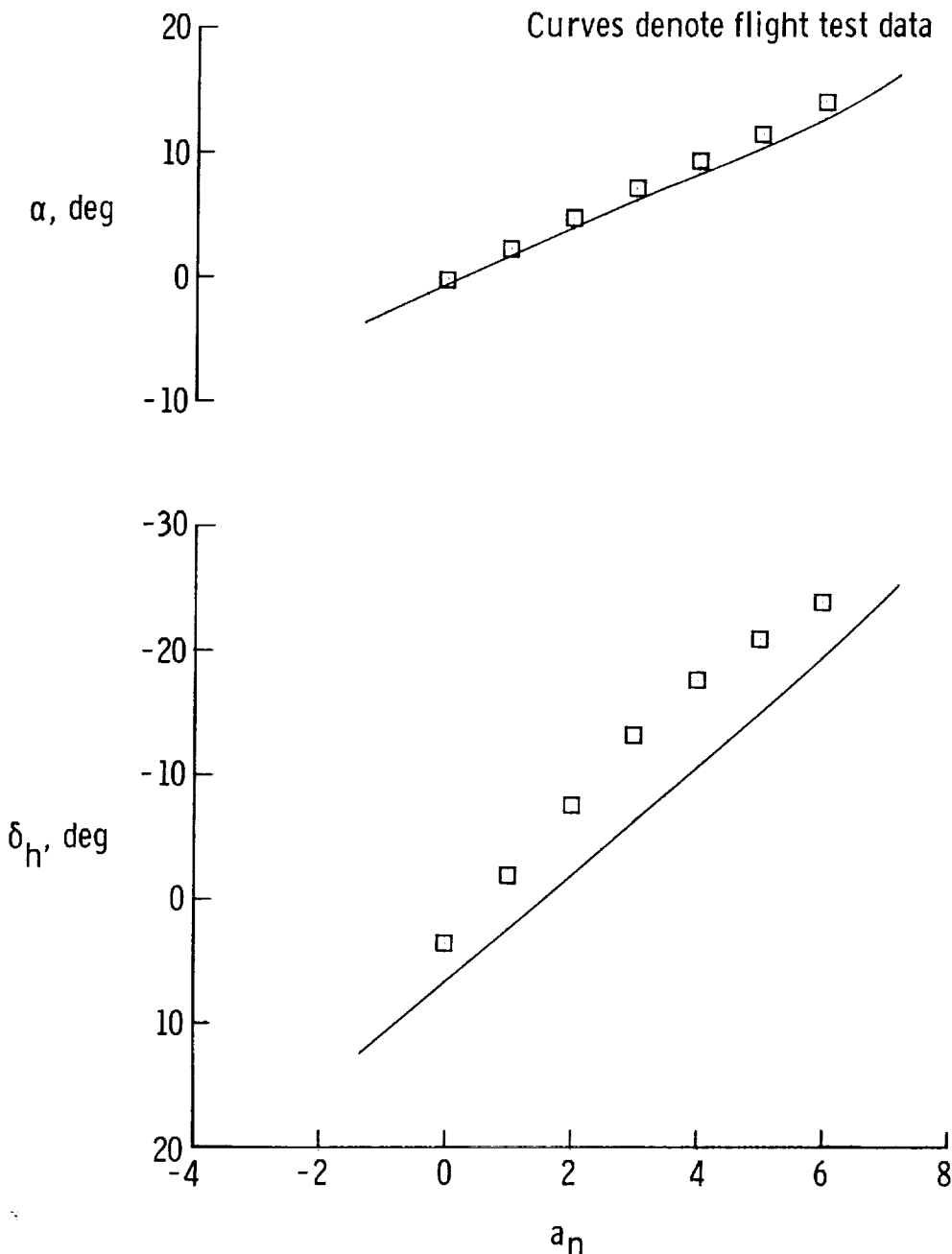
UNCLASSIFIED

APPENDIX D

Dynamic pressure

DMS data N/m² lb/ft²
□ 19 152 400

Curves denote flight test data



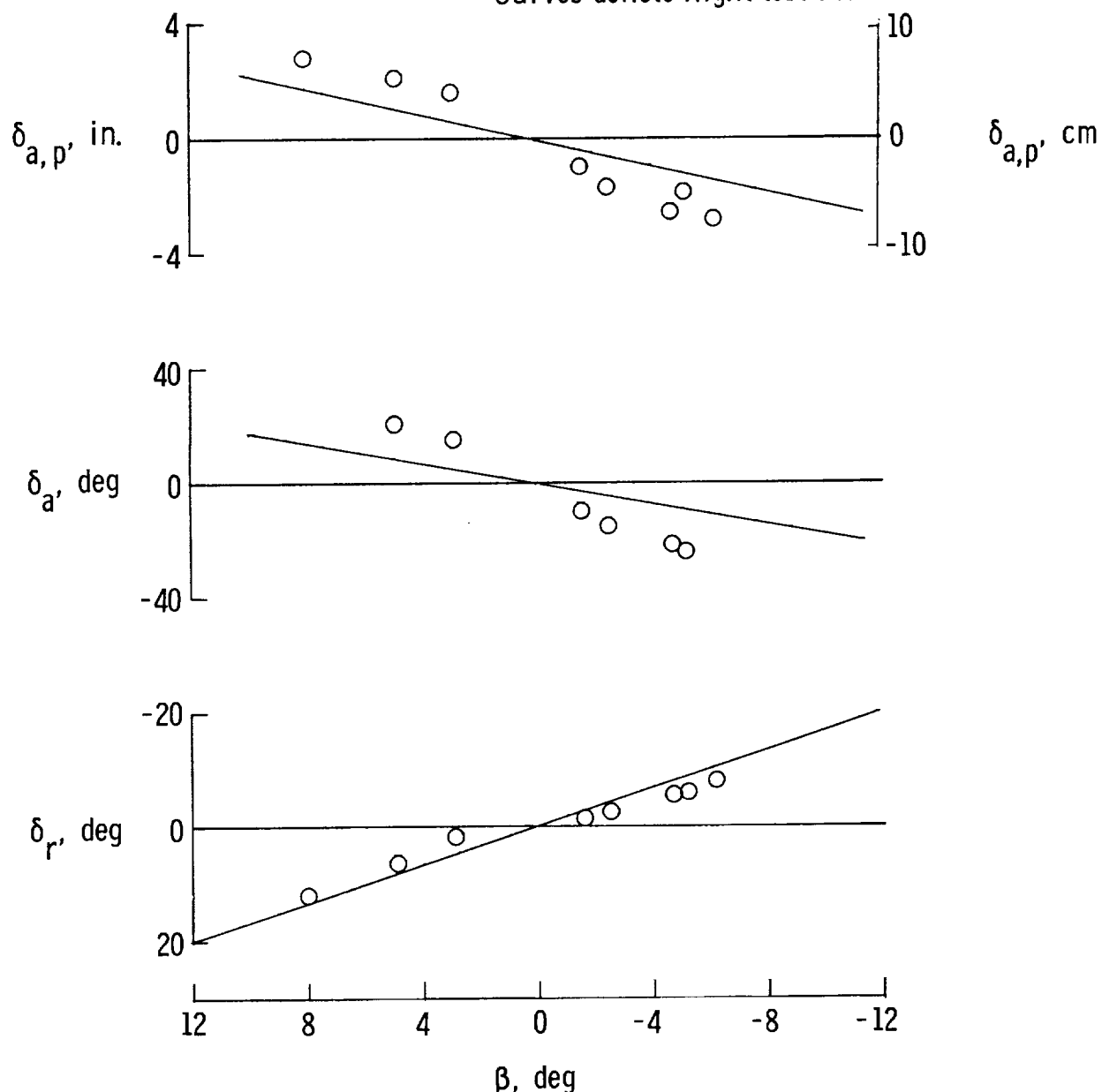
(d) M = 1.2.

(U) Figure D3.- Concluded. (U)

UNCLASSIFIED

APPENDIX D

Symbols denote DMS data
Curves denote flight test data



(a) $\bar{q} = 4788 \text{ N/m}^2 (100 \text{ lb/ft}^2)$.

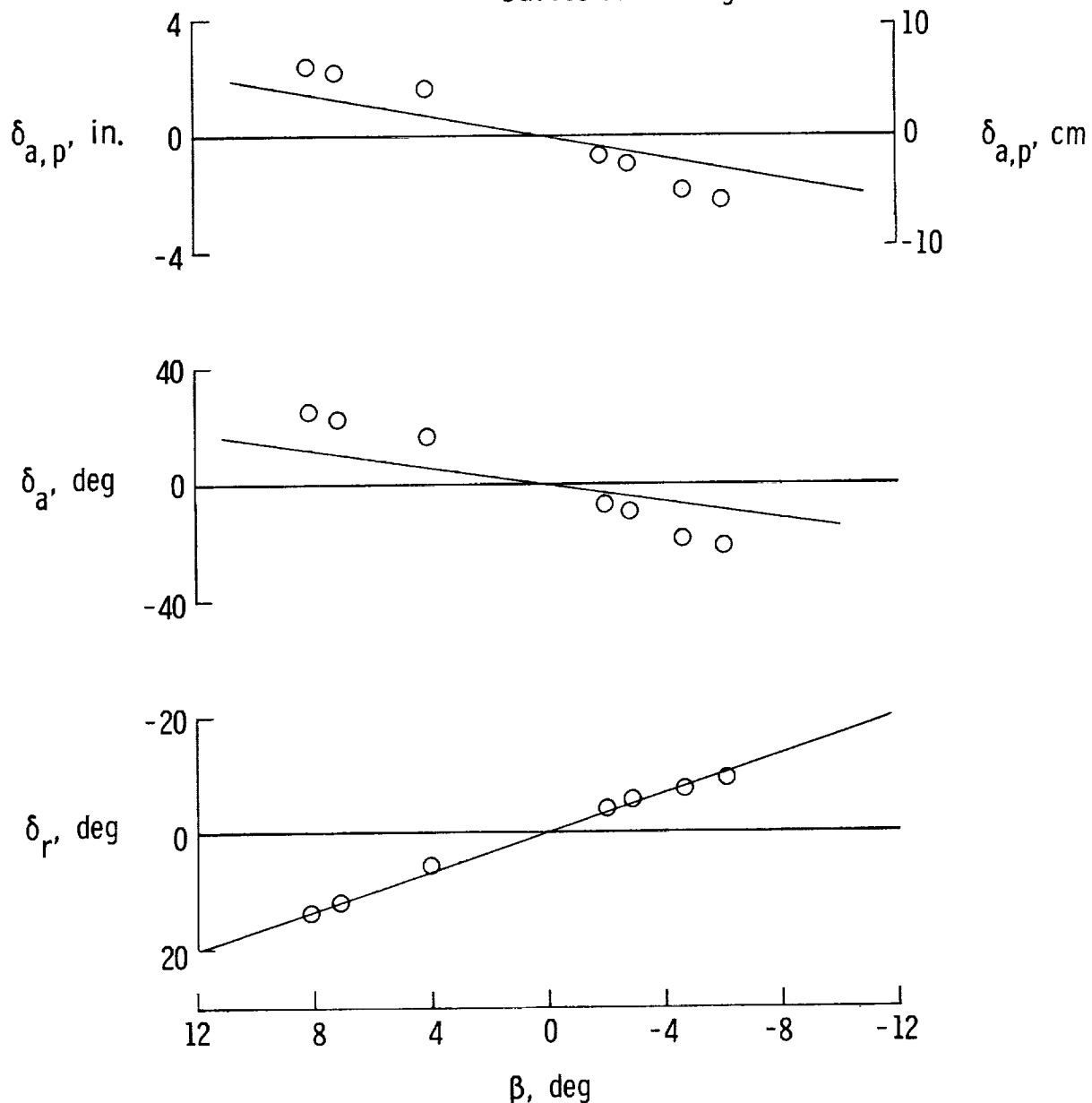
(U) Figure D4.- Static lateral-directional stability at $M = 0.6$. (U)

UNCLASSIFIED

UNCLASSIFIED

APPENDIX D

Symbols denote DMS data
Curves denote flight test data



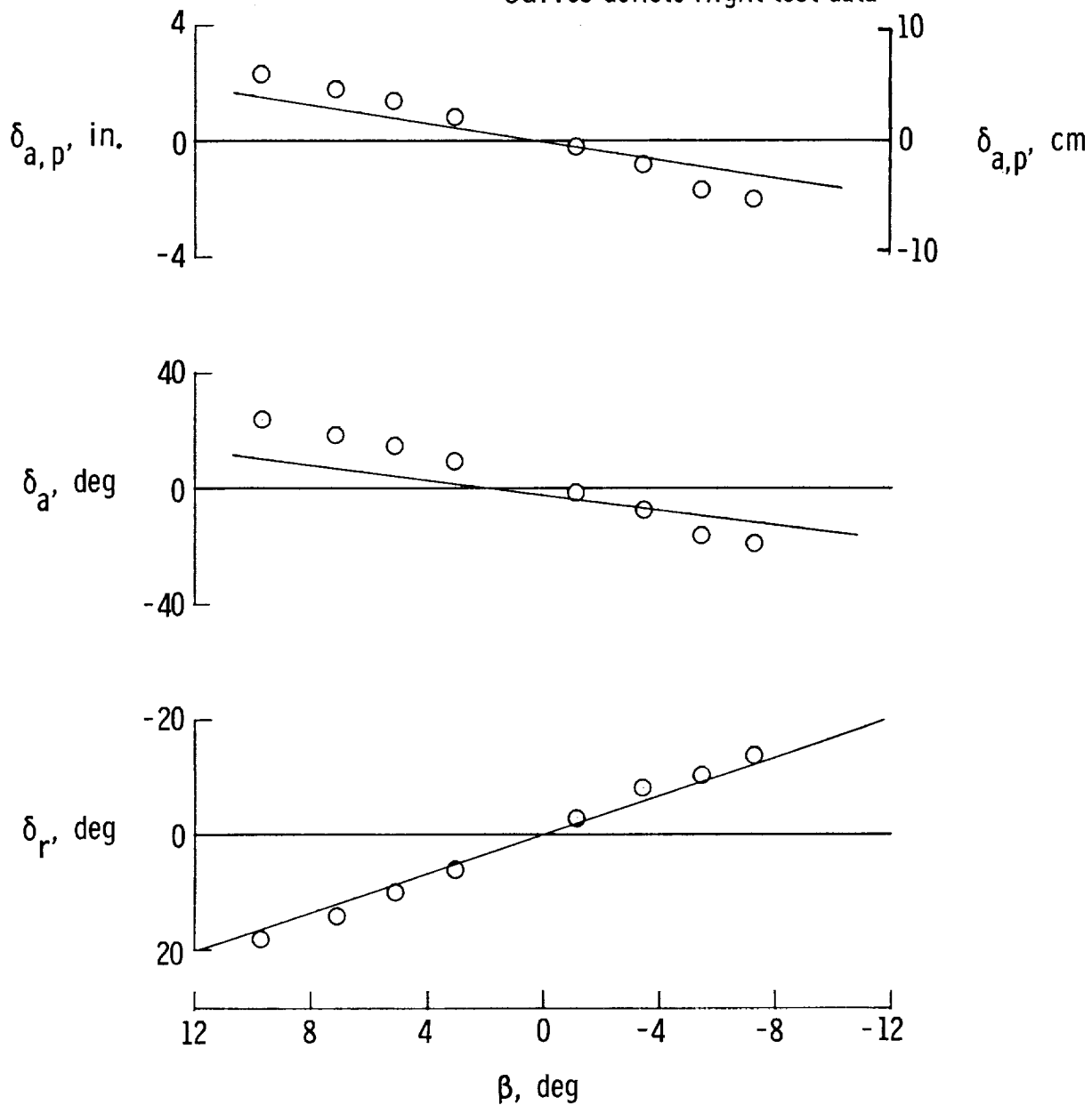
(b) $\bar{q} = 9576 \text{ N/m}^2$ (200 lb/ft^2).

(U) Figure D4.- Continued. (U)

UNCLASSIFIED

APPENDIX D

Symbols denote DMS data
Curves denote flight test data



(c) $\bar{q} = 19\ 152 \text{ N/m}^2 (400 \text{ lb/ft}^2)$.

(U) Figure D4.- Concluded. (U)

UNCLASSIFIED

UNCLASSIFIED

APPENDIX D

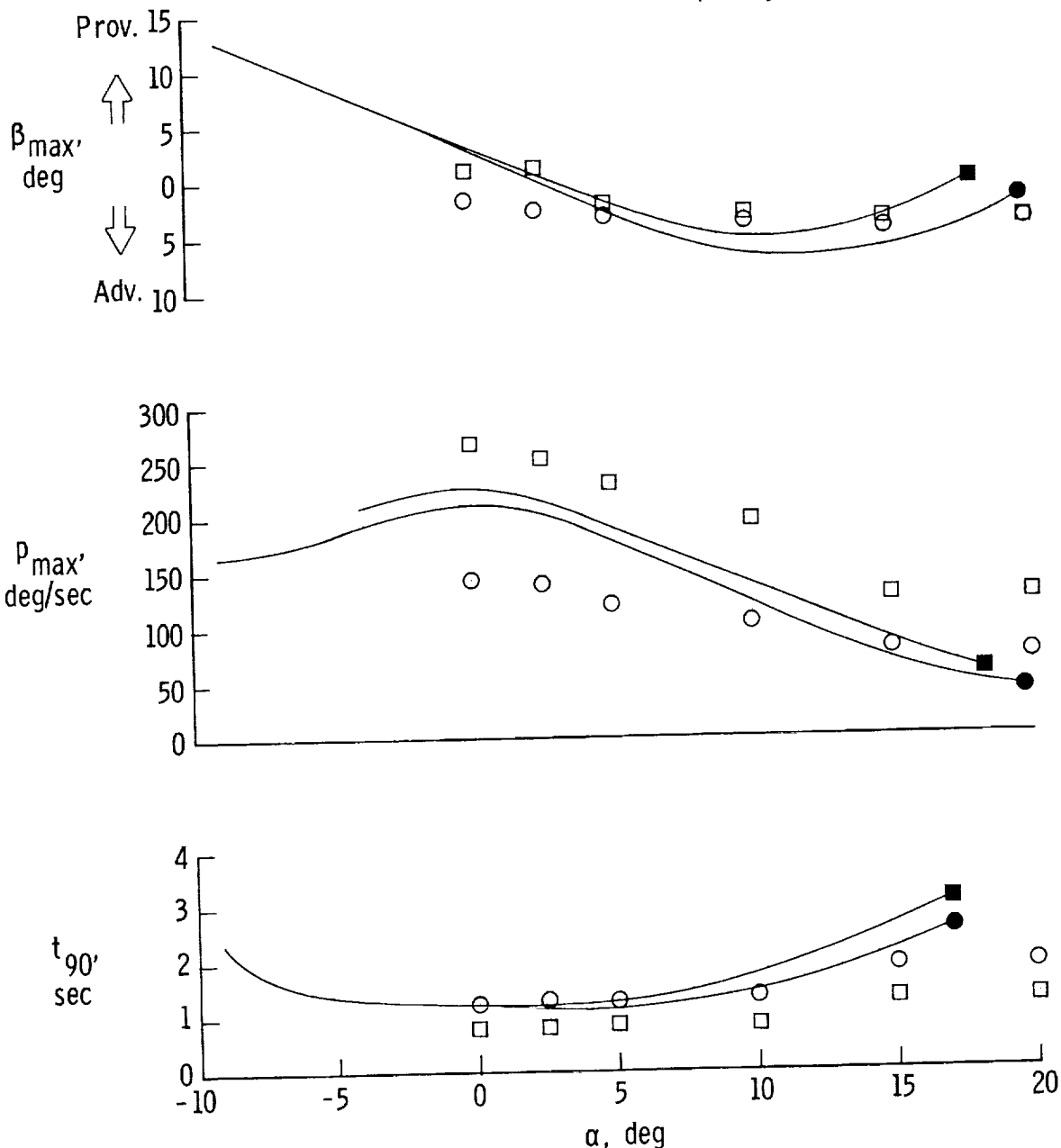
Flight data

- $M = 0.4 - 0.6, \bar{q} < 400 \text{ psf} (19152 \text{ N/m}^2)$
- $M = 0.8 - 0.9, \bar{q} < 400 \text{ psf} (19152 \text{ N/m}^2)$

Curves denote flight test data

Mach	Dynamic pressure	
	N/m^2	lb/ft^2
0.4	9576	200
0.8	19152	400

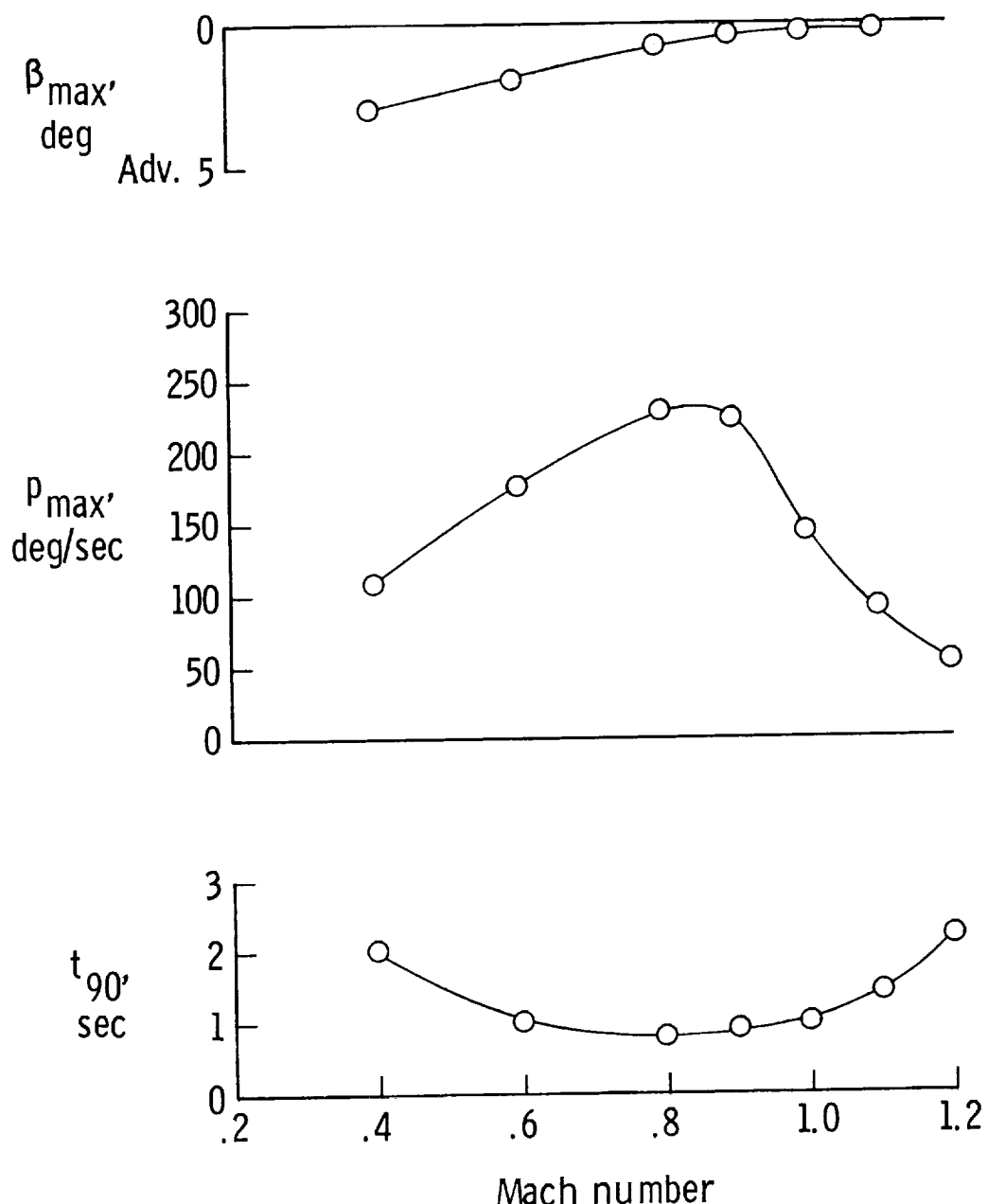
Open symbols denote DMS data



(U) Figure D5.- Roll response. (U)

UNCLASSIFIED

APPENDIX D



(U) Figure D6.- Roll response in 1g flight ($h = 9144$ m). (U)

UNCLASSIFIED

UNCLASSIFIED

APPENDIX E

(U) EQUATIONS FOR REAL-TIME GUN SIMULATION (U)

(U) This appendix presents the equations used in the real-time gun simulation. The ballistics equations are based on work done by the University of Texas for the U.S. Air Force Avionics Laboratory, Wright-Patterson Air Force Base, Ohio, and reported in reference 24. Since NASA is not involved in weapons systems research, the Department of Defense and industry are relied upon for data with which to modify and improve the weapons models in the DMS.

(U) Ballistics Model (U)

(U) The equations used for bullet trajectory computations are given in the following paragraphs.

(U) Projectile velocity in body axes.- The equation for the projectile velocity in body axes is

$$\bar{v}_{bo} = \bar{v} + \bar{v}_M + \bar{\omega} \times \bar{R}_{gcg}$$

where \bar{v} is the aircraft velocity

$$\bar{v} = \begin{Bmatrix} u \\ v \\ w \end{Bmatrix}$$

and u , v , and w are components of airplane velocity in the airplane body axis system.

(U) \bar{v}_M is the muzzle velocity where

$$\bar{v}_M = \begin{Bmatrix} u_M \\ v_M \\ w_M \end{Bmatrix} = \begin{Bmatrix} v_M \cos A_g \cos E_g \\ v_M \sin A_g \cos E_g \\ -v_M \sin E_g \end{Bmatrix}$$

where A_g and E_g are the gun azimuth and elevation angles, respectively.

UNCLASSIFIED

APPENDIX E

$$\bar{\omega} = \begin{Bmatrix} p \\ q \\ r \end{Bmatrix}$$

and p , q , and r are aircraft roll, pitch, and yaw rates (in radians per second) referenced to the body axis system. R_{gcg} is the displacement of the gun from the airplane center of gravity where

$$R_{gcg} = \begin{Bmatrix} x_{gcg} \\ y_{gcg} \\ z_{gcg} \end{Bmatrix}$$

The components of \bar{v}_{bo} in body axes are

$$\bar{v}_{bo} = \begin{Bmatrix} \dot{x}_{Bbo} \\ \dot{y}_{Bbo} \\ \dot{z}_{Bbo} \end{Bmatrix}$$

(U) Projectile yaw angle.- The projectile yaw angle δ_o is the angle (in radians) between \bar{v}_{bo} and \bar{v}_M .

$$\delta_o = \cos^{-1} \left(\frac{\dot{x}_{Bbo}u_M + \dot{y}_{Bbo}v_M + \dot{z}_{Bbo}w_M}{v_{bo}v_M} \right)$$

where v_{bo} and v_M are the magnitudes of \bar{v}_{bo} and \bar{v}_M .

$$v_M = 1006 \text{ m/sec (3300 ft/sec)}$$

(U) X_1, Y_1, Z_1 and X_2, Y_2, Z_2 coordinate systems.- Now it is necessary to introduce two new fixed coordinate systems: the X_1, Y_1, Z_1 system and the X_2, Y_2, Z_2 system. These are shown in figure E1. The X_1, Y_1 axes lie in the horizontal

UNCLASSIFIED

APPENDIX E

(X_I, Y_I) plane, with Z_I aligned with the $-Z_I$ axis (positive up). This is an orthogonal, but not right-hand system. Assuming a transformation matrix [D]

$$\begin{Bmatrix} X_I \\ Y_I \\ Z_I \end{Bmatrix} = [D] \begin{Bmatrix} X_1 \\ Y_1 \\ Z_1 \end{Bmatrix}$$

$$[D] = \begin{bmatrix} \cos \psi_o & \sin \psi_o & 0 \\ -\sin \psi_o & \cos \psi_o & 0 \\ 0 & 0 & -1 \end{bmatrix}$$

The X_1 axis lies along the projection of \bar{v}_{bo} on the horizontal plane. The X_2, Y_2, Z_2 axis system is defined by a rotation about Y_1 through an angle θ_o so that the X_2 axis lies along \bar{v}_{bo} . Thus, the X_1, X_2, Z_I, Z_1 , and Z_2 axes all lie in a vertical plane containing \bar{v}_{bo} . The matrix [E] transforms coordinates from the X_1, Y_1, Z_1 axis system to the X_2, Y_2, Z_2 system.

$$\begin{Bmatrix} X_2 \\ Y_2 \\ Z_2 \end{Bmatrix} = [E] \begin{Bmatrix} X_1 \\ Y_1 \\ Z_1 \end{Bmatrix}$$

$$[E] = \begin{bmatrix} \cos \theta_o & 0 & \sin \theta_o \\ 0 & 1 & 0 \\ -\sin \theta_o & 0 & \cos \theta_o \end{bmatrix}$$

The angles ψ_o and θ_o are defined by the inertial components of \bar{v}_{bo} .

$$\begin{Bmatrix} \dot{x}_{Ibo} \\ \dot{y}_{Ibo} \\ \dot{z}_{Ibo} \end{Bmatrix} = [C]^{-1} \begin{Bmatrix} \dot{x}_{Bbo} \\ \dot{y}_{Bbo} \\ \dot{z}_{Bbo} \end{Bmatrix}$$

UNCLASSIFIED

APPENDIX E

where $[C]^{-1}$ is the inverse of the body-to-inertial transformation matrix $[C]$ having element C_{ij} .

$$\theta_O = \sin^{-1} \left(\frac{-\dot{z}_{Ibo}}{v_{bo}} \right)$$

$$\psi_O = \tan^{-1} \left(\frac{\dot{y}_{Ibo}}{\dot{x}_{Ibo}} \right)$$

(U) Inertial projectile precession angle ϕ_O . - Referring to figure E1, the inertial projectile precession angle ϕ_O is defined as the projection of the gun boreline (or \bar{V}_M) on the Y_2, Z_2 plane. The components of \bar{V}_M in the X_2, Y_2, Z_2 system are

$$\begin{Bmatrix} u_M' \\ v_M' \\ w_M' \end{Bmatrix} = [E][D][C]^{-1} \begin{Bmatrix} u_M \\ v_M \\ w_M \end{Bmatrix}$$

and $\phi_O = \tan^{-1} \left(\frac{v_M'}{w_M'} \right)$

(U) Projectile coordinates and windage jump. - The position of the projectile is computed in the X_1, Y_1, Z_1 coordinate system, with the origin at the aircraft center of gravity at time of fire.

$$x_1 = P \cos \theta_O + s_x$$

$$y_1 = s_y$$

$$z_1 = P \sin \theta_O - Q + s_z$$

where P is the Sciatti range, Q is the gravity drop, and s_x , s_y , s_z are windage jump displacements.

$$s_x = C_x P$$

$$s_y = C_y P$$

UNCLASSIFIED

UNCLASSIFIED

APPENDIX E

$$S_z = C_z P$$

$$C_x = -\delta_o(a \cos \phi_o - b \sin \phi_o) \sin \theta_o$$

$$C_y = \delta_o(a \sin \phi_o + b \cos \phi_o)$$

$$C_z = \delta_o(a \cos \phi_o - b \sin \phi_o) \cos \theta_o$$

where a and b are constants, $a = 0.00751$ and $b = 0.0564$. The inertial position of the projectile is given, then, by

$$\begin{Bmatrix} x_{Ib} \\ y_{Ib} \\ z_{Ib} \end{Bmatrix} = [D]^{-1} \begin{Bmatrix} x_1 \\ y_1 \\ z_1 \end{Bmatrix}$$

Note that P and Q are not perpendicular. P is along initial direction of travel (\bar{v}_{bo}) and Q is vertical.

(U) Equations of Motion (U)

(U) The equations of motion for Sciatti range and gravity drop are:

$$\ddot{P} = \frac{-\rho d^2 v_p K_D}{m_p} (1 + K_o e^{-KP}) \dot{P}$$

$$\ddot{Q} = \frac{-\rho d^2 v_p K_D}{m_p} (1 + K_o e^{-KP}) \dot{Q} + g$$

where

m_p bullet mass, 101.7 grams (0.00696 slug)

d bullet diameter, 20 mm (0.06562 ft)

UNCLASSIFIED

APPENDIX E

$$g = 9.81 \text{ m/sec}^2 (32.2 \text{ ft/sec}^2)$$

$$K_0 = \frac{(13.2)(S_0 - 1/2)\delta_0^2}{(S_0 - 1)}$$

$$K = 2\sigma c$$

σ atmospheric density ratio, (ρ/ρ_0)

ρ_0 atmospheric density at sea level

$$c = c_1 + \frac{c_2}{(S_0 - 1)}$$

$$c_1 = 0.00755 \text{ m}^{-1} (0.0023 \text{ ft}^{-1})$$

$$c_2 = 0.000344 \text{ m}^{-1} (0.000105 \text{ ft}^{-1})$$

$$S_0 = \frac{s_s}{\sigma} \left(\frac{v_M}{v_{bo}} \right)^2$$

$$s_s = 3.5655$$

K_D is the drag function, given in table E1.

$$v_p = \sqrt{\dot{P}^2 + \dot{Q}^2 - 2\dot{P}\dot{Q} \sin \theta_0}$$

where v_p is projectile speed and $M_p = \frac{v_p}{v_s}$ where M_p = projectile Mach number and v_s = speed of sound.

UNCLASSIFIED

APPENDIX E

(U) TABLE E1.- BALLISTIC DRAG FUNCTION (U)

M_p	K_D	M_p	K_D
≤ 0.7	0.0958	3.7	0.1296
1.2	.2219	4.2	.1217
1.7	.1936	4.7	.1155
2.2	.1700	5.2	.1100
2.7	.1516	5.7	.1052
3.2	.1394	≥ 6.2	.1013

at $t = 0$, $\dot{P} = V_{bo}$ and $\dot{Q} = P = Q = 0$.

(U) Number of Bullet Hits (U)

(U) The steps involved in computing probability of hit and expected number of hits are summarized.

1. The target airplane is modeled as a rectangle located in the plane normal to the bullet trajectory and centered at the target center of gravity.
2. The angular size of the rectangle (in mils) is computed.
3. The angular displacement in azimuth and elevation between the impact point and target center is determined.
4. Assuming that the rounds are distributed about the pattern center (impact point) by a bivariate normal distribution (ballistic dispersion), the single-shot probability of hit P_{HSS} is given by integral of the bullet pattern over the projected target area.

In DMS simulations, a "nominal" bullet will be "fired" every 1/8 sec and each nominal bullet represents 10 actual bullets. Therefore, the expected number of hits associated with the nominal bullet will be

$$E_H = 10P_{HSS}$$

If the pilot fires a gun burst involving n iterations (burst length = $n/8$ sec) then the expected number of hits for the burst will be

UNCLASSIFIED

APPENDIX E

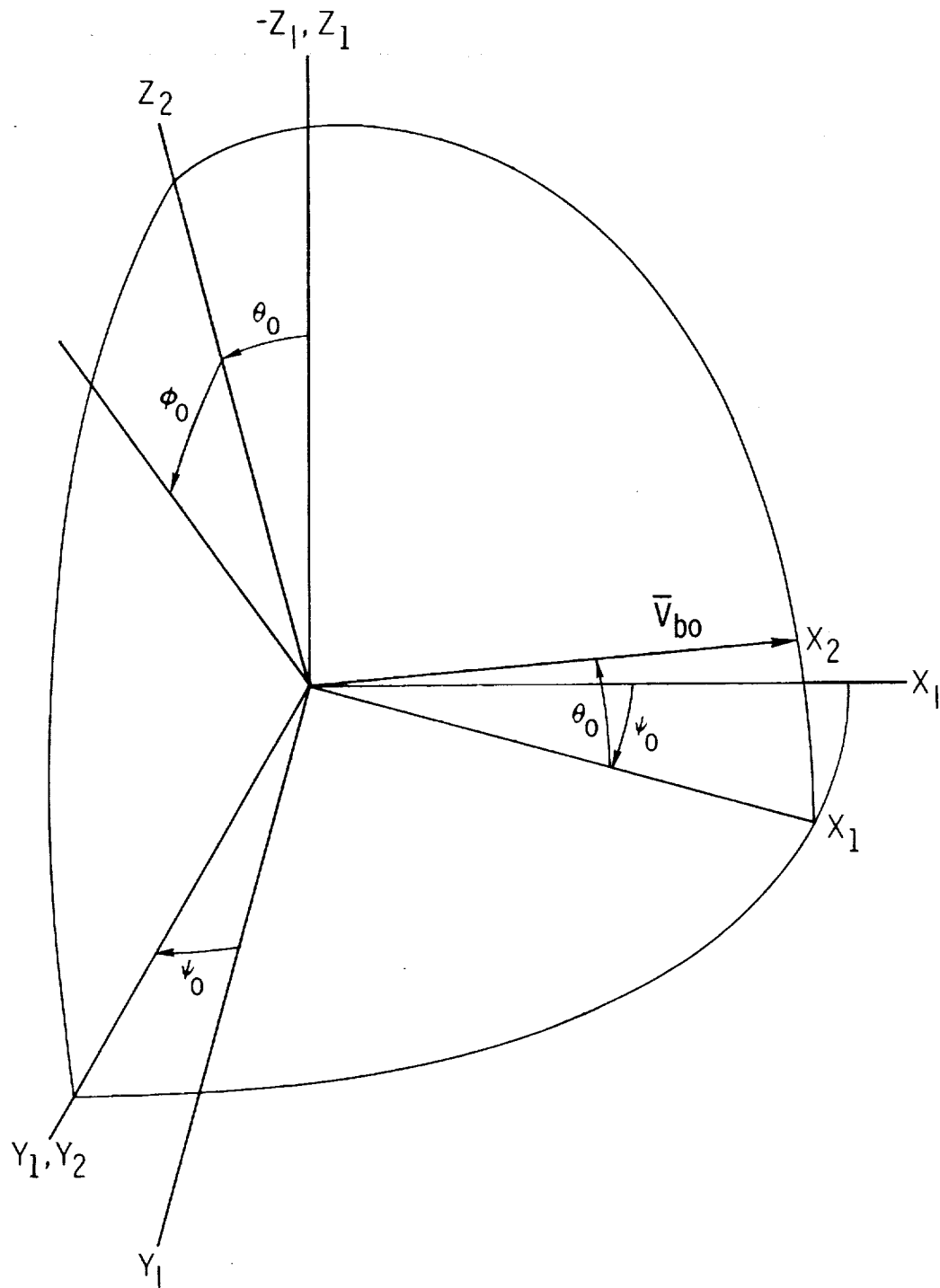
$$E_{H,\text{burst}} = \sum_{i=1}^n E_{H,i}$$

where $E_{H,i}$ is E_H at the ith iteration.

(U) The DMS program does not contain a vulnerability model for the simulated airplane, so it does not calculate probability of kill. Probability of kill would be useful in a multiaircraft scenario or a weapons system analysis. It was not considered necessary for one-on-one simulations investigating airplane performance and flying qualities.

UNCLASSIFIED

APPENDIX E



(U) Figure E1.- Relation of the X_1, Y_1, Z_1 and X_2, Y_2, Z_2 axis systems to the internal axis system and definition of the projectile precession angle ϕ_0 . (U)

UNCLASSIFIED

(U) REFERENCES (U)

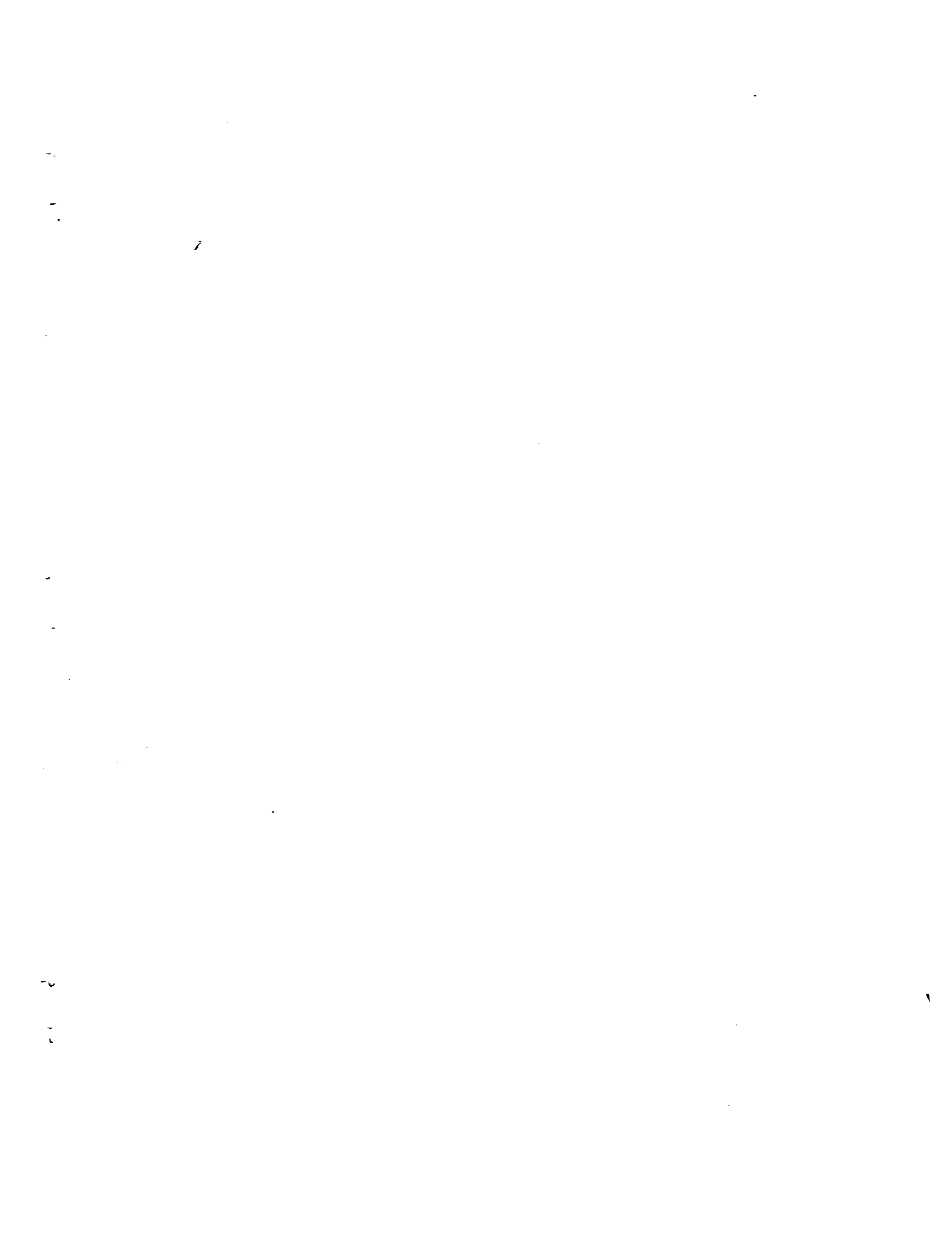
1. Runckel, Jack F.: Interference Between Exhaust System and Afterbody of Twin-Engine Fuselage Configurations. NASA TN D-7525, 1974.
2. Maiden, Donald L.; and Petit, John E.: Investigation of Two-Dimensional Wedge Exhaust Nozzles for Advanced Aircraft. AIAA Paper No. 75-1317, Sept.-Oct. 1975.
3. Capone, Francis J.: A Summary of Experimental Research on Propulsive-Lift Concepts in the Langley 16-Foot Transonic Tunnel. AIAA Paper No. 75-1315, Sept.-Oct., 1975.
4. Berrier, Bobby L.; and Re, Richard J.: Effect of Several Geometric Parameters on the Static Internal Performance of Three Nonaxisymmetric Nozzle Concepts. NASA TP-1468, 1979.
5. Capone, Francis J.: The Effects on Propulsion-Induced Aerodynamic Forces of Vectoring a Partial-Span Rectangular Jet at Mach Numbers From 0.40 to 1.20. NASA TN D-8039, 1975.
6. Berrier, Bobby L.; Palcza, J. Lawrence; and Richey, G. Keith: Nonaxisymmetric Nozzle Technology Program - An Overview. AIAA Paper 77-1225, Aug. 1977.
7. Gowadia, N. S.; Bard, W. D.; and Wooten, W. H.: YF-17/ADEN System Study. NASA CR-144882, 1979.
8. Capone, Francis J.; Gowadia, Noshir S.; and Wooten, W. H.: Performance Characteristics of Nonaxisymmetric Nozzles Installed on the F-18 Aircraft. AIAA Paper 79-0101, Jan. 1979.
9. F-15 2-D Nozzle System Integration Study. Volume I - Technical Report. NASA CR-145295, 1978.
10. F-15 2-D Nozzle System Integration Study. Volume III - Appendices. NASA CR-145297, 1978.
11. Ashworth, B. R.; and Kahlbaum, William M., Jr.: Description and Performance of the Langley Differential Maneuvering Simulator. NASA TN D-7304, 1973.
12. Beasley, Gary P.; and Sigman, Richard S.: Differential Maneuvering Simulator Data Reduction and Analysis Software. NASA TM X-2705, 1973.
13. Hankins, Walter W., III: Computer-Automated Opponent for Manned Air-to-Air Combat Simulations. NASA TP-1518, 1979.
14. Beasley, Gary P.; and Beissner, Fred L., Jr.: Correlation of Aircraft Maneuvering Parameter for One-On-One Air Combat. NASA TM X-3023, 1974.

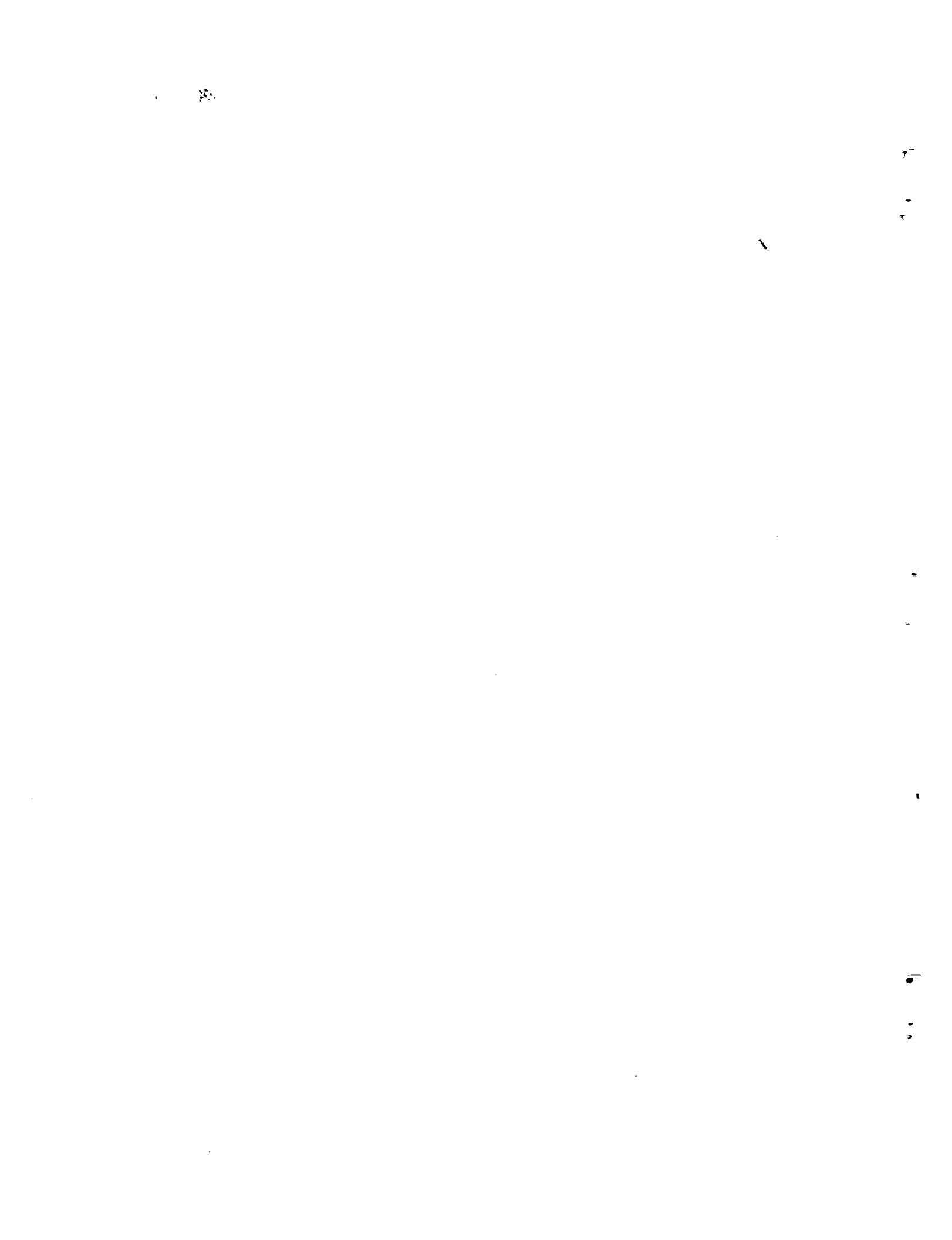
UNCLASSIFIED

177

UNCLASSIFIED

15. Pennington, Jack E.: Simulation Study of Effects of Thrust Vectoring and Induced Lift Due to Thrust Vectoring on Combat Effectiveness of a Fighter Aircraft. NASA TM X-3202, 1975.
16. Pennington, Jack E.; and Meintel, Alfred J., Jr.: Simulation Study of Thrust Vectoring for Air Combat Maneuvering for a Lightweight Fighter-Class Aircraft. NASA TM X-3270, 1975.
17. Thelander, J. A.: Aircraft Motion Analysis. FDL-TDR-64-70, U.S. Air Force, Mar. 1965. (Available from DTIC as AD 617 354.)
18. Etkin, Bernard: Dynamics of Flight. John Wiley & Sons, Inc., c.1959.
19. Robinson, Alfred C.: On the Use of Quaternions in Simulation of Rigid-Body Motion. WADC Tech. Rep. 58-17, U.S. Air Force, Dec. 1958. (Available from DTIC as AD 234 422.)
20. McDonald, Edward H.: F-15 Eagle Flight Control System. Advances in Control Systems, AGARD-CP-137, May 1974, pp. 11-1 - 11-8.
21. Burrows, Irving L.: F-15 Progress Report: Part II. 1973 Report to the Aerospace Profession, Tech. Rev., vol. 11, no. 4, Soc. Exp. Test Pilots, c.1974, pp. 13-22.
22. Jones, G. L.; and Winters, C. P.: Initial Air Force Development Test and Evaluation of the Flying Qualities of the F-15A Aircraft IAFDT and E-1. AFFTC-TR-74-8, U.S. Air Force, Apr. 1974. (Available from DTIC as AD C007 938L.)
23. Tanaka, A. Y.; and Huete, R. J.: F/TF-15A Flying Qualities Air Force Development Test and Evaluation, Volume 1. AFFTC-TR-76-48-VOL-1, U.S. Air Force, July 1977. (Available from DTIC as AD B021 782L.)
24. Norwood, J. M.: Gun Fire Control System Analysis. Volume 2: Ballistic Calculations in Airborne Gun Fire Control Systems. ARL-TR-76-49-VOL-2, U.S. Air Force, Mar. 1977. (Available from DTIC as AD B019 174L.)





[REDACTED]

7

[REDACTED]

[REDACTED]

[REDACTED]

1. Report No. NASA TM-80230	2. Government Accession No.	3. Recipient's Catalog No.	
4. Title and Subtitle SIMULATION STUDY OF NONAXISYMMETRIC NOZZLE FOR AIR-COMBAT MANEUVERING FOR AN F-15 CLASS AIRPLANE (U)		5. Report Date August 1980	
7. Author(s) Jack E. Pennington and Alfred J. Meintel		6. Performing Organization Code	
9. Performing Organization Name and Address NASA Langley Research Center Hampton, VA 23665		8. Performing Organization Report No. L-13357	
12. Sponsoring Agency Name and Address National Aeronautics and Space Administration Washington, D.C. 20546		10. Work Unit No. 505-43-33-03	
15. Supplementary Notes Appendix B by Fred L. Biessner, Jr., Kentron International, Inc., Hampton, Virginia.		11. Contract or Grant No.	
16. Abstract <p>(U) In 1978 an F-15 class airplane and a similar airplane having a non-axisymmetric two-dimensional nozzle were simulated on the Langley Differential Maneuvering Simulator. A series of simulated engagements were flown by combat-qualified pilots to assess the benefits of the two-dimensional nozzle. This report presents the equations and data used to represent both airplanes, describes the tests used to validate the simulation, compares the performance characteristics of the two airplanes, and presents the results of the piloted simulation.</p>			
17. Key Words (Suggested by Author(s)) F-15 Two-dimensional nozzle Simulation		18. Distribution Statement [REDACTED]	
Subject Category 05			
19. Security Classif. of this report [REDACTED]	20. Security Classif. (of this page) Unclassified	21. No. of Pages 178	22. Price
"NATIONAL SECURITY INFORMATION" Unauthorized Disclosure Subject to Criminal Sanctions.		Classified by: ASD-23 August 1973 Declassify on: December 31, 1988	